History of Quantum Chromodynamics

Harald Fritzsch (Munich, Germany)

On the Phase Structure and Dynamics of QCD

Jan M. Pawlowski (Heidelberg, Germany)

QCD phase structure

Estimate for CEP

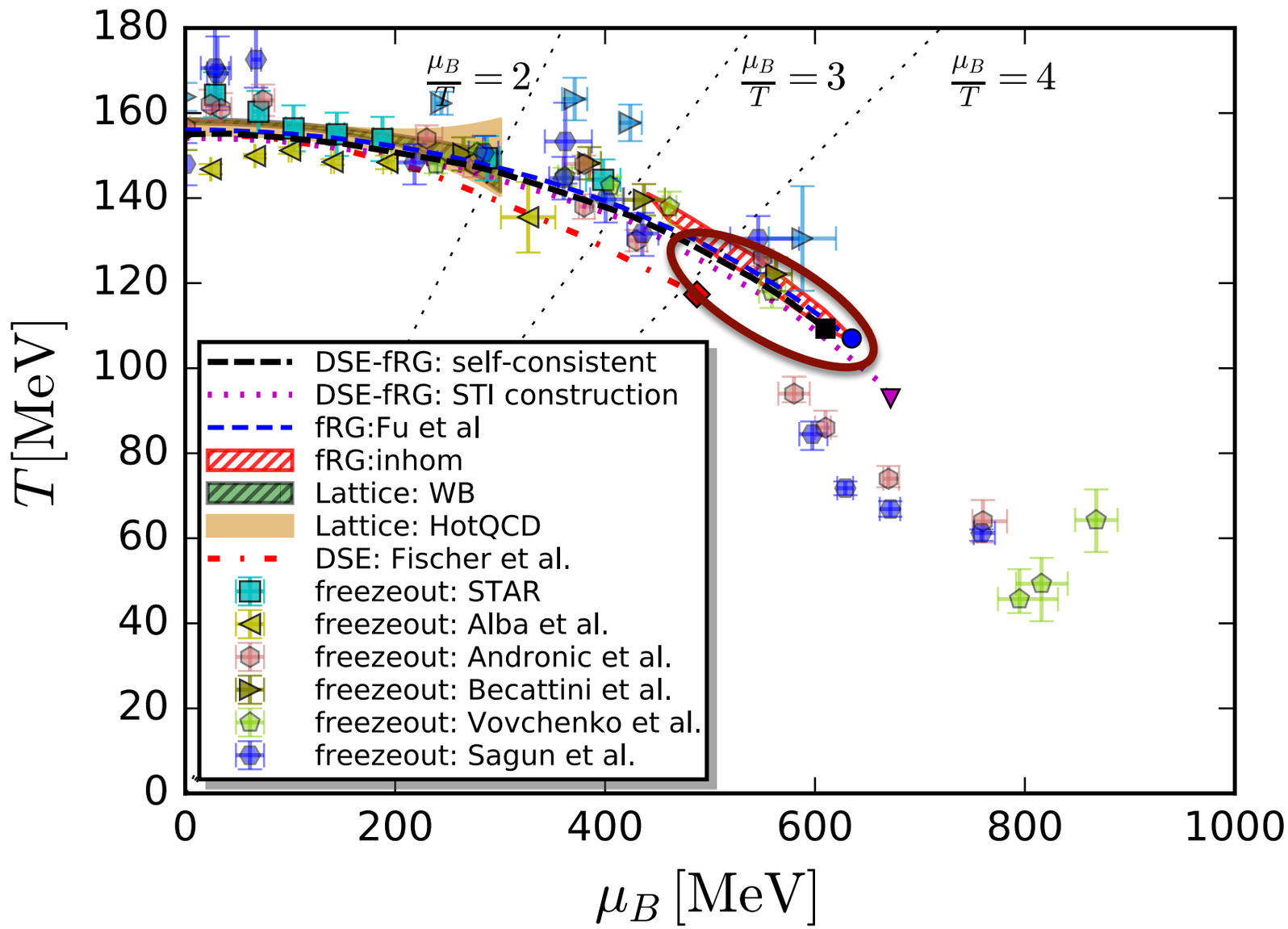

Stay tuned!

CEP-estimate fRG-DSE

$$(135\,,\,450\,)\,\mathrm{MeV} \lesssim (T_{\mathrm{CEP}}\,,\,\mu_{B_{\mathrm{CEP}}}) \lesssim (100\,,\,650)\,\mathrm{MeV}$$

fRG: Fu, JMP, Rennecke, PRD 101, (2020) 054032
DSE: Gao, JMP, PLB 820 (2021) 136584

Fluctuations of conserved charges

QCD-assisted LEFT

Benchmark at vanishing density

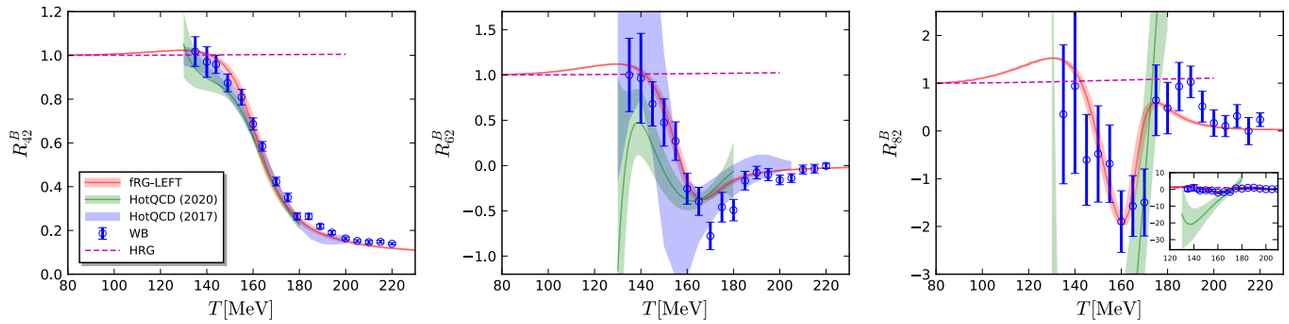

Freezeout curve

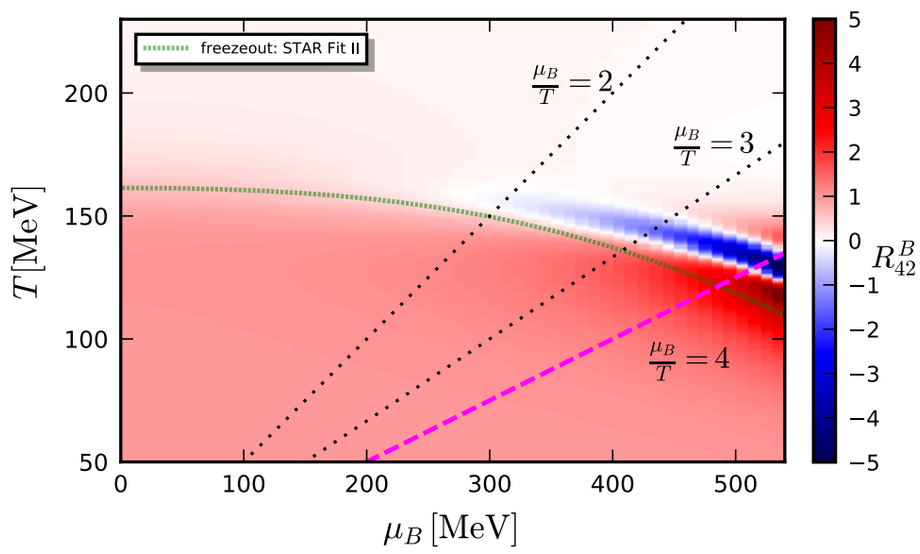

Great opportunity for a combined analysis
-Exp. data, lattice QCD, functional QCD-
of high density QCD

Fu, Luo, JMP, Rennecke, Wen, Yin, 2101.06035

QCD-assisted LEFT

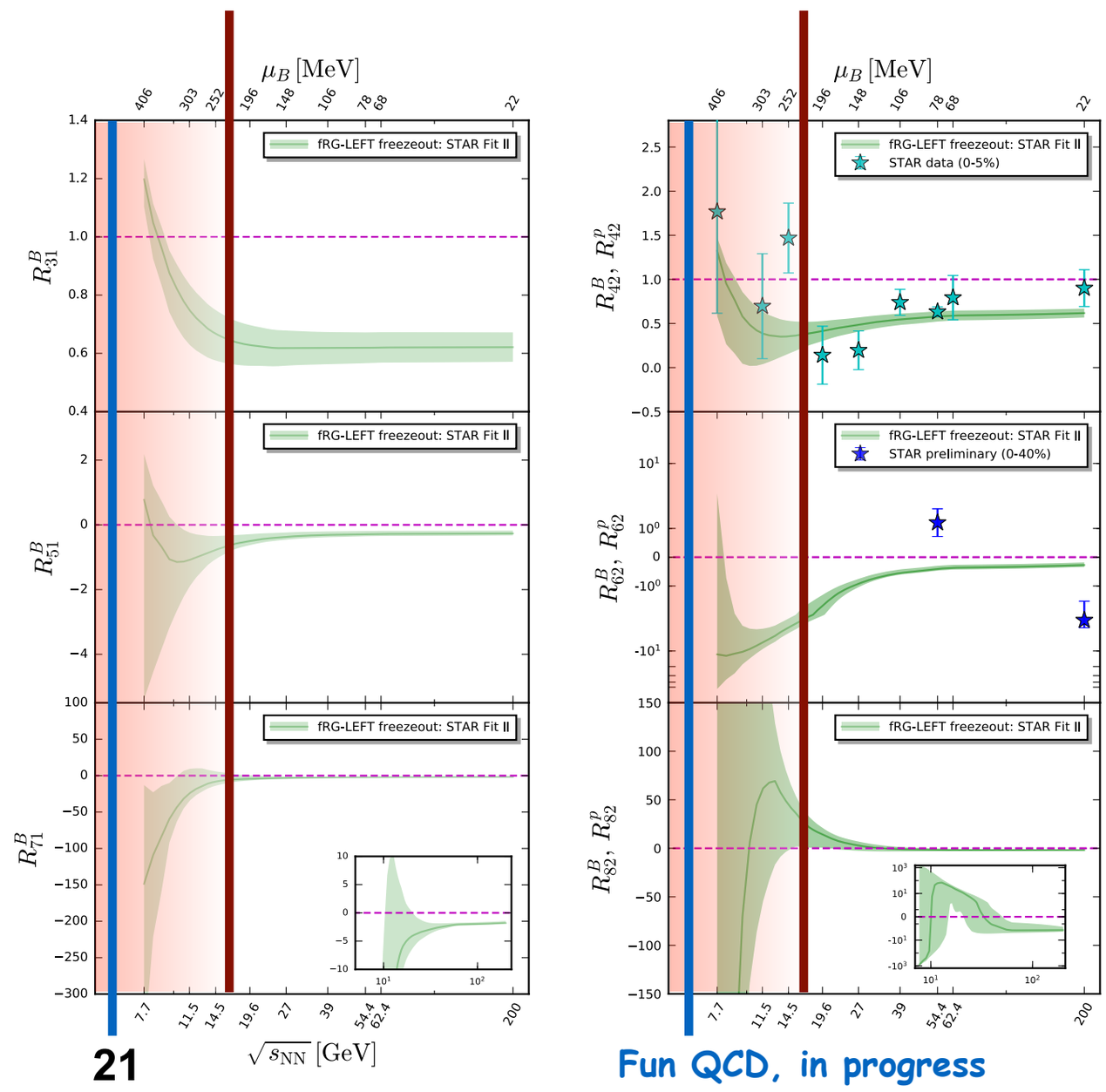

Fun QCD, in progress

Exploring the QCD phase diagram with Dyson-Schwinger equations

Philipp Isserstedt (Giessen, Germany)

Thermodynamics from DSEs ($\mu = 0$)

P.I., Fischer, Steinert, PRD 103 (2021) 054012

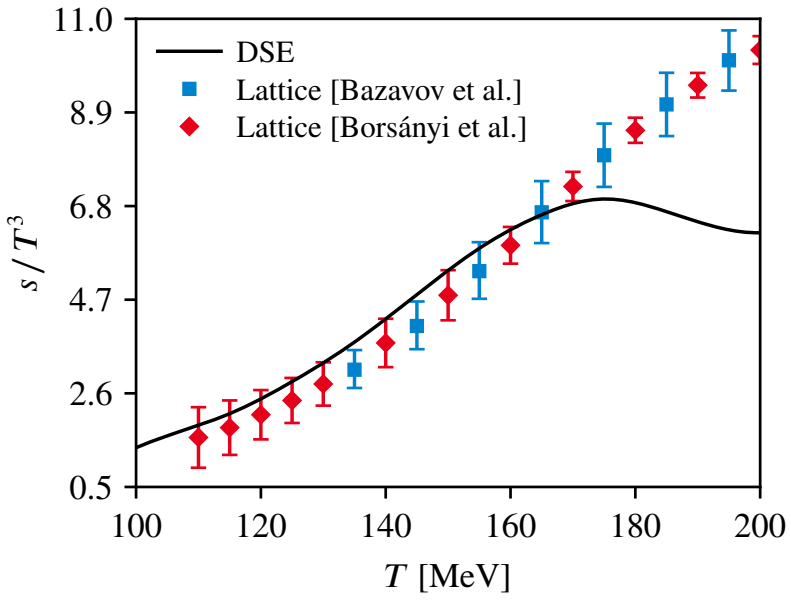

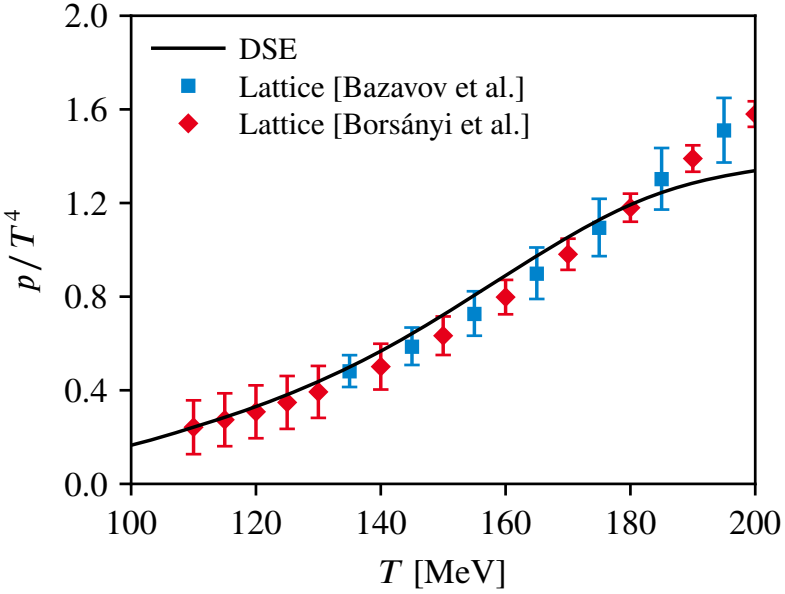

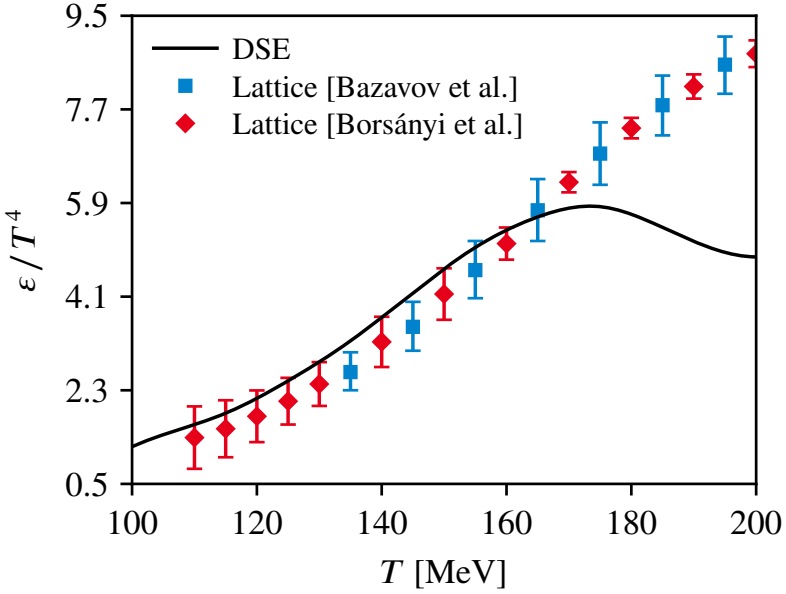

Thermodynamics from DSEs ($\mu \neq 0$)

P.I., Fischer, Steinert, PRD 103 (2021) 054012

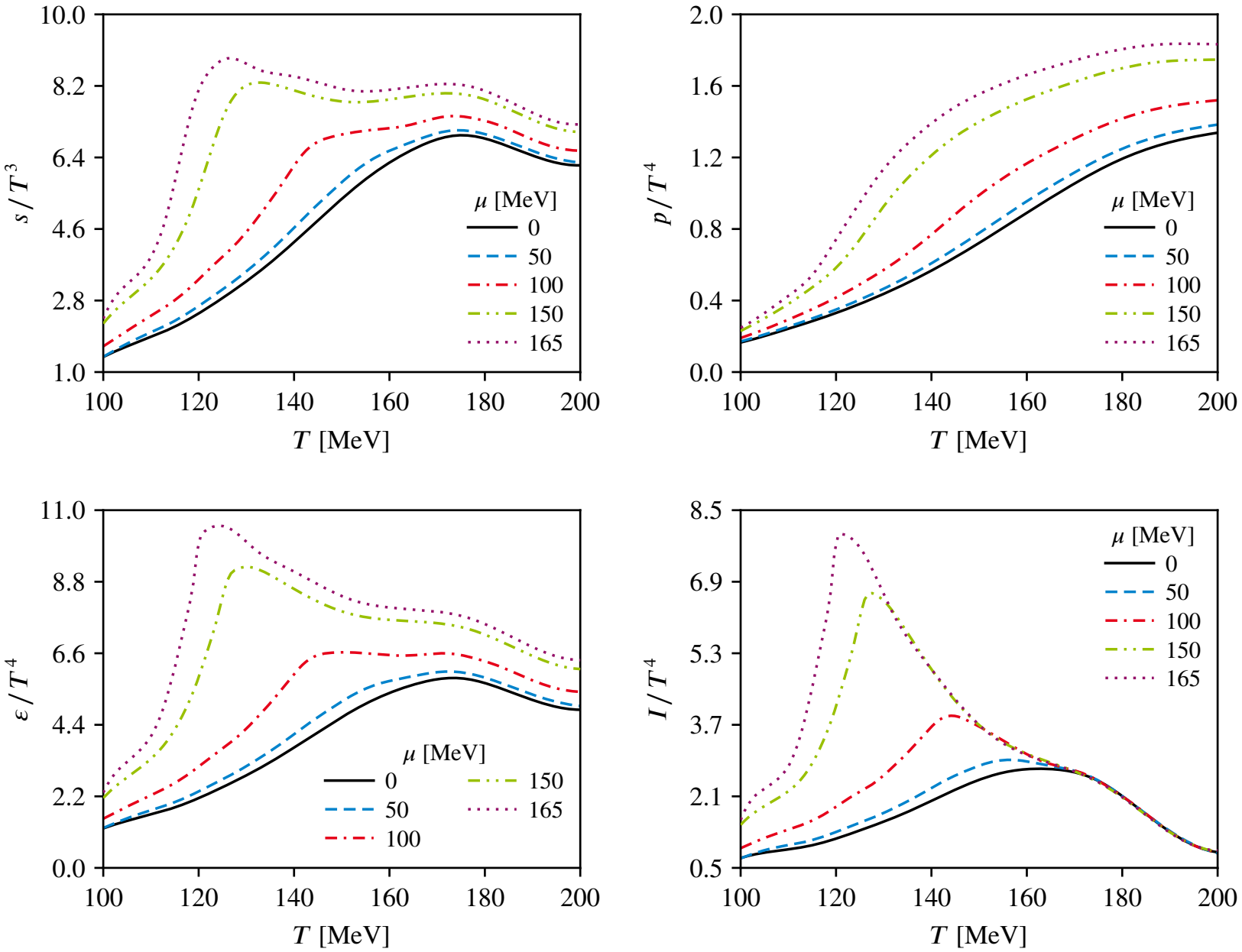

The critical endpoint of QCD in a finite volume

Julian Bernhardt (Giessen, Germany)

Results: Mass Function at $T = 130\,\mathrm{MeV}$ and $\mu_\mathrm{B} = 0$

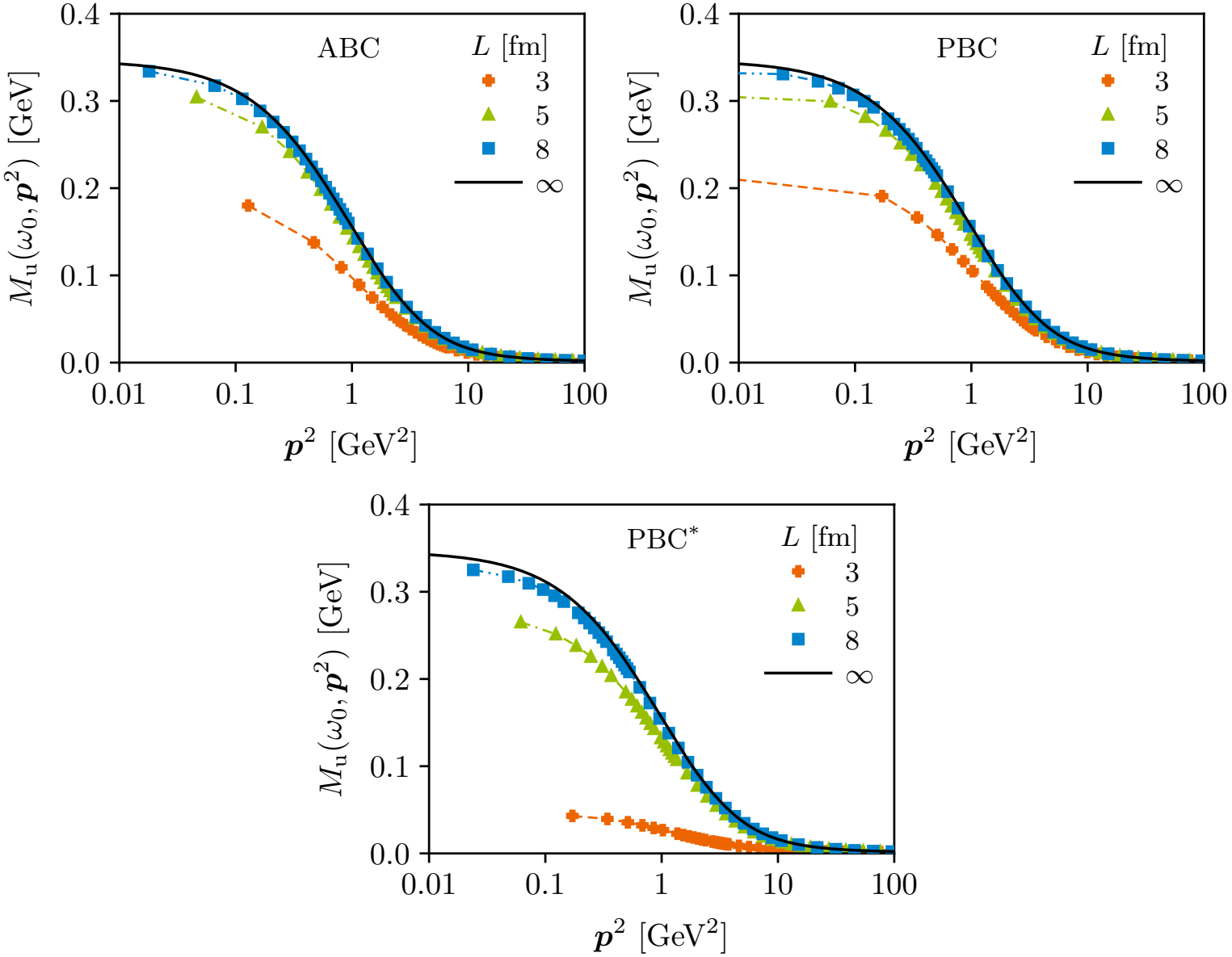

Results: QCD Phase Diagram

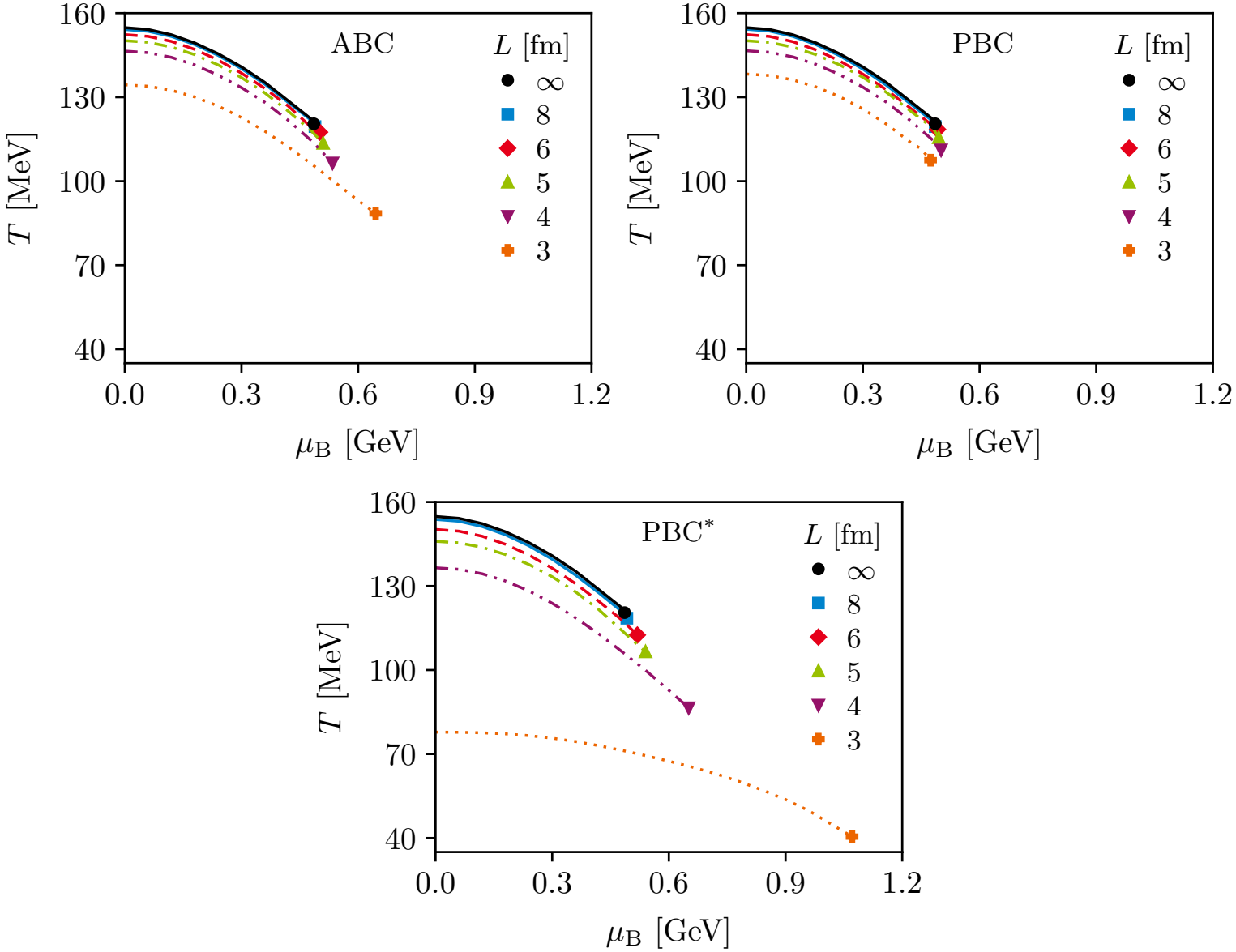

JB, Fischer, Isserstedt, Schaefer (arXiv:2107.05504)

Influence of quark masses and strangeness degrees of freedom on inhomogeneous chiral phases

Michael Buballa (Darmstadt, Germany)

Inhomogeneous chiral phases

TECHNISCHE UNIVERSITÄT DARMSTADT

NJL model, including inhomogeneous phase

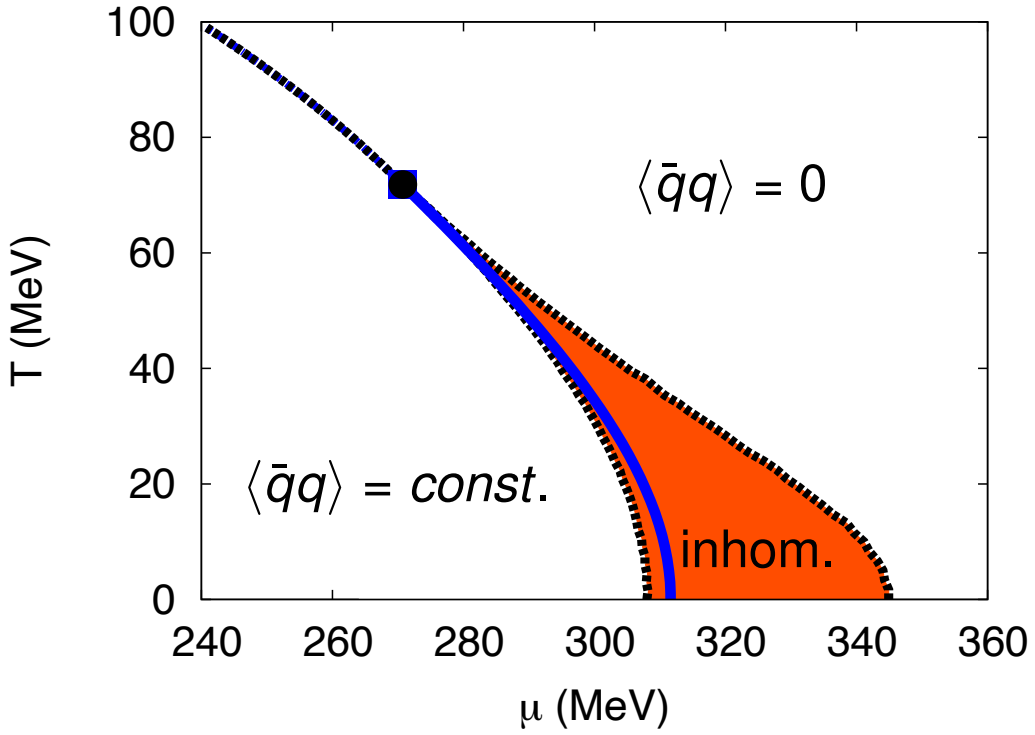

[D. Nickel, PRD (2009)]

$M \propto \langle \bar{q}q \rangle$

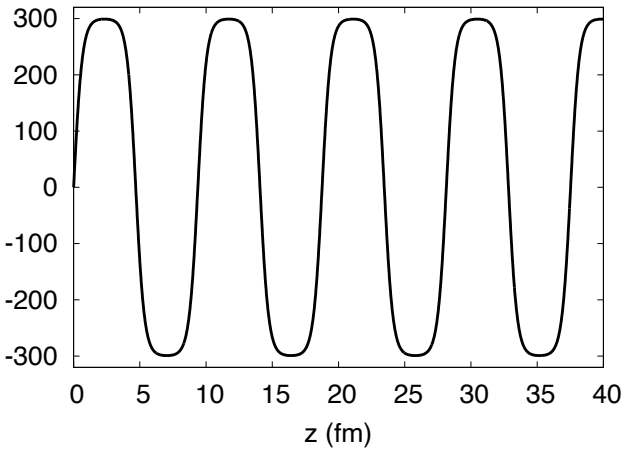

- 1st-order phase boundary completely covered by the inhomogeneous phase!
- Critical point $\rightarrow$ Lifshitz point
  [D. Nickel, PRL (2009)]

Effect of explicit chiral-symmetry breaking

TECHNISCHE UNIVERSITÄT DARMSTADT

GL results for critical points and Lifshitz points:

	chiral limit	explicitly broken
NJL model	LP = TCP [Nickel, PRL (2009)]	PLP = CEP [MB, Carignano, PLB (2019)]
QM model	LP = TCP if $m_\sigma = 2\bar{M}$ [MB, Carignano, Schaefer, PRD (2014)]	PLP = CEP if $m_\sigma = 2\bar{M}$ in the chiral limit [MB, Carignano, Kurth EPJST (2020)]

- No qualitative changes by explicit chiral-symmetry breaking
- Model results, but independent of model parameters

→ Model predictions of an inhomogeneous phase should be taken as seriously as those of a CEP!

Crossover width criteria for the two-flavor NJL-type models

Enrique Valbuena-Ordonez (San Nicolas de los Garza, Mexico)

NJL phase diagrams (local extended)

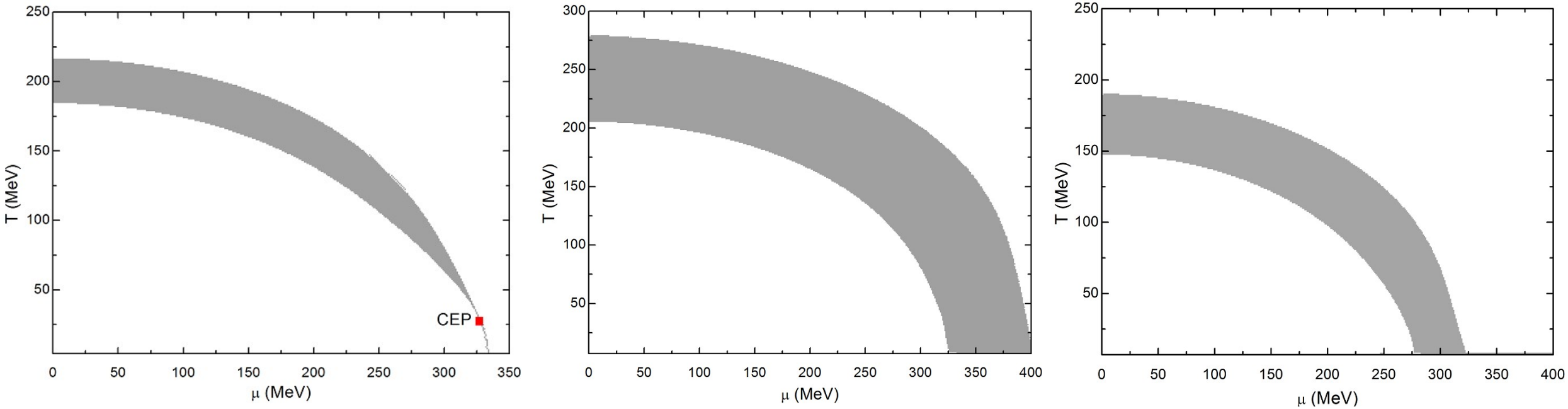

a. UV cutoff: Kohyama, H., Kimura, D., Inagaki, T.; Nucl. Phys. B 896, 2015
b. PTR: Cui, Z.-F.; Zhang, J.-L., Zong, H.-S.; Sci. Rep. 7, 2017
c. PV: Klevansky, S. P.; Rev. Mod. Phys. 64, 1992

PNJL phase diagrams (local)

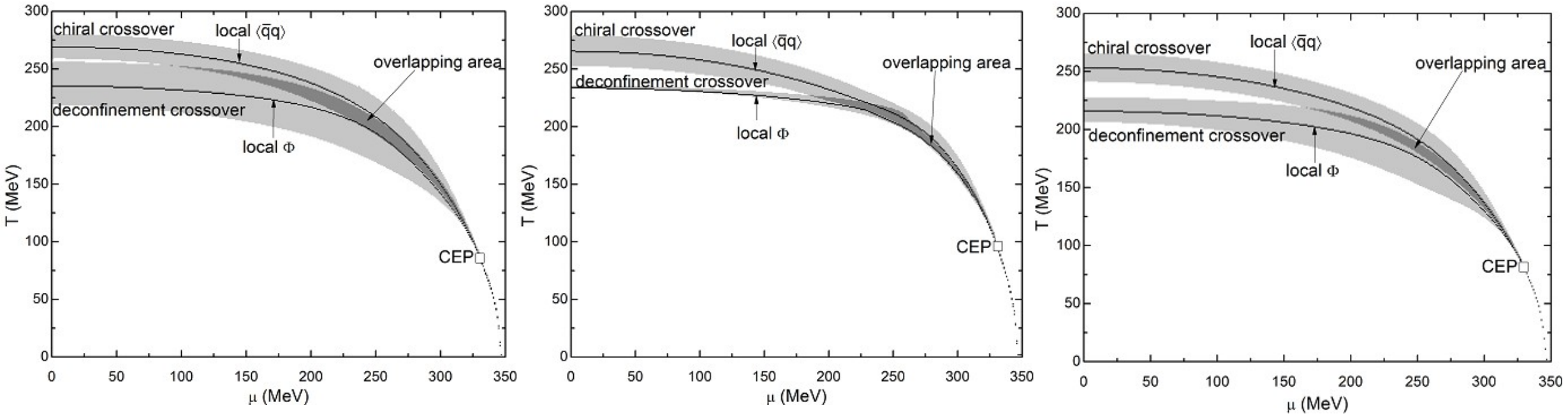

a b c

a. Ratti, C., Thaler, M. A., Weise, W.; Phys. Rev. D 73, 2006
b. Rößner, S., Ratti, C., Weise, W.; Phys. Rev. D 75, 2007
c. Fukushima, K.; Phys. Rev. D 77, 2008

Quasiparticle approach to strangeness and charm production in hot QCD

Valeriya Mykhaylova (Wroclaw, Poland)

Quasiparticle model with charm quarks: $N_f = 2+1$ vs $N_f = 2+1+1$

$N_f = 2+1$: non-thermalized charm quarks, $m_c = 1.3$ GeV

$N_f = 2+1+1$: charm quarks thermalize & contribute to EoS at $T \geq 300$ MeV ($\simeq 2T_c$)*1

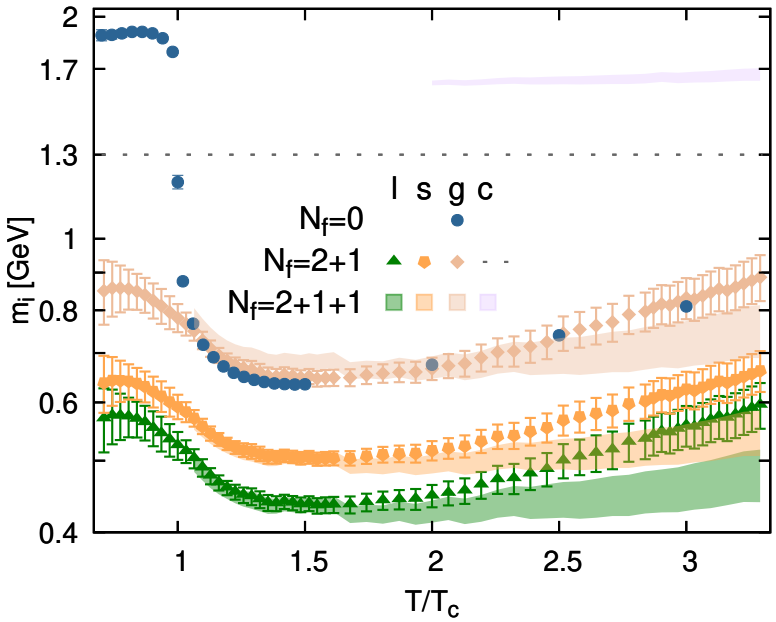

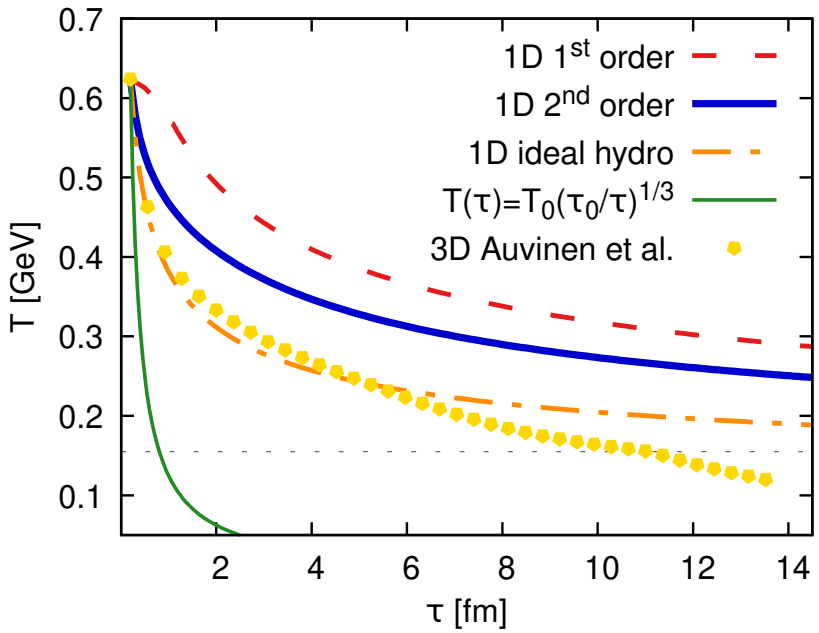

Interactions are encoded in the effective masses m_i: smooth change $2+1 \to 2+1+1$ for $m_{l,s,g}$, but m_c should be defined differently to connect constant and dynamically generated parts

$\tau_0 = 0.2$ fm, $T_0 = 0.624$ GeV*2

Time evolution of the QGP strongly depends on the order of hydrodynamics. Qualitative description in 3D[2] considers shear viscosity η/s for $N_f = 2+1$*3

[*1 Sz. Borsanyi et al., Nature 539 (2016), *2 J. Auvinen et al., PRC 102 (2020) , *3V.M., M. Bluhm, K. Redlich, C.Sasaki PRD 100 (2019)] Preliminary

Quasiparticle model with charm quarks: $N_f = 2+1$ vs $N_f = 2+1+1$

$$\text{Rate equations}^{*4}: \frac{dn_{s(c)}}{d\tau} = R^{gain}_{s(c)} - R^{loss}_{s(c)} = R^{tot}_{s(c)};$$

$$R^{tot}_{s(c)} = \frac{1}{2}\,\bar{\sigma}_{gg\to s\bar{s}(c\bar{c})}\, n_g^2 + \bar{\sigma}_{q\bar{q}\to s\bar{s}(c\bar{c})}\, n_q^2 + \bar{\sigma}_{c\bar{c}\leftrightarrow s\bar{s}}\, n^2_{c(s)} - \cdots$$

Cross sections depend on quasiparticle masses m_i^{*5}

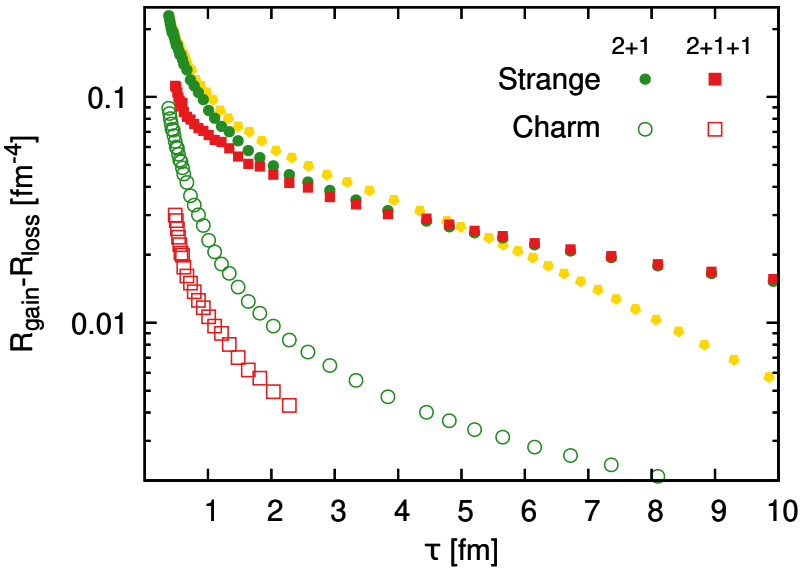

Ideal 1D

Viscous 3D

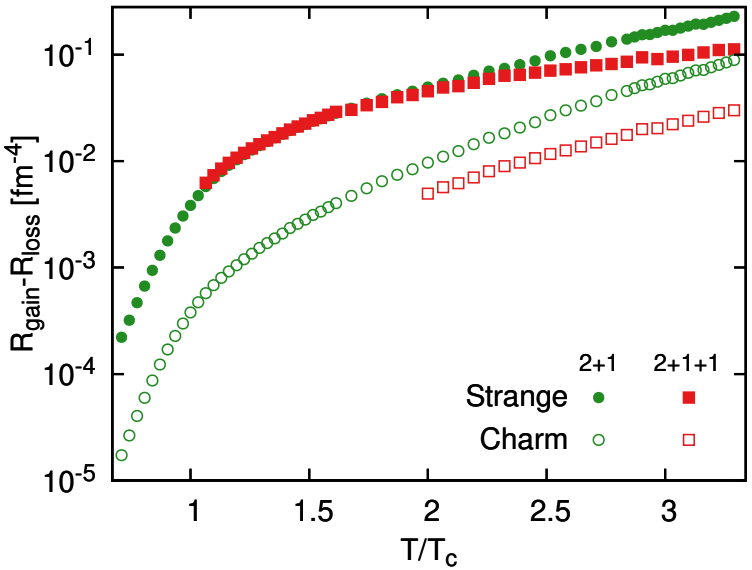

1D evolution of ideal QGP vs 3D evolution of viscous QGP: hadronization is faster in viscous 3D-expanding fireball

Suppression of strange and charm production rates at$(\simeq 2T_c)$ due to charm quark thermalization

[*4 T.S. Biro et al., PRC 48 (1993); J. Rafelski et al., Acta Phys.Polon.B 27 (1996); T.Matsui et al., PRD 34(4) (1986), *5 V.M., M. Bluhm, K. Redlich, C.Sasaki PRD 100 (2019), V.M., C. Sasaki, PRD 103 (2021)] Preliminary

Dualities of three colour and two colour QCD phase diagram

Roman Zhokhov (Troitsk, Moscow, Russia)

Dualities

$$(a) \qquad \mathcal{D}_1 : \qquad \mu \longleftrightarrow \nu, \qquad \text{PC} \longleftrightarrow \text{BSF}$$

$$(b) \qquad \mathcal{D}_3 : \qquad \nu \longleftrightarrow \nu_5, \qquad \text{PC} \longleftrightarrow \text{CSB}$$

$$(c) \qquad \mathcal{D}_2 : \qquad \mu \longleftrightarrow \nu_5, \qquad \text{CSB} \longleftrightarrow \text{BSF}$$

Phase diagram is **highly symmetric** due to **dualities** and highly constrained by them

A lot of interesting features of two color case remains qualitatively true in three color one

Dualities have been shown in two colour QCD itself not just in effective models

Hyperon-anti-hyperon polarization asymmetry in relativistic heavy-ion collisions as an interplay between chiral and helical vortical effects

Victor E. Ambrus (Frankfurt am Main, Germany)

Polarisation of Λ-hyperons [STAR Collaboration, Nature **548** (2017) 62]

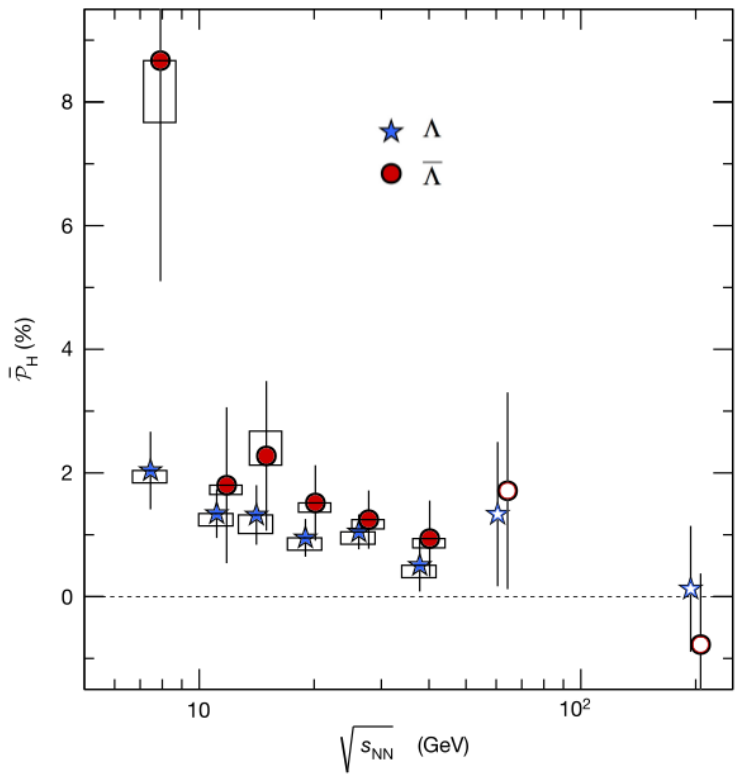

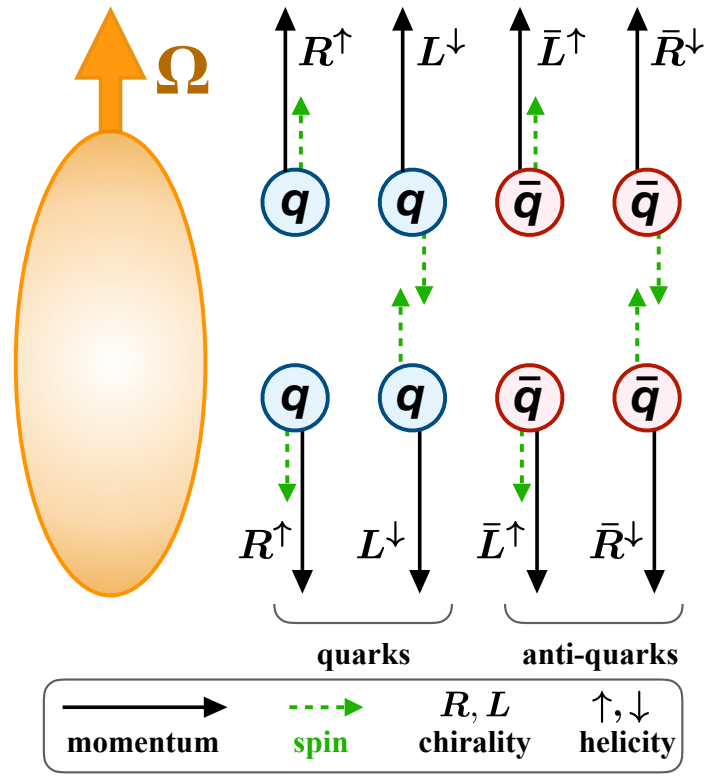

- Persistent polarization $\overline{\mathcal{P}}_{\Lambda/\bar{\Lambda}}$ measured by STAR. **Q: Why is $\overline{\mathcal{P}}_{\bar{\Lambda}} > \overline{\mathcal{P}}_{\Lambda}$?**
- Proposition: $\mathcal{P}$ due to Chiral+Helical Vortical Effects in thermalized QGP:

$$J_A = \sigma_A |\boldsymbol{\omega}| = J_\uparrow + \bar{J}_\uparrow - J_\downarrow - \bar{J}_\downarrow, \qquad \sigma_A = \frac{T^2}{6} + \frac{\mu_B^2}{18\pi^2},$$
$$J_H = \sigma_H |\boldsymbol{\omega}| = J_\uparrow + \bar{J}_\downarrow - J_\downarrow - \bar{J}_\uparrow, \qquad \sigma_H = \frac{2\mu_B T}{3\pi^2} \ln 2 + O(\mu_B^3/T).$$

[V. E. Ambruș, M. N. Chernodub, arXiv:1912.11034 [hep-th]; V. E. Ambruș, arXiv:1912.09977 [nucl-th]]

Result

[V. E. Ambruș, M. Chernodub, arXiv:2010.05831 [hep-ph]]

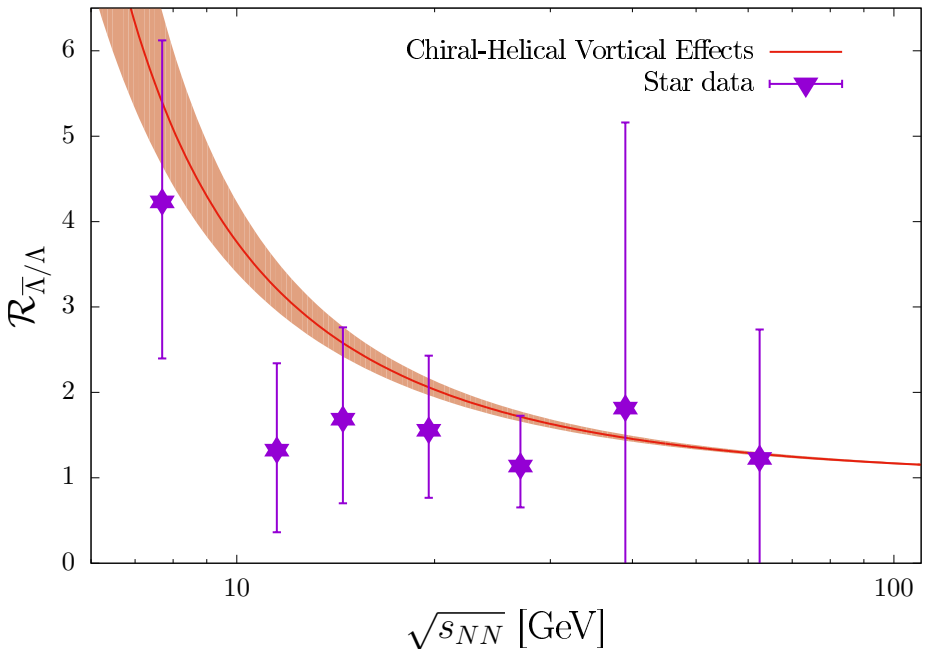

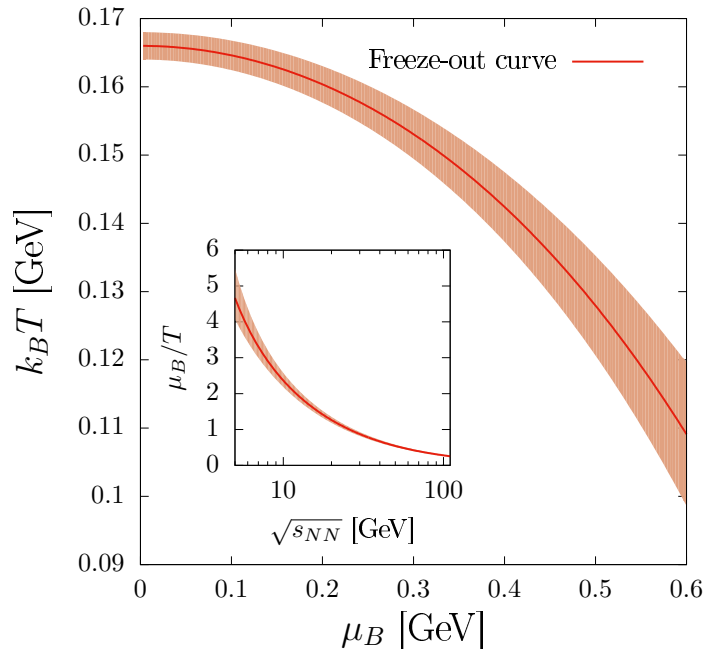

- The total $\mathcal{P}$ can be obtained by integration over the FO hypersurface:

$$\mathcal{P}_{q/\bar{q}} = \frac{1}{2}\kappa_{qj}(\sigma_A^\omega \pm \sigma_H^\omega)\int d\Sigma_\mu \omega^\mu.$$

- $\mathcal{R}_{\bar{\Lambda}/\Lambda}$ depends only on μ_B, T at freezeout: [Cleymans *et al.* PRC **73** (2006) 034905]

$$\mathcal{R}_{\bar{\Lambda}/\Lambda} = \frac{\mathcal{P}_{\bar{\Lambda}}}{\mathcal{P}_{\Lambda}} = \frac{\mathcal{P}_q}{\mathcal{P}_{\bar{q}}} = \frac{\sigma_A^\omega + \sigma_H^\omega}{\sigma_A^\omega - \sigma_H^\omega} = 1 + \frac{8\ln 2}{\pi^2}\frac{\mu_B}{T} + O(\mu_B^2/T^2).$$

- Connection between $\mathcal{R}_{\bar{\Lambda}/\Lambda}$ and μ_B/T easily established via CVE+HVE.

How can we understand spin polarization of Lambda hyperons using spin hydrodynamics?

Rajeev Singh (Krakow, Poland)

Perfect-fluid background and spin components evolution:

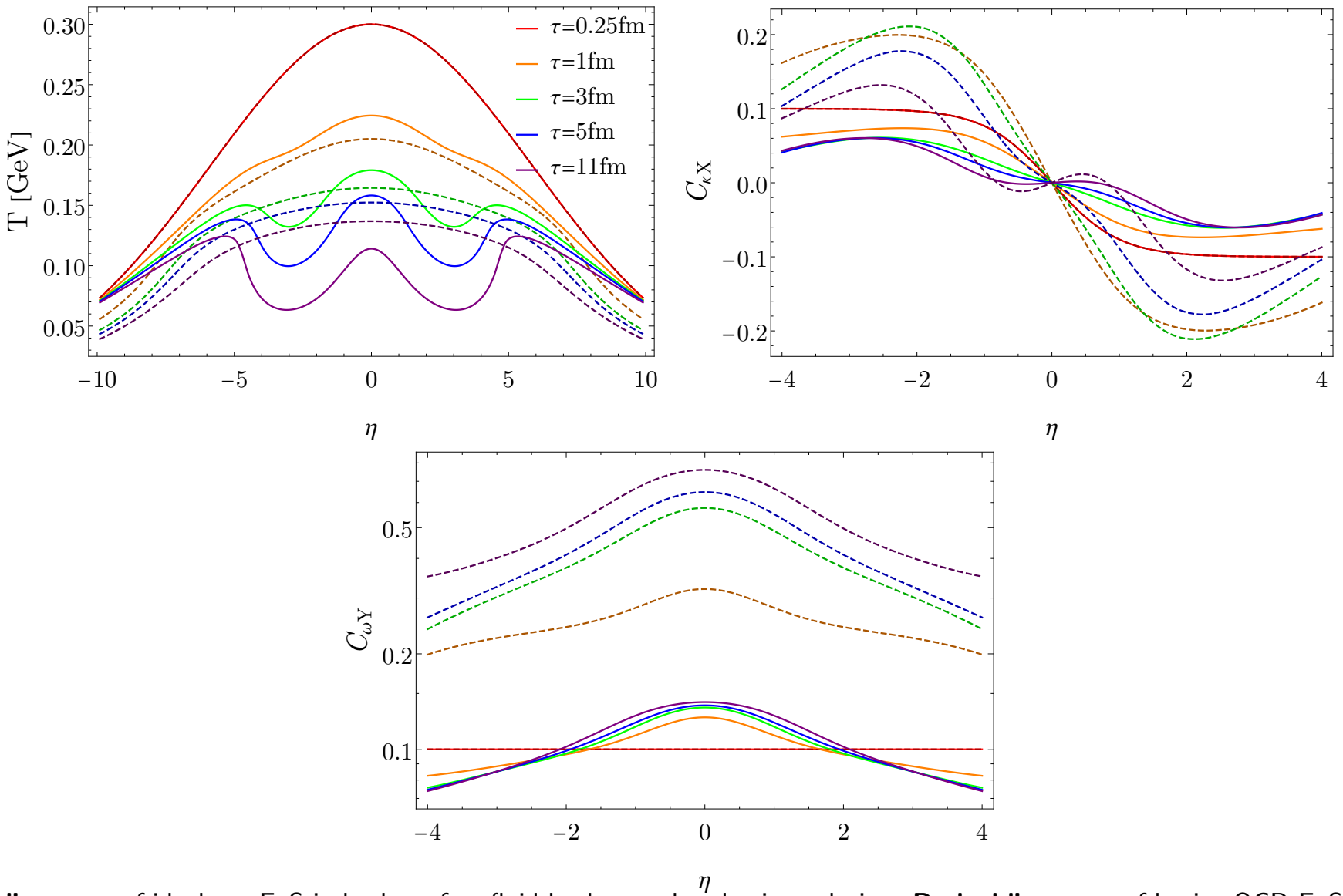

Solid lines: use of ideal gas EoS in both perfect fluid background and spin evolution. **Dashed lines**: use of lattice QCD EoS in background and ideal gas EoS for the spin evolution. Bumps in T are due to boundary effects. 3+1 D simulation in progress.

Exploring microscopic properties of matter across the QCD phase diagram with dileptons

Tetyana Galatyuk (Darmstadt, Germany)

EM SPECTRAL FUNCTION TO PROBE FIREBALL

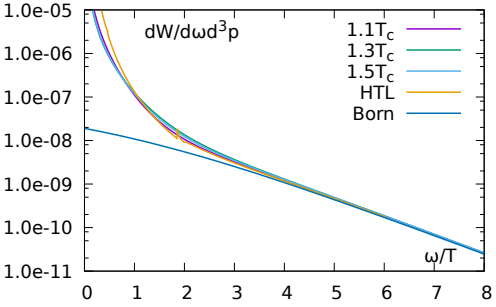

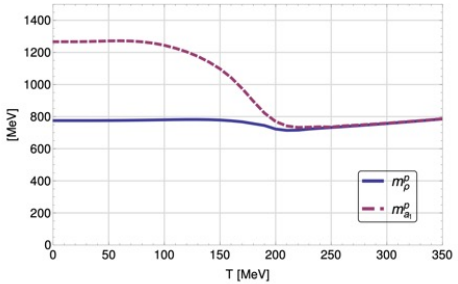

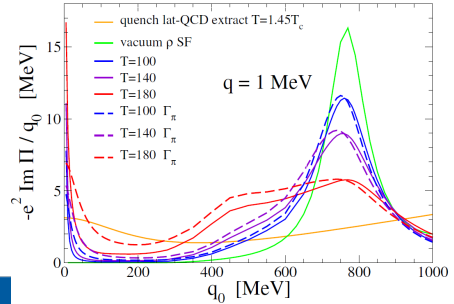

- Degrees of freedom of the medium: spectral function merges into QGP description as evidence for transition to quarks and gluons

  Rapp and Wambach, Adv.Nucl.Phys. (2000) 25
  Ding *et al.*, Phys.Rev.D 94 (2016) 3, 034504

- Chiral symmetry restoration: $\boldsymbol{\rho}$ meson melts, $\boldsymbol{a_1}$ mass decreases and degenerates with near ground-state mass

  Hohler and Rapp, Phys. Lett. B 731 (2014) 103
  Jung, Rennecke, Tripolt, at al., PRD95 (2017) 036020
  Sasaki, Phys.Lett. B801 (2020) 135172
  Aarts *et al.*, Phys. Rev. D 92 (2015) no.1, 014503

- Transport properties $\sigma_{el}(T) = -e^2 \lim_{q_0 \to 0} \frac{\delta}{\delta q_0} Im\Pi_{em}(q_0, q = 0; T)$
  - Electrical conductivity probes soft limit of EM spectral function

    Moore and Robert, arXiv:hep-ph/0607172
    Atchison, and Rapp, Phys. Conf.Ser. 832 (2017) 012057
    Greif, Greiner, Denicol, Phys.Rev. D93 (2016) 096012
    Gebhardt, Flörchinger in preparation

- Phenomenological tool (excitation functions)
  - temperature, excess yield and shape, T_{eff} vs mass, v_2 vs mass, polarization

    Speranza, Jaiswal, Friman, PLB782 (2018) 395
    R. Chatterjee et al., PRC 75 (2007), 054909

FUTURE

Signatures for phase transition (and critical end point?)

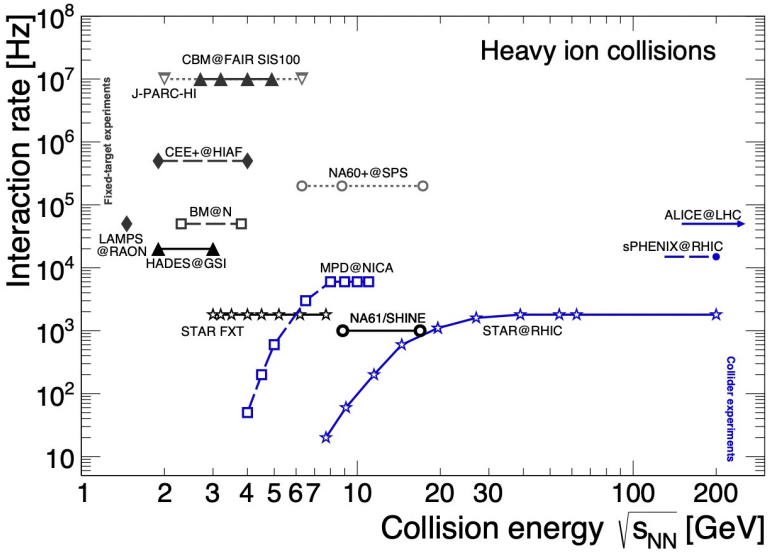

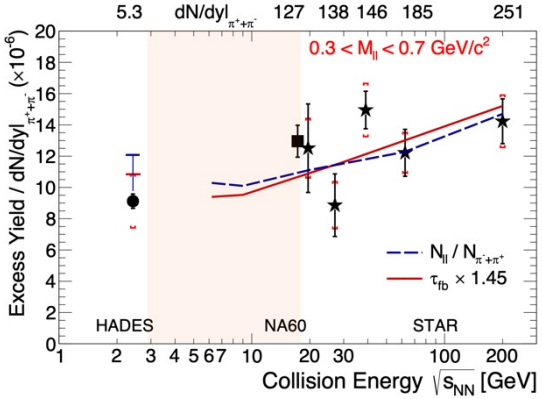

Low mass dilepton excess yield:

⇝ latent heat ⇝ longer life time ⇝ extra radiation

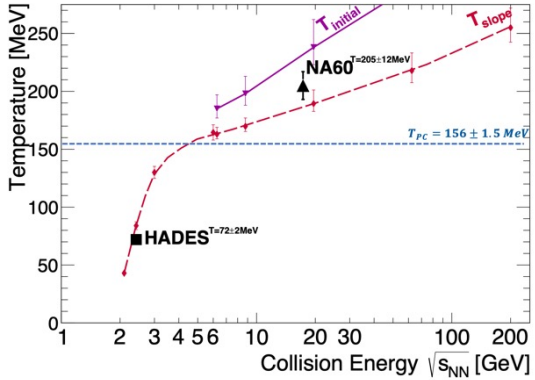

Unique temperature measurement (no blue-shift!)

⇝ phase transition may show up as a plateau

https://github.com/tgalatyuk/interaction_rate_facilities
https://github.com/tgalatyuk/QCD_caloric_curve

COARSE-GRAINED MICROSCOPIC TRANSPORT

- necessary ingredients to understand dilepton production in HIC:
  - realistic emission rates
  - accurate description of fireball evolution
  - sensitivity studies for the Equation of State
- use UrQMD, SMASH, HSD, GiBUU transport models to establish a **base line** for further comparisons of EM spectral functions

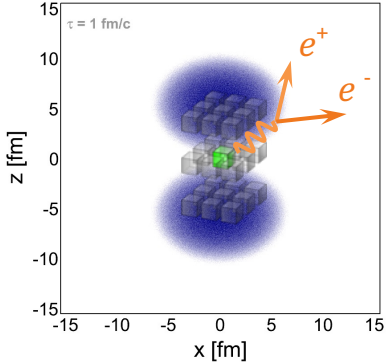

equilibrium properties in a local space-time volume from coarse-grained approach

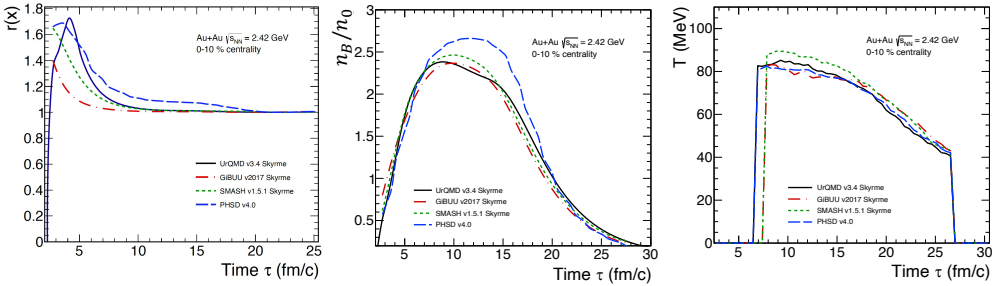

apply in-medium SF to compute EM rates

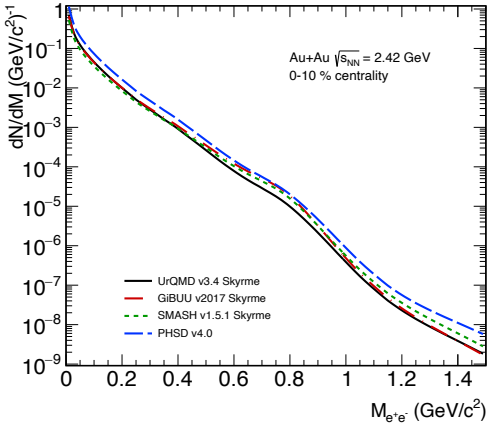

Galatyuk, Hohler, Rapp, Seck, Stroth, EPJA52 (2016) 131
Similar approaches: Staudenmaier, Weil, Steinberg, Endres, Petersen, PRC98 (2018) 054908
Endres, v. Hees, Bleicher, PRC94 (2016) no.2, 024912

Exploring the high-μ_B region of the QCD phase diagram with HADES

Joachim Stroth (Frankfurt am Main, Germany)

Proton higher-order flow components ($Au + Au$ $\sqrt{s} = 2.42$ AGeV)

The collective motion (flow) of protons, deuterons and tritons shows a distinct pattern which encodes properties of the fireball (e.g. equation-of-state).

Hillmann, Steinheimer et al., J.Phys.G 45 (2018)

The flow is encoded in the transverse mass spectra and in the angular variation of the yields.

$$\frac{\mathrm{d}N}{\mathrm{d}\varphi} \propto 1 + 2\sum_{n=1}^{\infty} v_n \cos\big(n(\varphi - \Psi_n)\big)$$

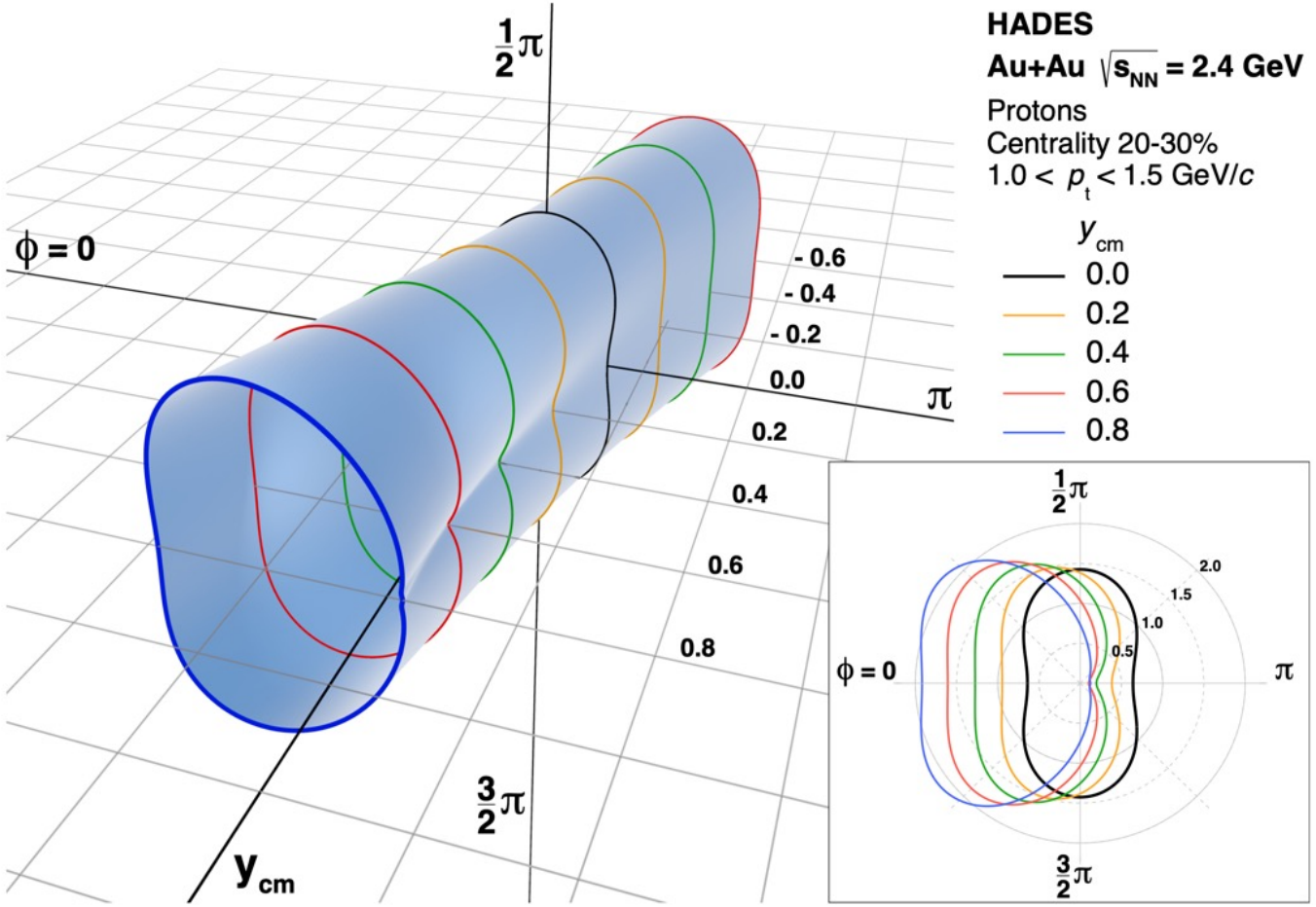

HADES, Phys. Rev. Lett. 125 (2020)

$\langle N_p \rangle$ scaling of factorial cumulants C_n

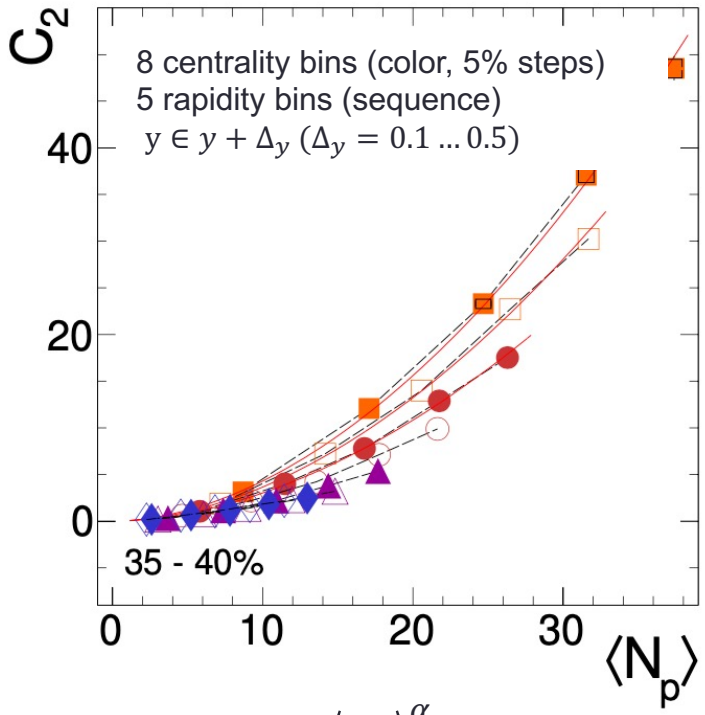

$C_2 \propto \langle N_p \rangle^{\alpha}$

$\alpha = 1.86 \pm 0.04$

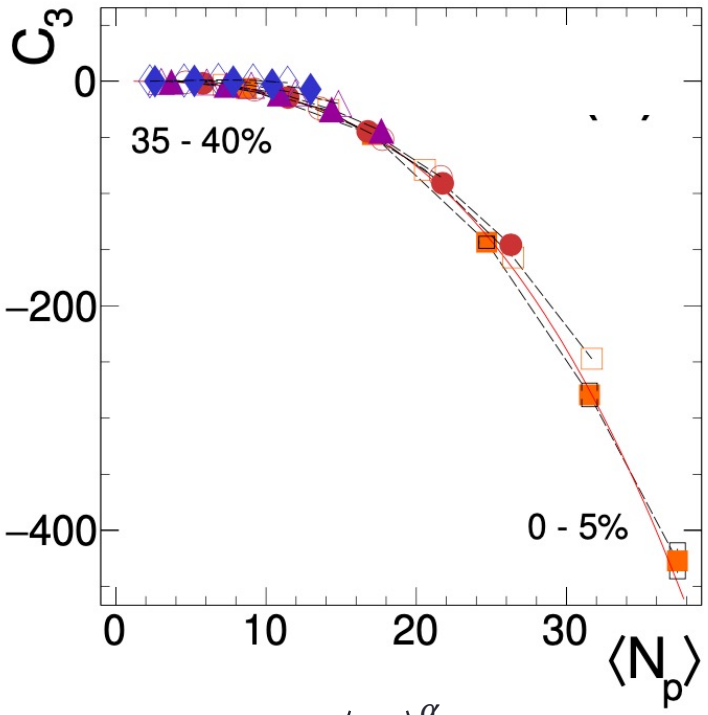

$C_3 \propto \langle N_p \rangle^{\alpha}$

$\alpha = 2.84 \pm 0.05$

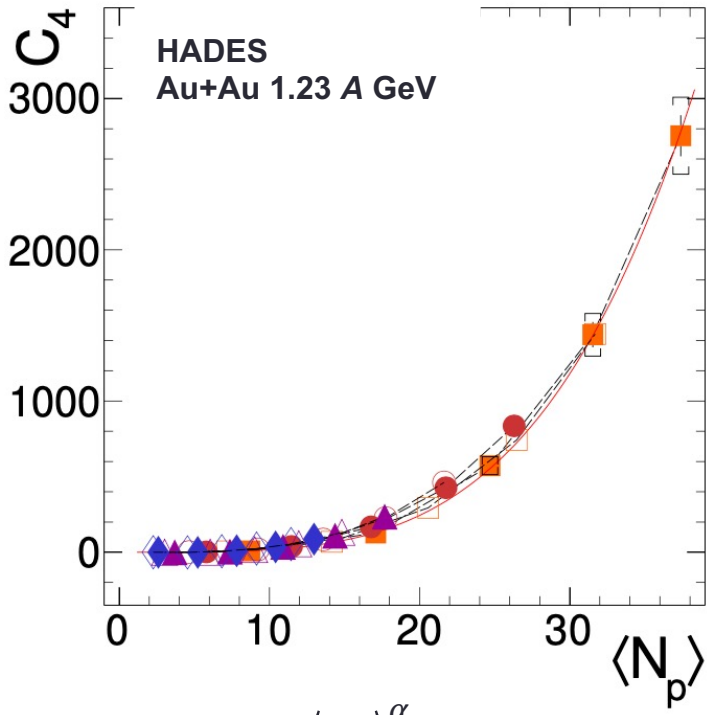

$C_4 \propto \langle N_p \rangle^{\alpha}$

$\alpha = 3.89 \pm 0.14$

$C_1 = K_1$
$C_2 = K_2 - K_1$
$C_3 = K_3 - 3K_2 + 2K_1$
$C_4 = K_4 - 6K_3 - 11K_2 + 6K_1$
K_n: cumulants
C_n: factorial cumulants/correlator

$\alpha \simeq n$ → signature of rather long-range correlation $(\Delta y_{corr} > \Delta_y)$

B. Ling, M.A. Stephanov; Phys.Rev:C 93, 034519

HADES Phys.Rev.C 102 (2020) 2, 024914

$\pi^- + p \rightarrow e^+e^- + n$

Effective transition form factor (time-like) extracted by subtracting QED expectation.

R-Dalitz decay:

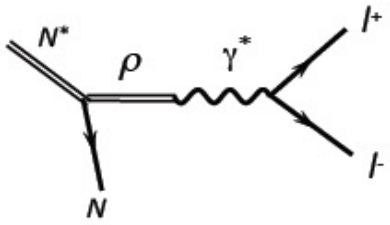

Baryonic contribution to in-mediumρ selfenergy

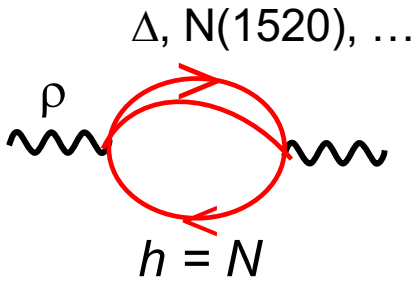

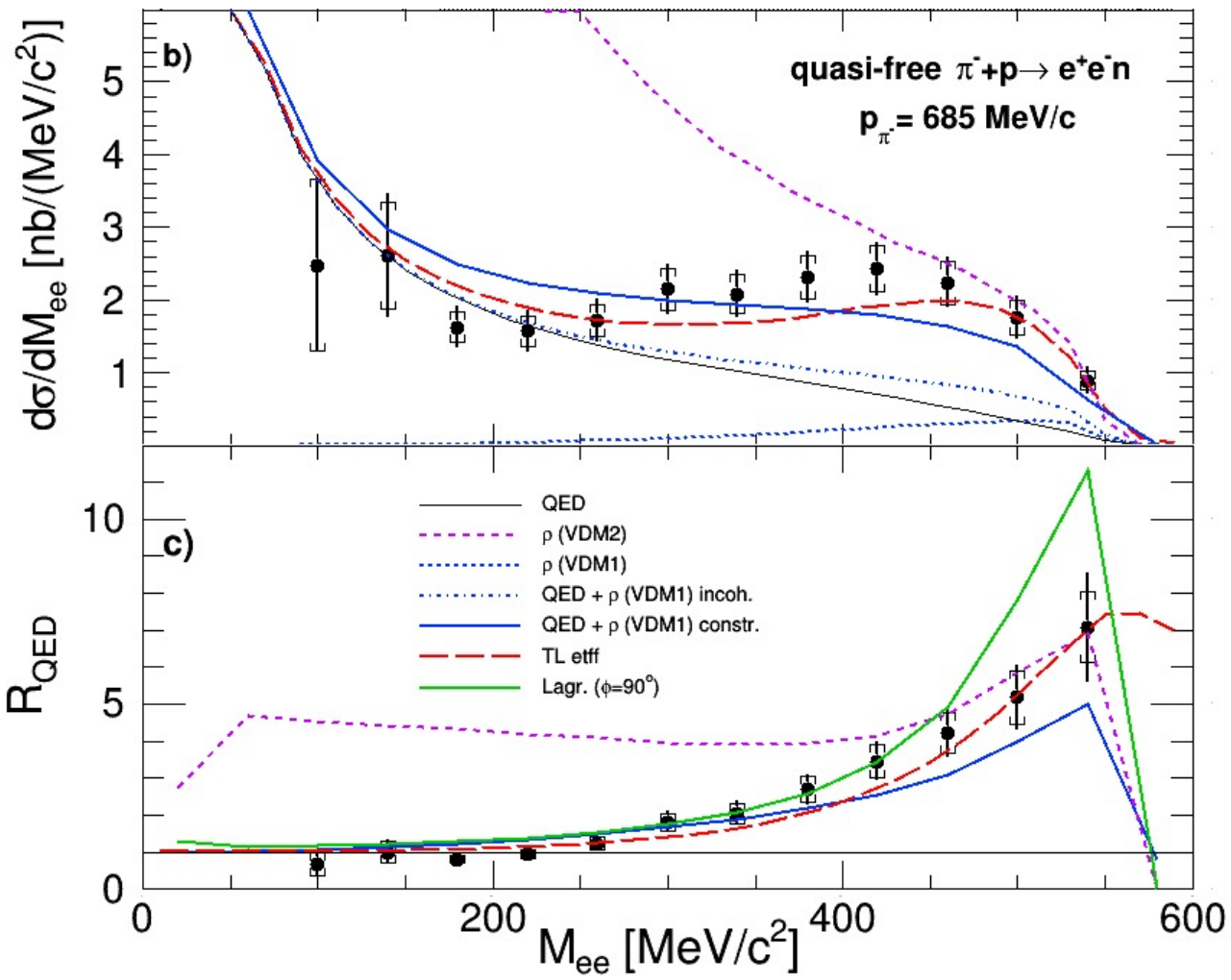

Dielectron reconstruction in Ag+Ag at $\sqrt{s_{NN}}$ = 2.55 GeV beam energy with HADES

Jan-Hendrik Otto (Giessen, Germany)

Ag+Ag at $\sqrt{s_{NN}} = 2.55\,GeV$

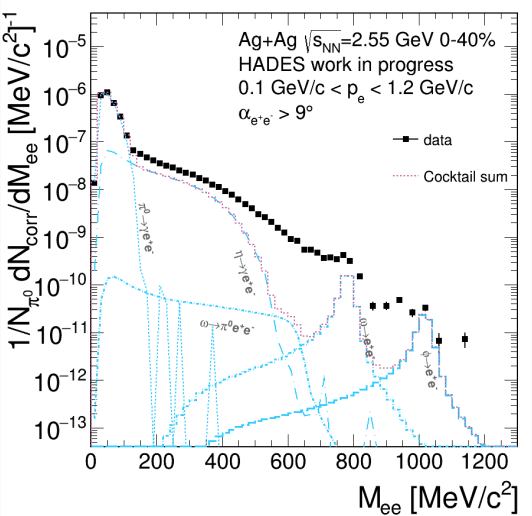

- DiElectrons are emitted throughout the whole evolution of the collision
- Interpolation of hadron multiplicities (HADES measurements in preparation) and NN reference simulation (GiBUU) allow to access the thermal radiation from the Fireball
- Clear excess above final freezeout hadrons observed

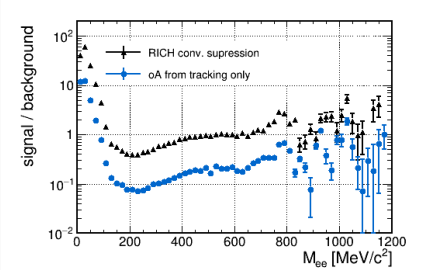

Pair momentum dependent analysis ($\sqrt{s_{NN}} = 2.55\,GeV$)

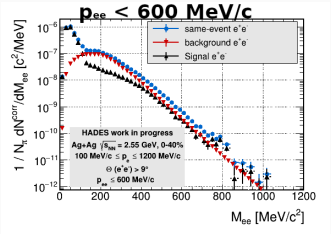

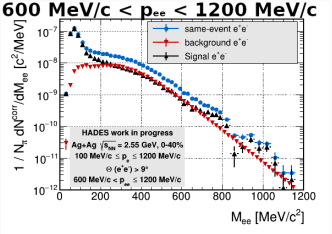

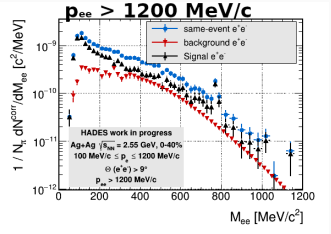

- Change of the line shape with momentum at the ω pole mass observed (similar to previous HADES p+Nb measurement, *Phys. Let. B 8 (2012), 10.1016*)
- ω multiplicity estimation possible for high momenta

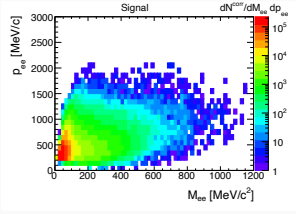

Search for critical point of strong interaction via proton intermittency

Haradhan Adhikary (Kielce, Poland)

Proton intermittency analysis result

(Search for QCD critical point by NA61/SHINE at CERN SPS)

Second scaled factorial moment dependence on the transverse momentum bin size for mid-rapidity protons produced in Pb+Pb at 30*A* GeV/*c* and Ar+Sc at 150*A* GeV/*c* using independent points and cumulative quantities:

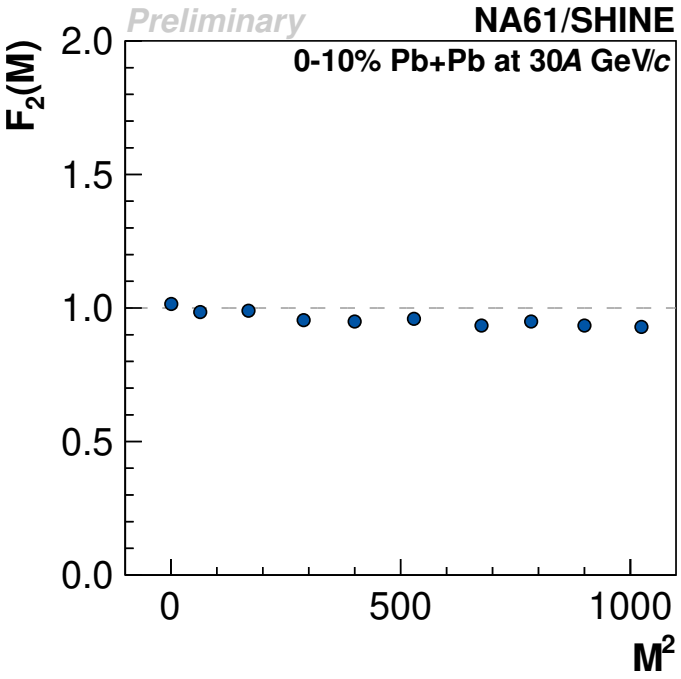

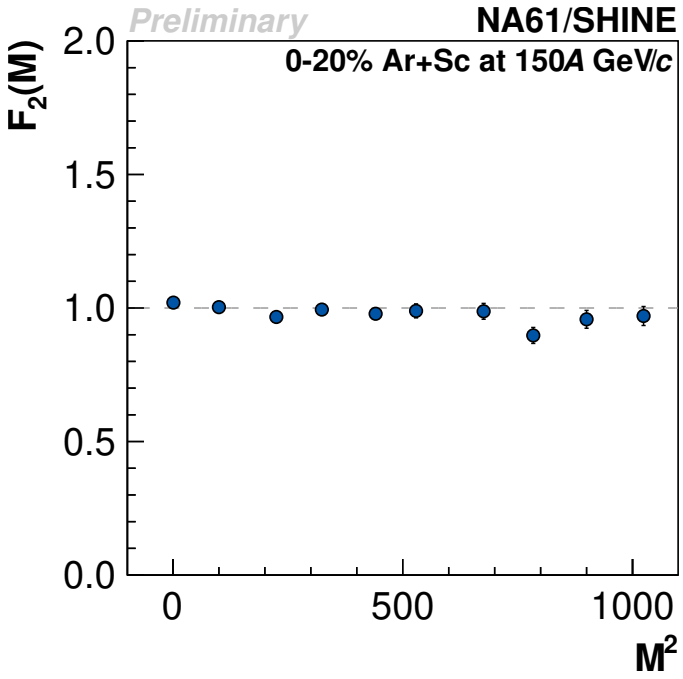

No significant critical signal is observed via proton intermittency analysis.... !

h^- (pion) intermittency analysis result

(Search for QCD critical point by NA61/SHINE at CERN SPS)

Scaled factorial moments (upto 4th order) dependence on the transverse momentum bin size for mid-rapidity pions produced in Pb+Pb at 30*A* GeV/c using independent points and cumulative quantities:

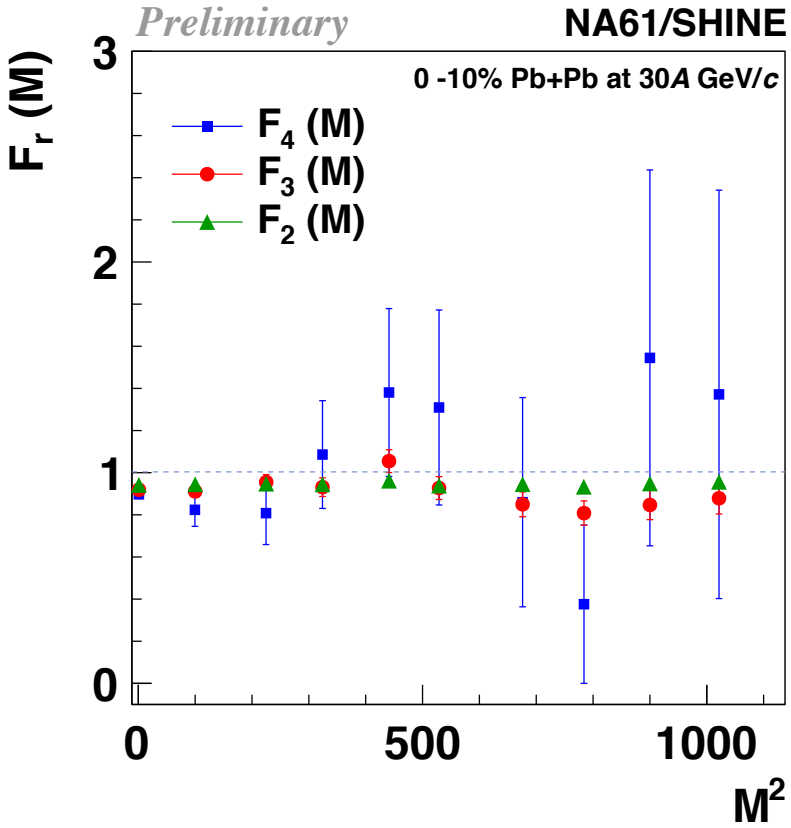

No significant critical signal is observed via pion intermittency analysis..!

Dense Baryonic Matter in QCD, and signatures from Heavy Ion Collisions and binary Neutron Star Matter

Horst Stoecker (Frankfurt am Main, Germany)

Kurtosis and the phase diagram

Kurtosis : $\chi_4^B/\chi_2^B, \quad \chi_n^B = \dfrac{\partial^n p/T^4}{\partial\left(\mu_B/T\right)^n}$

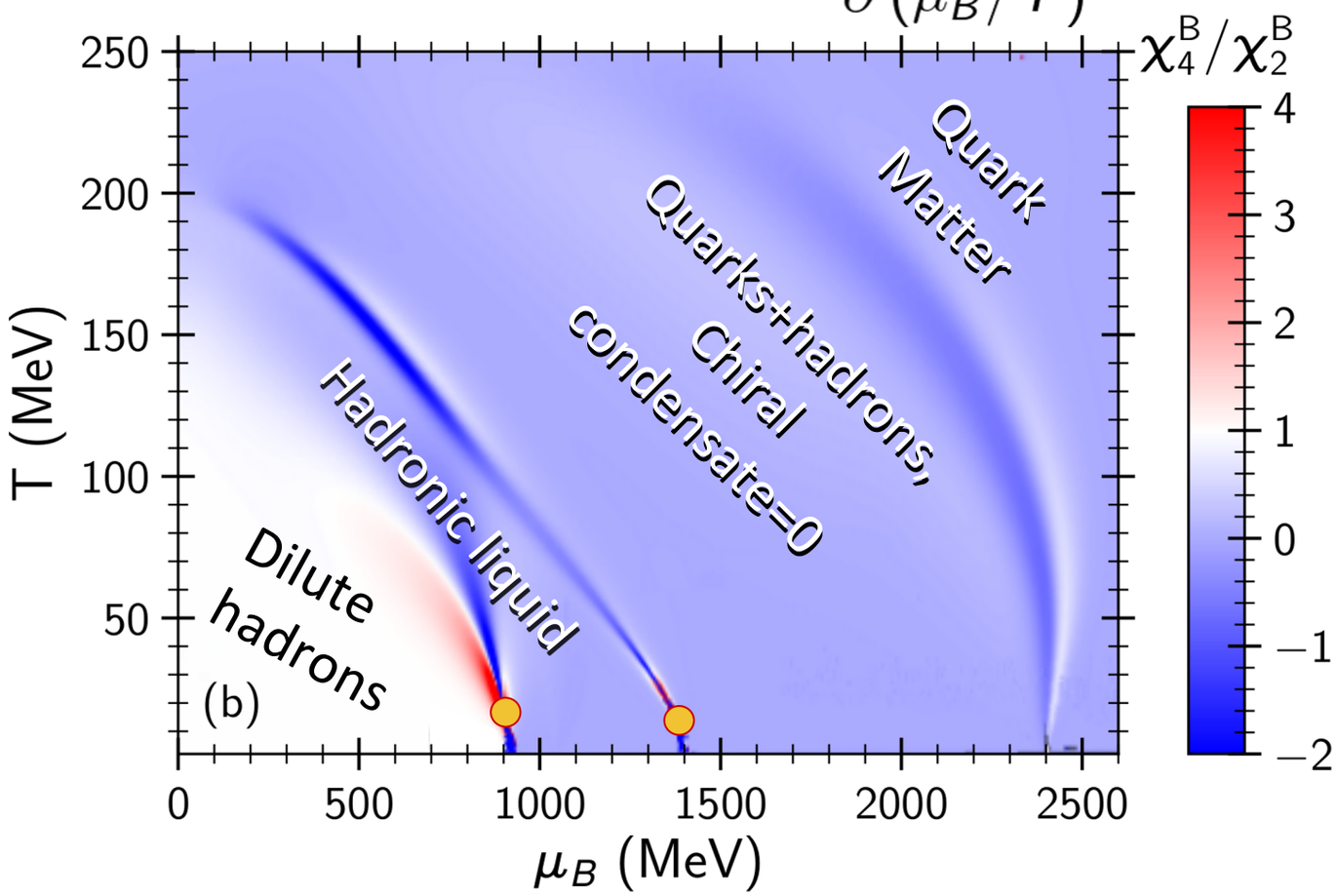

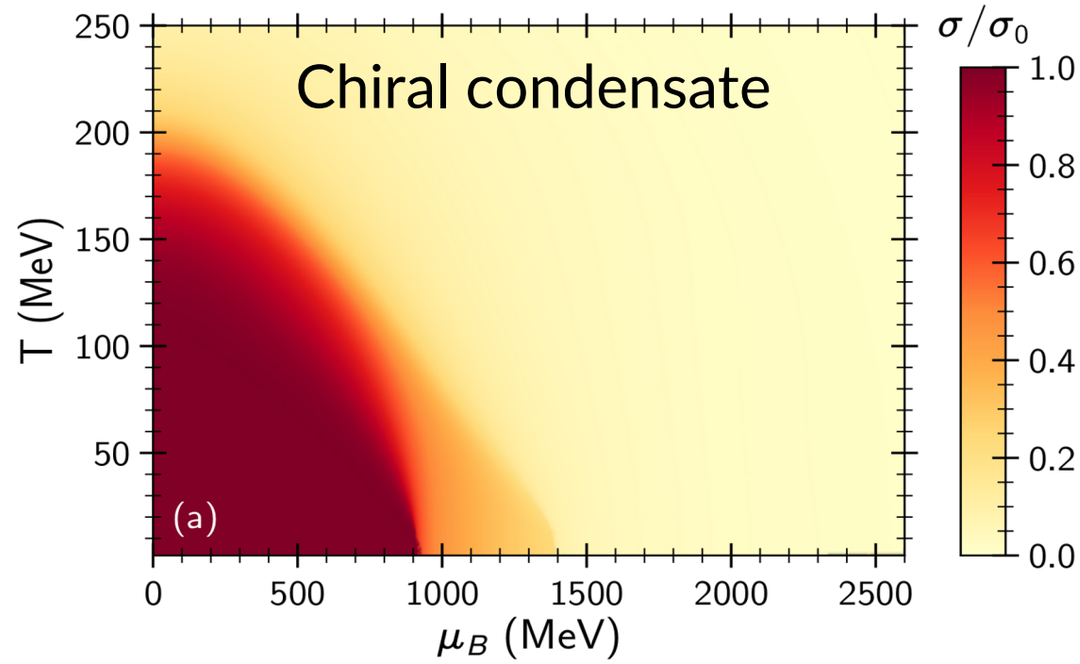

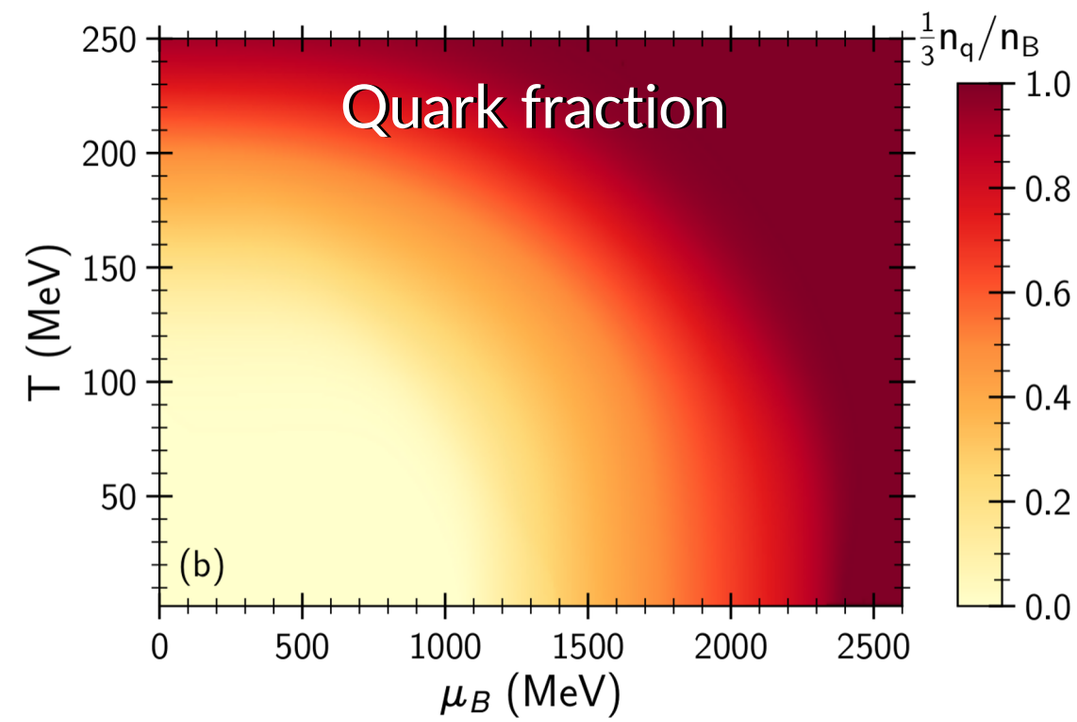

Gravitational Wave Emission from BNSM!

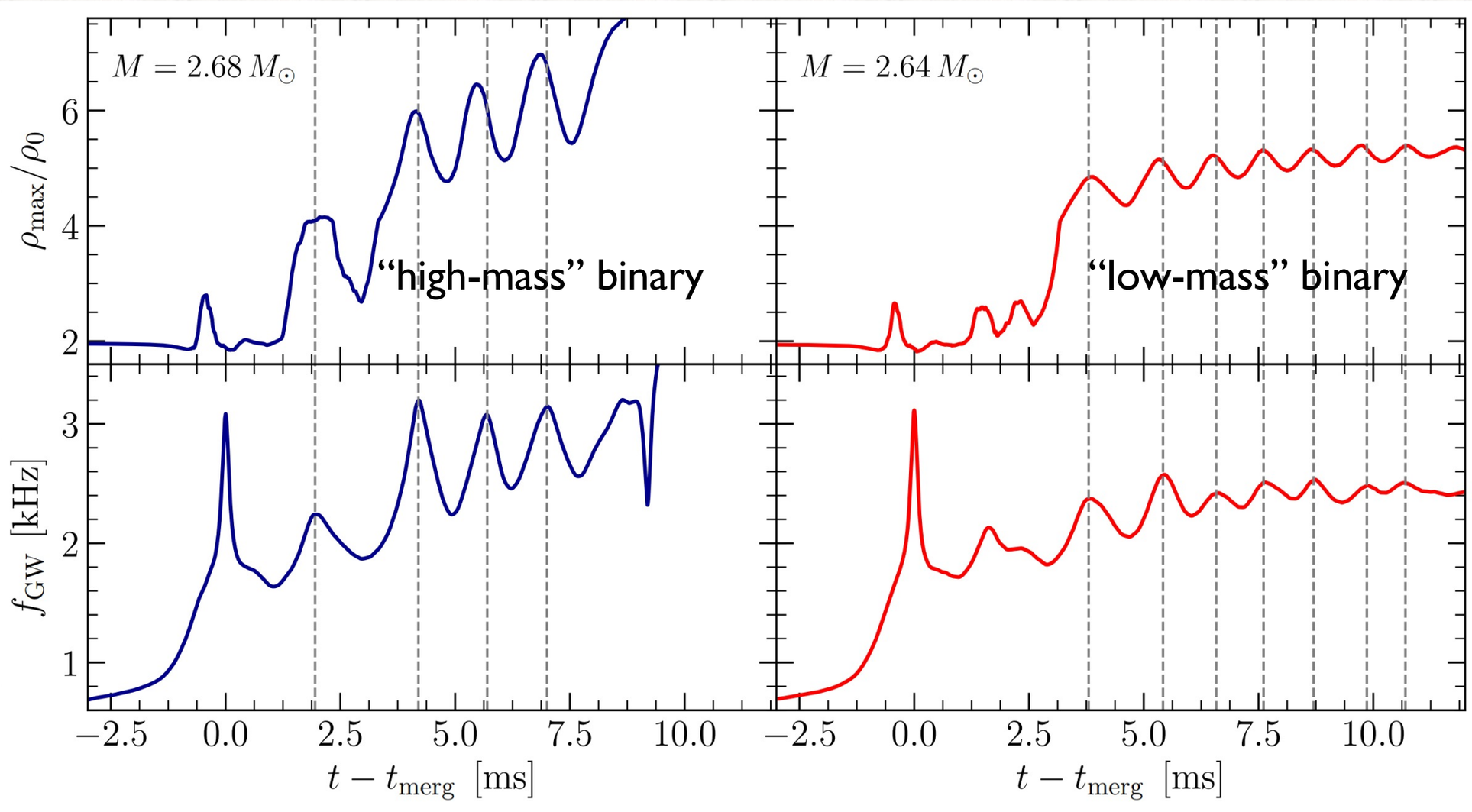

- Time dependence of instantaneous GW frequencies perfectly in phase with maximum density peaks

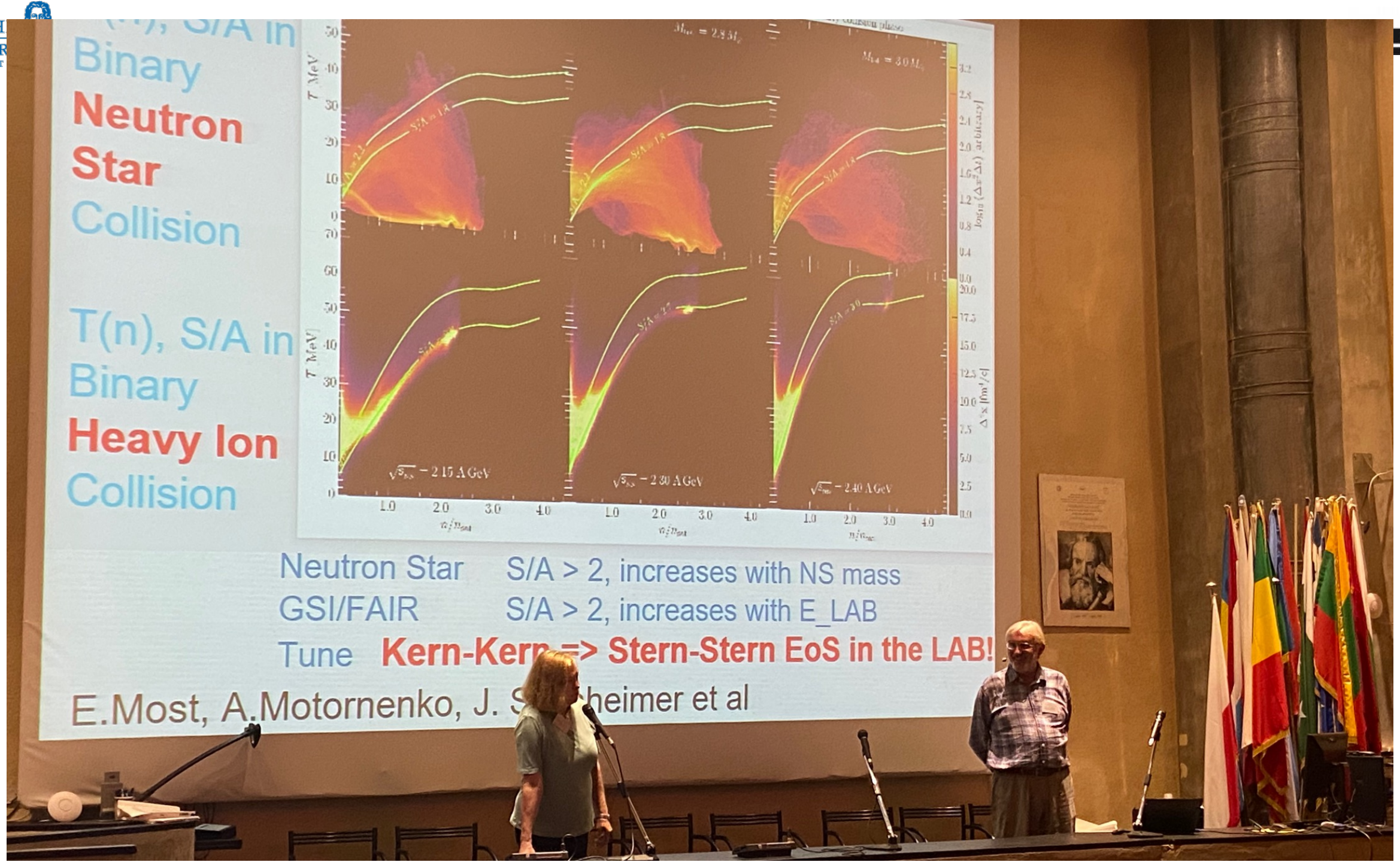
T(n), S/A in
Binary
Neutron
Star
Collision
T(n), S/A in
Binary
Heavy Ion
Collision
Neutron Star S/A > 2, increases with NS mass
GSI/FAIR S/A > 2, increases with E_LAB
Tune Kern-Kern => Stern-Stern EoS in the LAB!
E.Most, A.Motornenko, J. S heimer et al

Effects of quark deconfinement in compact stars and in heavy-ion collisions at NICA/FAIR energies

David Blaschke (Wroclaw, Poland)

New paradigm: hybrid stars larger and heavier

Work based on **Special Point location** with M. Cierniak, 2106.06986; Astron. N. 342 (2021)819

Dense quark plasma in color superconducting phase: nlNJL model

Constant-speed-of-sound (CSS) Equation of state (EoS)

$$p(\mu) = A(\mu/\mu_0)^{1+c_s^{-2}} - B$$

$$p = c_s^2\varepsilon - (1 + c_s^2)B$$

Perfect mapping
2SC nonlocal NJL → CSS ,
Antic et al., arxiv:2105.00029

Maxwell construction with
(1st order phase transition)
Relativistic Density Functional
EoS "DD2-Y-T" by S. Typel
With density-dependent coupling

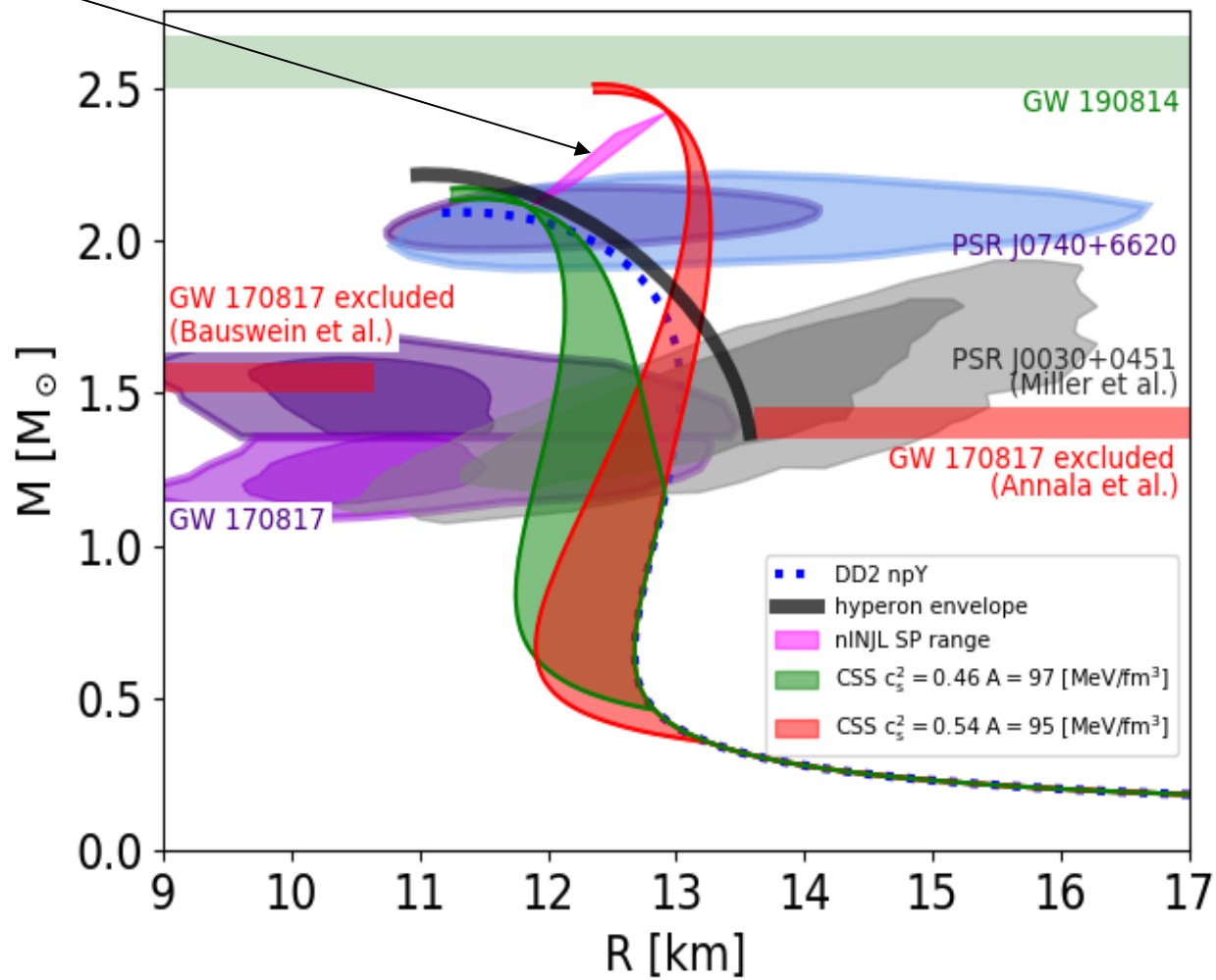

2.5 M_sun object can by a hybrid neutron star! With early onset of deconfinement!
NICER radius measurement on PSR J0740+6620 best described by hybrid stars!

Population of the QCD Phase Diagram

Binary NS merger,
1.35+1.35 M_sun

SN explosion,
Progenitor 50 M_sun

Ultrarelativistic HIC,
√s [GeV]=16, 10, 7, 4

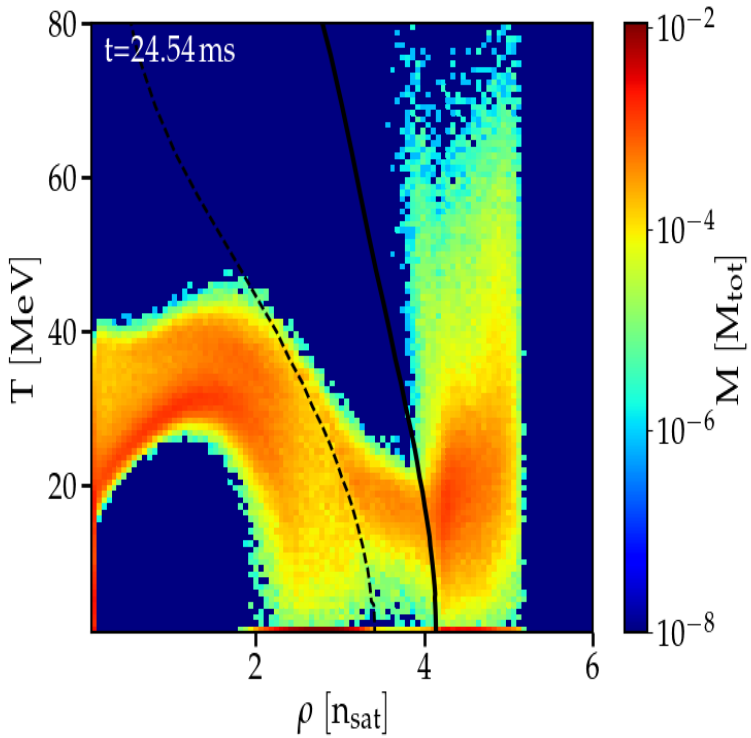

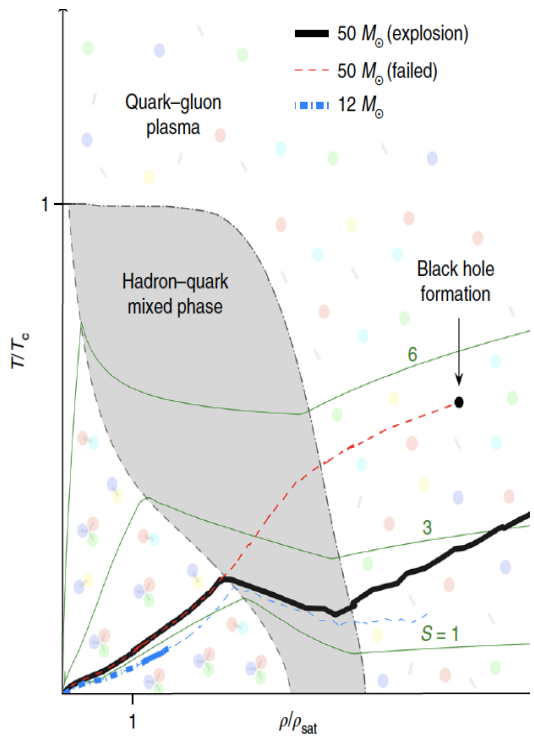

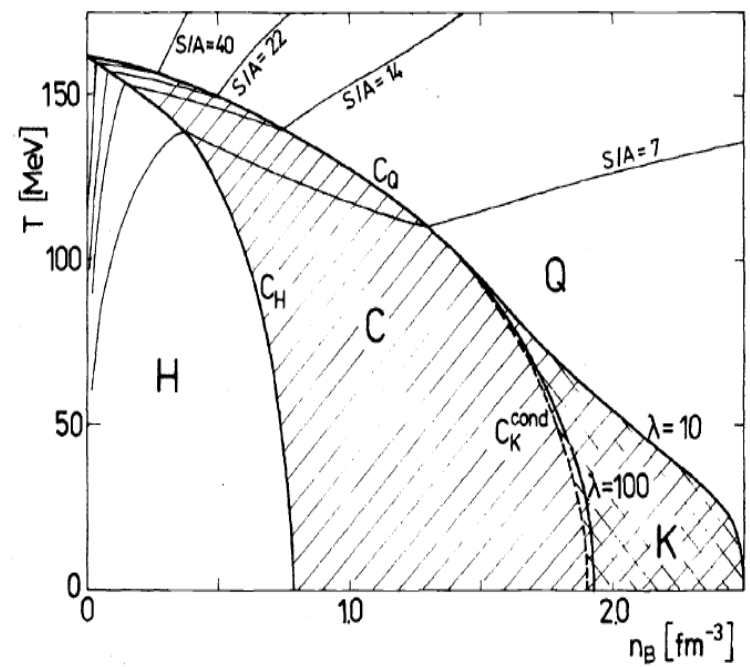

S. Blacker, A. Bauswein et al.,
PRD 102 (2020) 123023
arXiv:2006.03789

T. Fischer et al.,
Nat. Astron. 2 (2018) 980
arXiv:1712.08788

H.W. Barz, B. Friman et al.,
PRD 40 (1989) 157
GSI Preprint, GSI-89-13

The NICA Facility at JINR Dubna

NICA Facility running plan

- **Year 2021:**
  - Extensive commissioning of Booster accelerator
  - Heavy-ion (Fe/Kr/Xe) run of full Booster+Nuclotron setup
- **Year 2022:**
  - Completion of NICA Collider and transfer lines
- **Year 2023:**
  - Initial run of NICA with Bi+Bi @ 9.2 AGeV (other energies a second priority)
  - Goal to reach luminosity of 10^{25} $cm^{-2}s^{-1}$
- **Year 2024:**
  - Goal to have Au+Au collisions and acceleration in NICA (up to 11 AGeV)
- **Beyond 2024:**
  - Maximizing luminosity, possibility of collision energy and system size scan

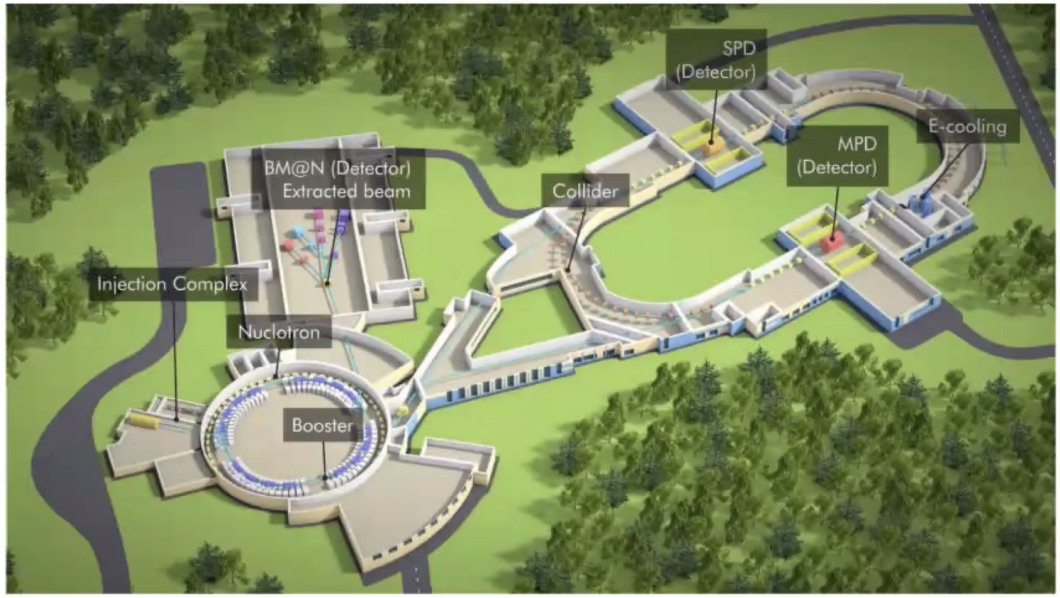

Probing Single and Double Beta Decay Nuclear Matrix Element in Heavy-Ion Reactions

Horst Lenske (Giessen, Germany)

MDCE and 0ν2β Double Beta-Decay

The Majorana Aspect

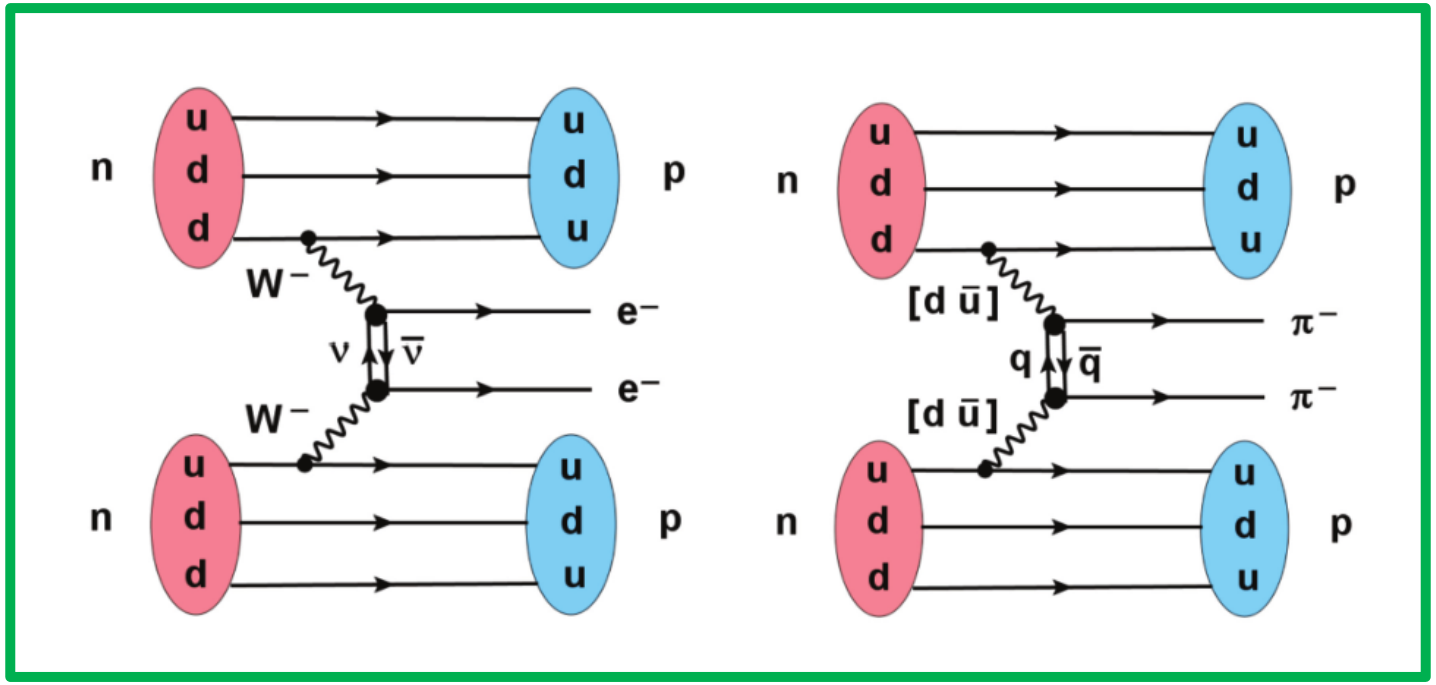

Ettore Majoran
*Aug., 5, 1906, at Catania
disappeared, Mar, 1938
+ 1959 in Venezuela?
+ in a Sicilian monastery?

- **Topological Correspondence on the Diagrammatic Level**
- **MDCE as a Surrogate Reaction for 0ν2β-NME**
- **DSCE as a Surrogate Reaction for 2ν2β-NME**

„BSM “-Physics and Neutrino-less Double-beta Decay: Dirac or Majorana Neutrinos?

GERDA, 2021: $T^{0\nu}_{1/2} > 10^{+26}$yr

$$\left[T^{0\nu}_{1/2}\right]^{-1} = G_{0\nu} g_A^4(0) \left|\frac{\langle m_\nu \rangle}{m_e}\right|^2 |M^{0\nu}(0_I^+ \to 0_F^+)|^2$$

Ejiri et al., Phys.Rept. 797 (2019) 1

$$\langle m_\nu \rangle = \left|\sum_k U_{ek}^2 m_k\right| = \left|\sum_k |U_{ek}|^2 m_k e^{i\alpha_k}\right|.$$

Pontecorvo–Maki–Nakagawa–Sakata (PMNS) Matrix

effective Majorana ν-Mass

$$M^{\mathrm{GT}}_{\beta\beta} = \sum_N G^{(i)}_{\beta\beta,N} \frac{\langle 0_F^+ || \tau^+ \vec{\sigma} || 1_N^+ \rangle \langle 1_N^+ || \tau^+ \vec{\sigma} || 0_I^+ \rangle}{\frac{1}{2}(Q_{\beta\beta} + 2m_e c^2) + E_N - E_I}$$

Nuclear Matrix Element
→ DCE Reactions as probes for nuclear models

H.L. et al., *Universe* 7 (2021) 4, 98

The Use of a Plasma Window as a Vacuum-Atmosphere Interface for Measurements of Stellar Neutron-Induced Reaction Cross Sections

Ophir Ruimi (Jerusalem, Israel)

Motivation

Characterization of neutron-induced reaction rates on unstable isotopes is essential for understanding the nucleosynthesis occurring in astrophysical events involving massive stars (s-processes - e.g., the s-process acting in the range from Ag to Sb):

$$n \rightarrow p + e^- + \bar{\nu}_e$$

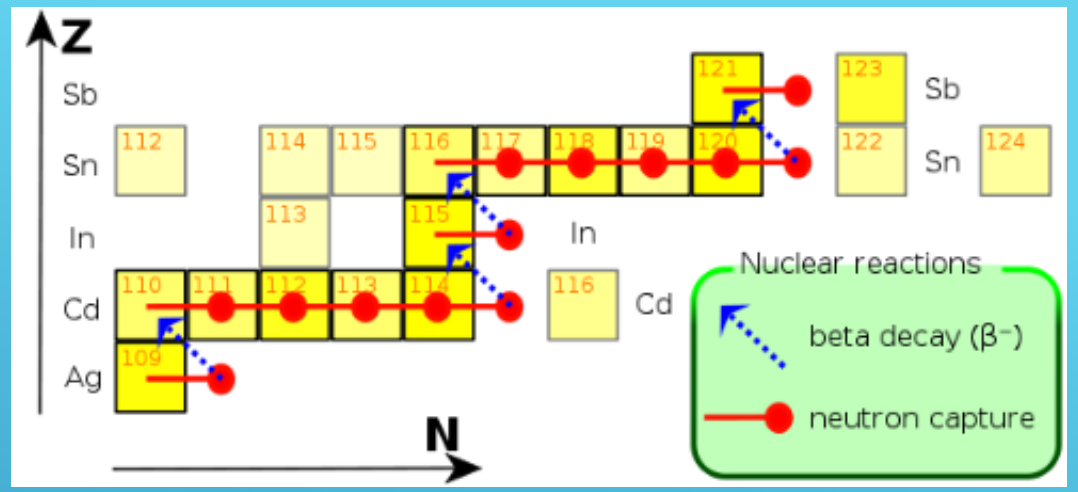

An enriched water ($H_2{}^{18}O$) target is under consideration at SARAF, for using the (p,n) reaction at an accelerated proton energy of 2.6 MeV in order to produce a 5 keV Quasi-Maxwellian neutron spectrum. So far, this reaction has been operated on solid targets, with corresponding low proton current and neutron flux. We aim to make use of the very high current available at SARAF-II to produce orders of magnitude more neutrons, and thus require a high-density target that is able to withstand high currents, which leads us to select a liquid based target. The only relevant liquid is $H_2{}^{18}O$.

$$MACS = \langle\sigma\rangle = \frac{\langle\sigma v\rangle}{v_T} = \frac{2}{\sqrt{\pi}} \frac{\int_0^\infty e^{-E/kT}\sigma(E)EdE}{\int_0^\infty e^{-E/kT}EdE}$$

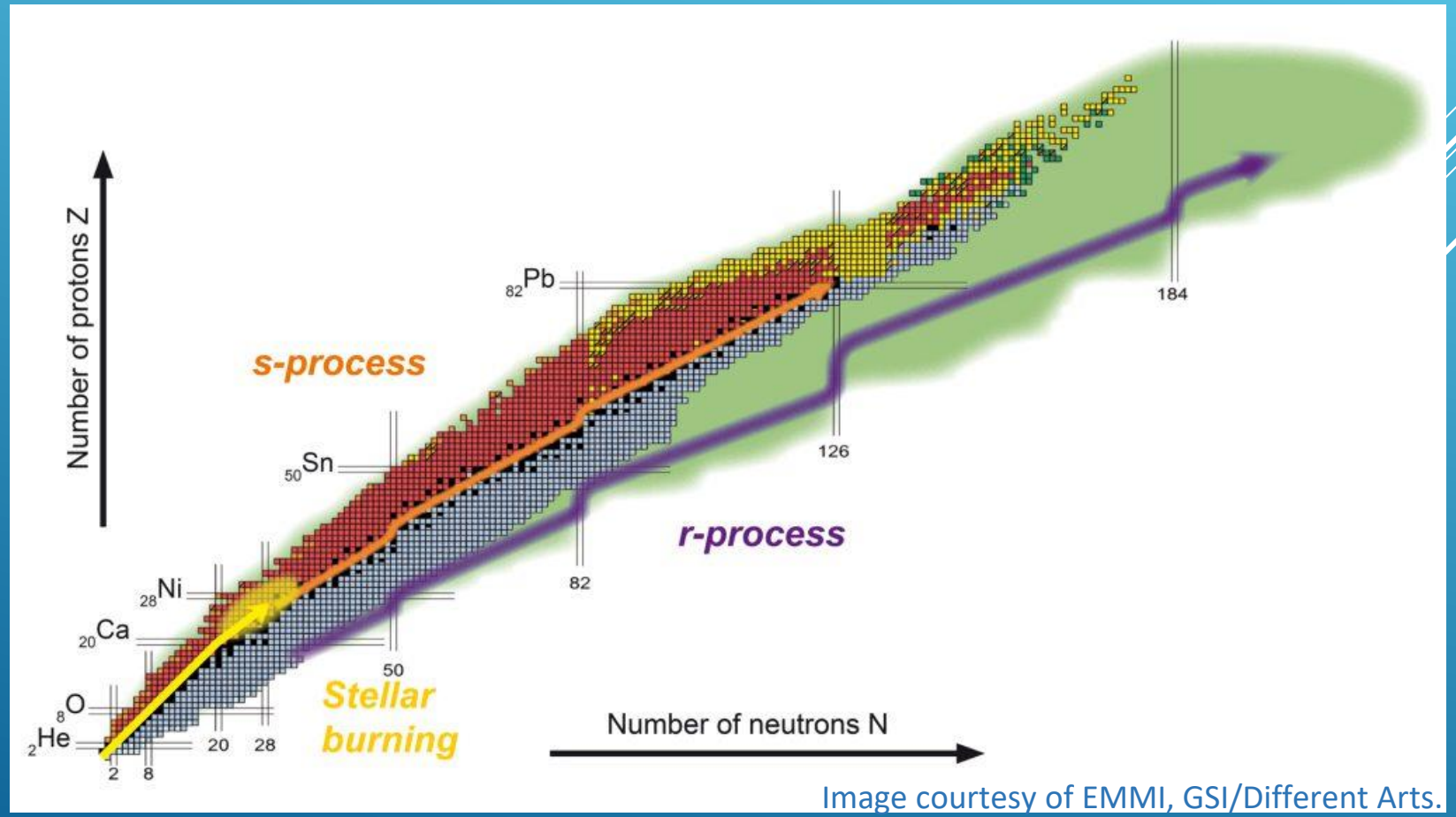

Image courtesy of EMMI, GSI/Different Arts.

Simulation of H energy and heat deposition in $H_2{}^{18}O$ target – preliminary results

Courtesy of Moshe Friedman (HUJI)

Energy loss and heat deposition probe of 2600-keV proton beam in $H_2{}^{18}O$. The volume power density plotted is the power deposited within one radial standard deviation.

Energy loss rate vs. initial beam energy

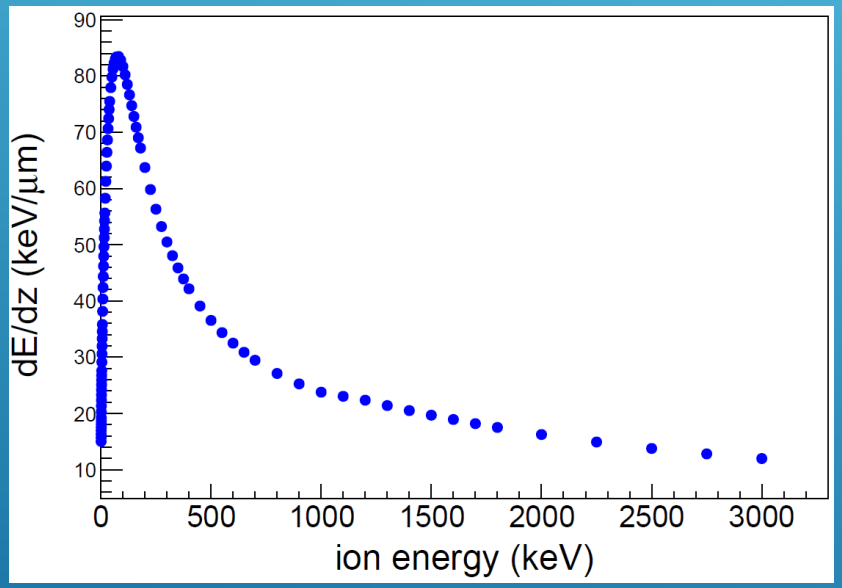

Energy loss vs. depth in the target

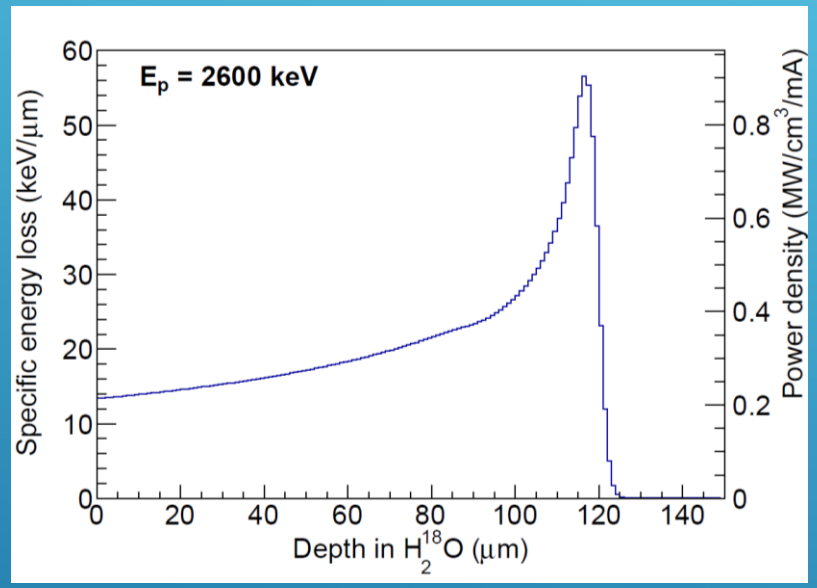

Heat deposition

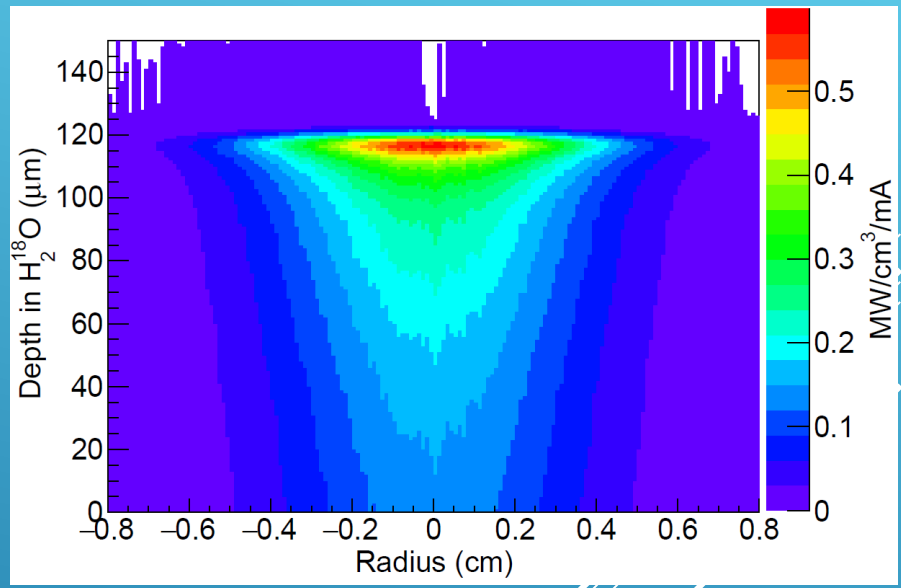

Conservation of the expensive $H_2{}^{18}O$ entails the use of a circulating target, containing a reservoir, a heat exchanger and a cooling loop, which controls the liquid's temperature and flow rate.

Required stream velocity on impact:

$$\frac{v}{i} \approx 38 \ \frac{\mathrm{m}}{\mathrm{s} \cdot \mathrm{mA}}$$

The high vapor pressure of $H_2{}^{18}O$ is incompatible with accelerator vacuum.
We opt to solve this by using a **Plasma Window.**

Plasma Window Terminology (cross section)

Cathode Housing

Insulating spacer: e.g. boron nitride (blue); FR4 [fire retardant form of G-10 (green); between them Viton O-ring)]

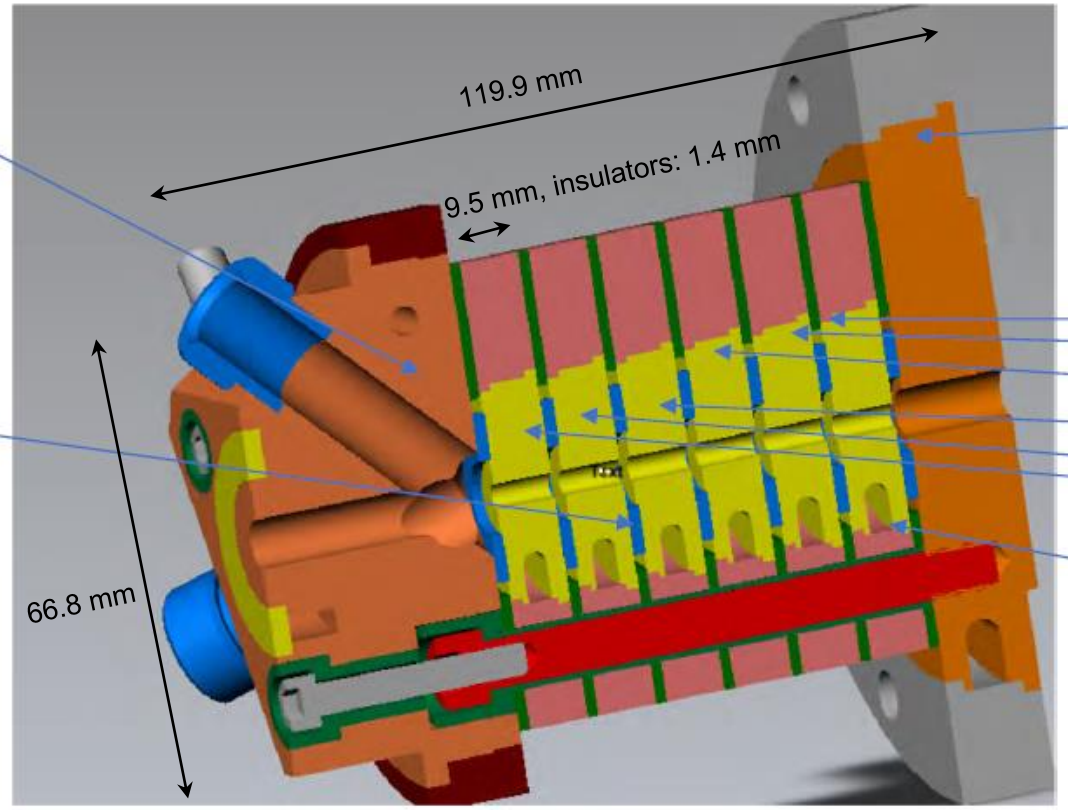

Central aperture: 5 mm

Anode

Cooling Plates
(OFHC Cu)

Cooling channel (only one shown)

QCD phase diagram and the equation of state from the lattice

Frithjof Karsch (Bielefeld, Germany)

Chiral PHASE TRANSITION temperature

(2+1)-flavor QCD

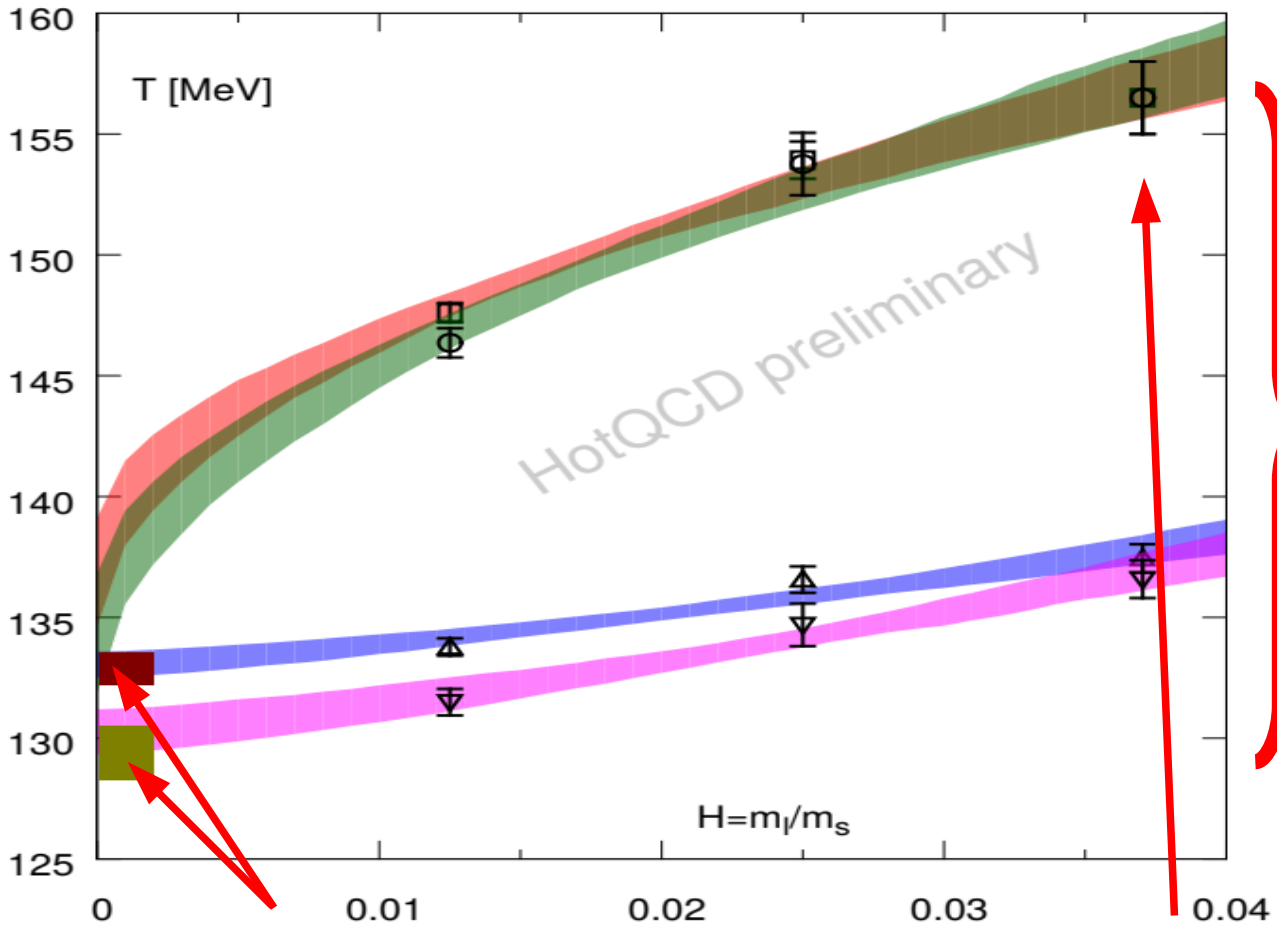

$$\Delta T \simeq 25 \text{ MeV}$$

A. Lahiri et al, arXiv:2010:15593

chiral limit extrapolations

physical masses

$$T_c^0 = 132^{+3}_{-6} \text{ MeV}$$

H.-T. Ding et al [HotQCD], arXiv:1903.04801

$$T_{pc}^{phys} = (156.5 \pm 1.5) \text{ MeV}$$

A. Bazavov et al [HotQCD], arXiv:1812.08235

Energy-like observables in the chiral limit

– **Polyakov loop is blind to chiral rotations ➡ energy like observable**

D.A. Clarke et al, arXiv:2008.11678

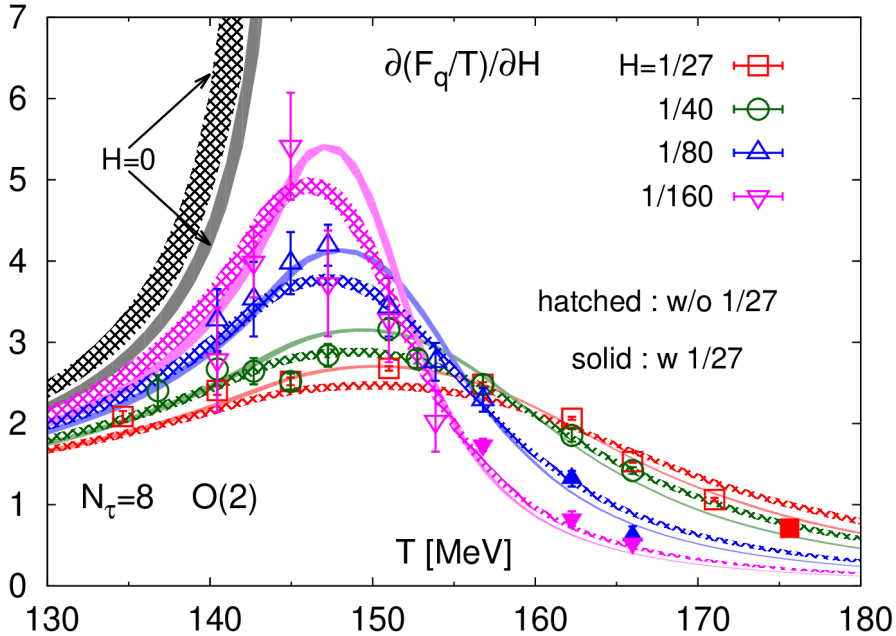

– H-derivative is a mixed susceptibility

$$\frac{\partial F_q(T,H)/T}{\partial H} = -\frac{1}{\langle P\rangle}\frac{\partial\langle P\rangle}{\partial H} \sim -AH^{(\beta-1)/\beta\delta} f'_G(z) + reg$$

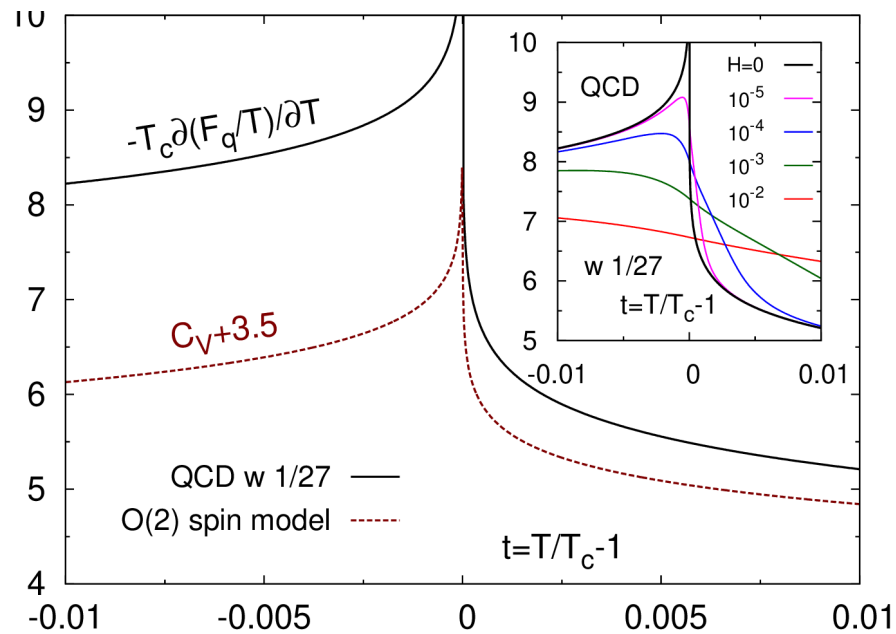

– T-derivative behaves like specific heat in O(N) spin models

$$T_c\frac{\partial F_q(T,H)/T}{\partial T} \sim -AH^{(-\alpha)/\beta\delta} f''_f(z) + reg$$

Specific heat in the 3d, O(2) spin model,
A. Cucchieri et al, J. Phys A 35 (2002) 6517

Conclusions

- close to the chiral limit thermodynamics in the vicinity of the QCD transition(s) is controlled by a universal scaling function

singular regular

$$\frac{p}{T^4} = \frac{1}{VT^3} \ln Z(V,T,\vec{\mu}) = -h^{(2-\alpha)/\beta\delta} f_f(t/h^{1/\beta\delta}) - f_r(V,T,\vec{\mu})$$

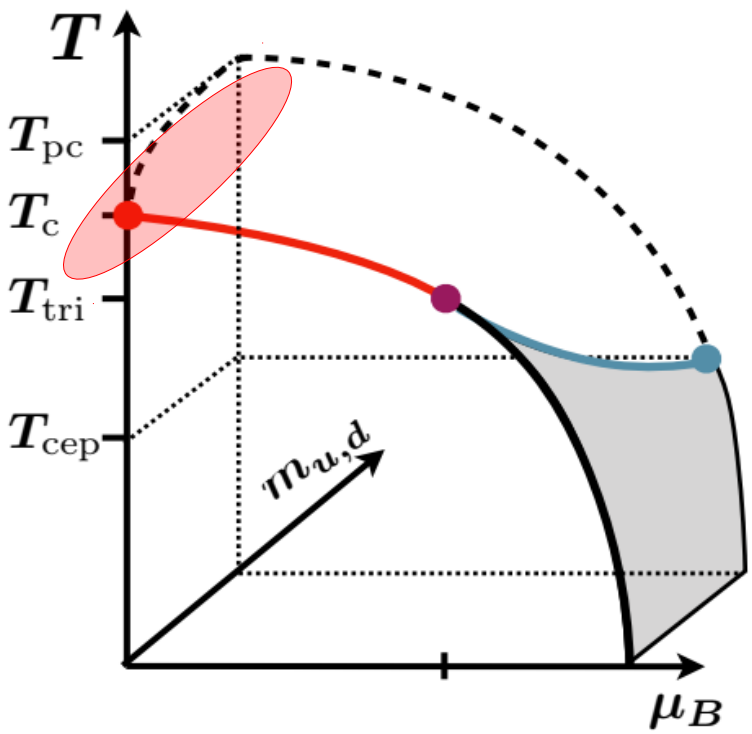

What we learned so far about the CEP in QCD from lattice QCD calculations:

I) the critical temperature is below Tc=132 MeV

II) curvature of the chiral critical line suggests an even lower bound

III) the corresponding critical chemical potential is likely to be above 400 MeV

→ Taylor expansions need to be resummed in order to reach CEP

QCD in the heavy dense regime

Owe Philipsen (Frankfurt am Main, Germany)

Deconfinement transition at finite density

[Fromm, Langelage, Lottini, O.P. JHEP (2012)]

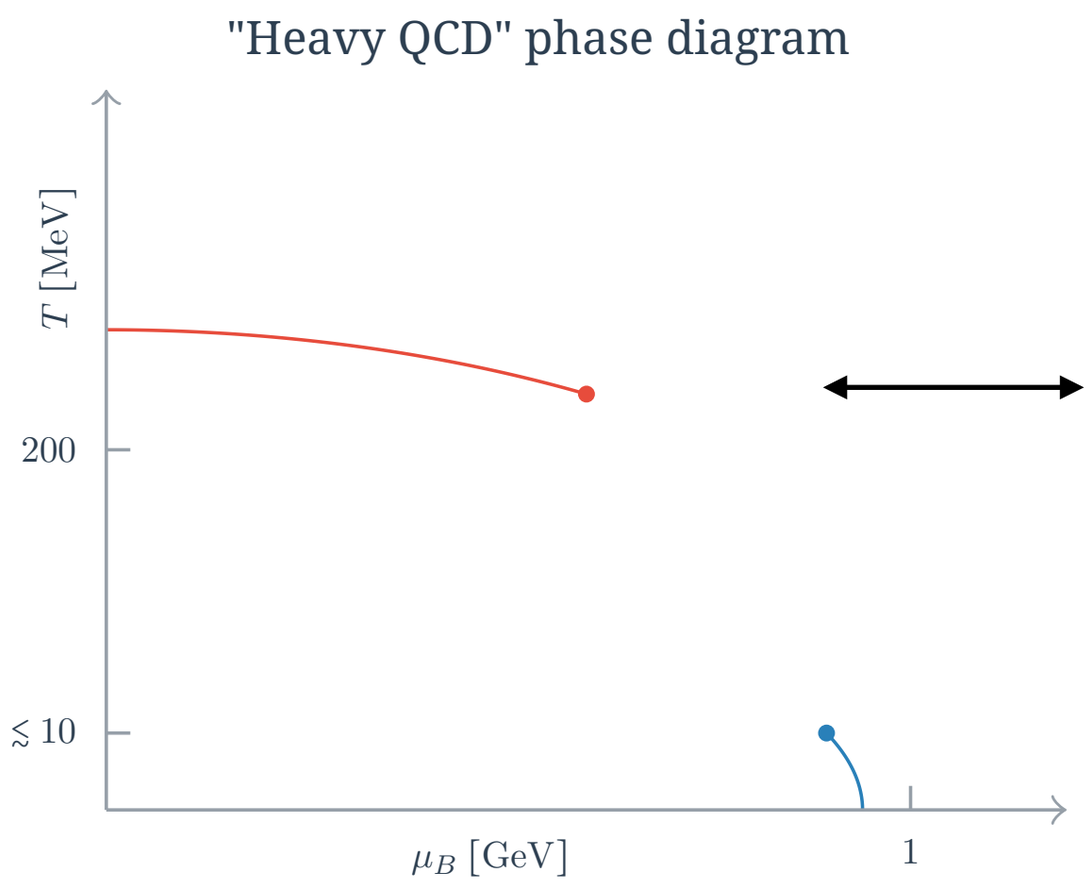

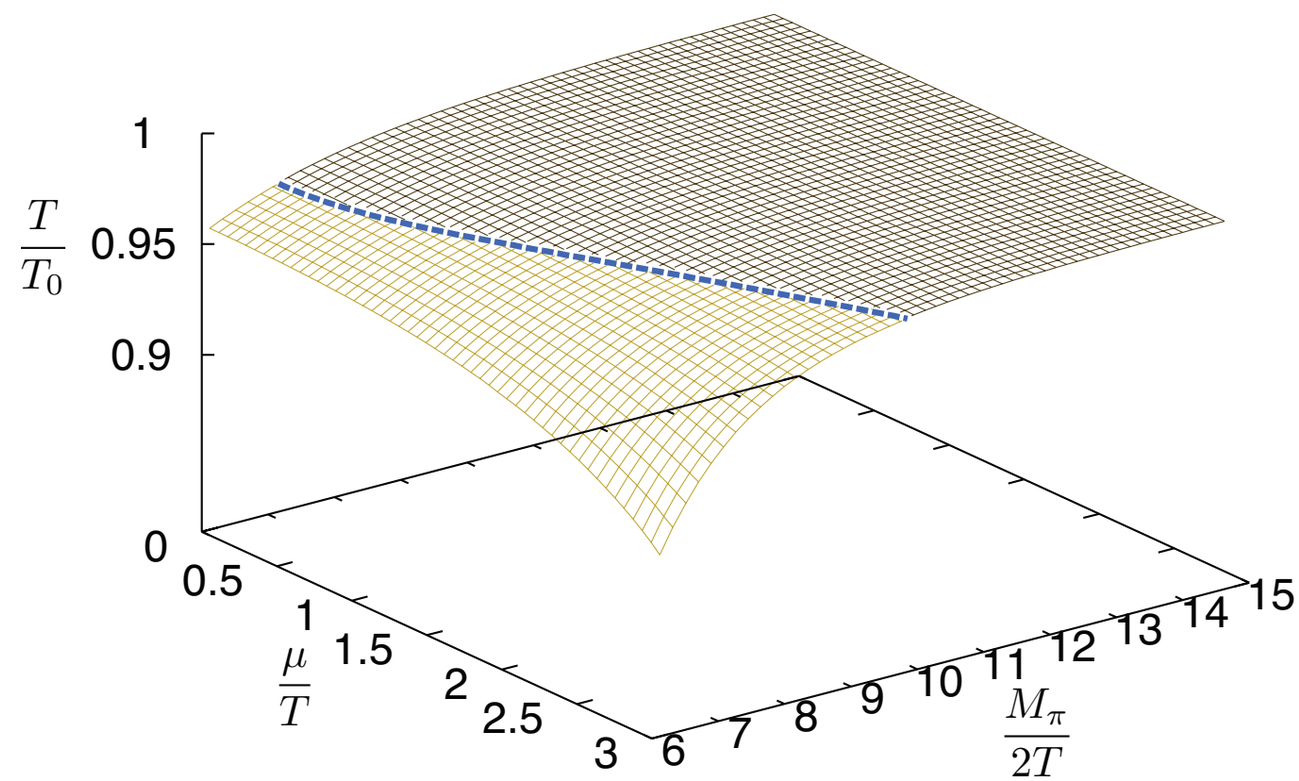

Same phase structure: continuum effective Polyakov loop theories, benchmarking possible!

[Fischer, Lücker, Pawlowski PRD (2015); Lo, Friman, Redlich PRD (2014)]

Light quarks: 1st order onset transition + endpoint

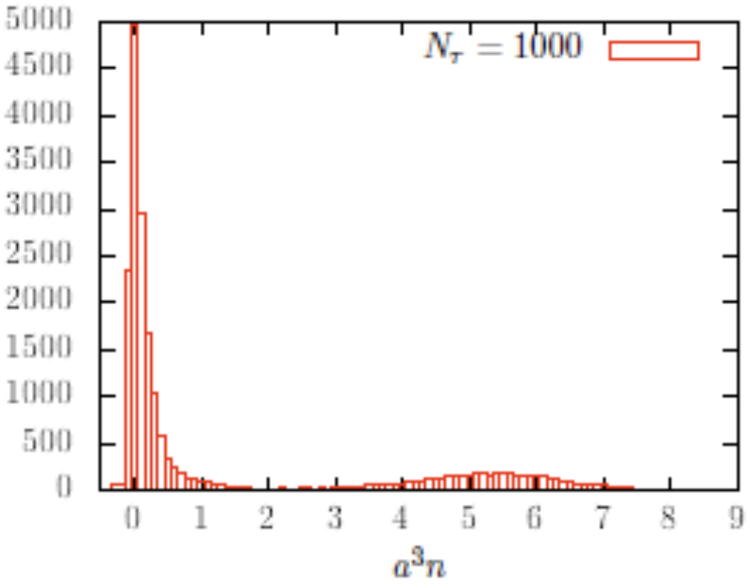

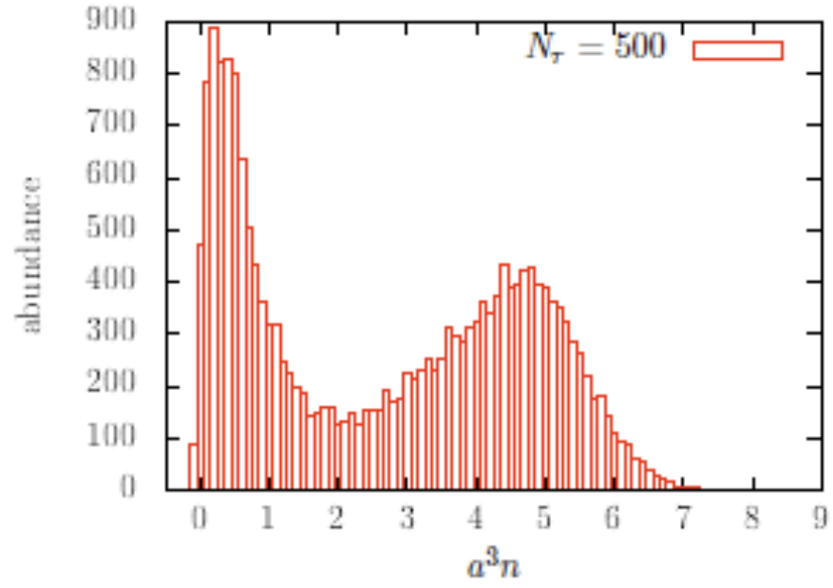

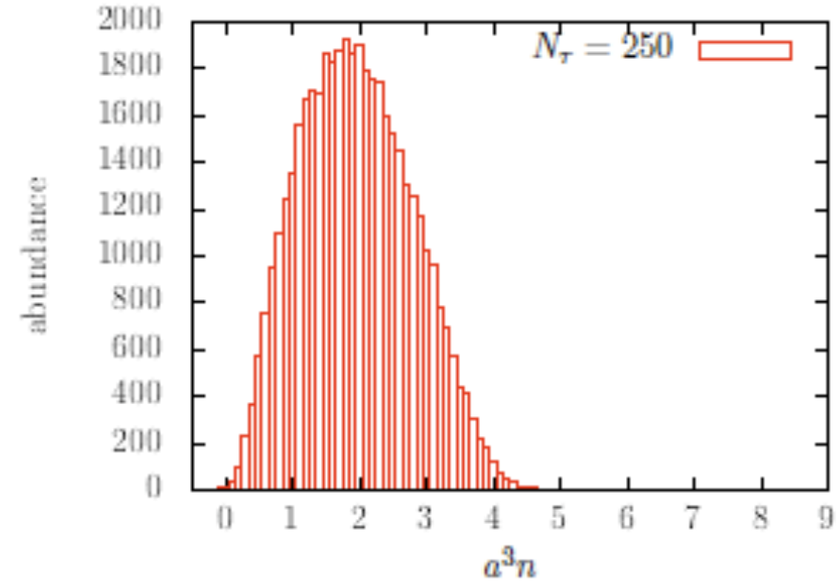

$\kappa = 0.12$

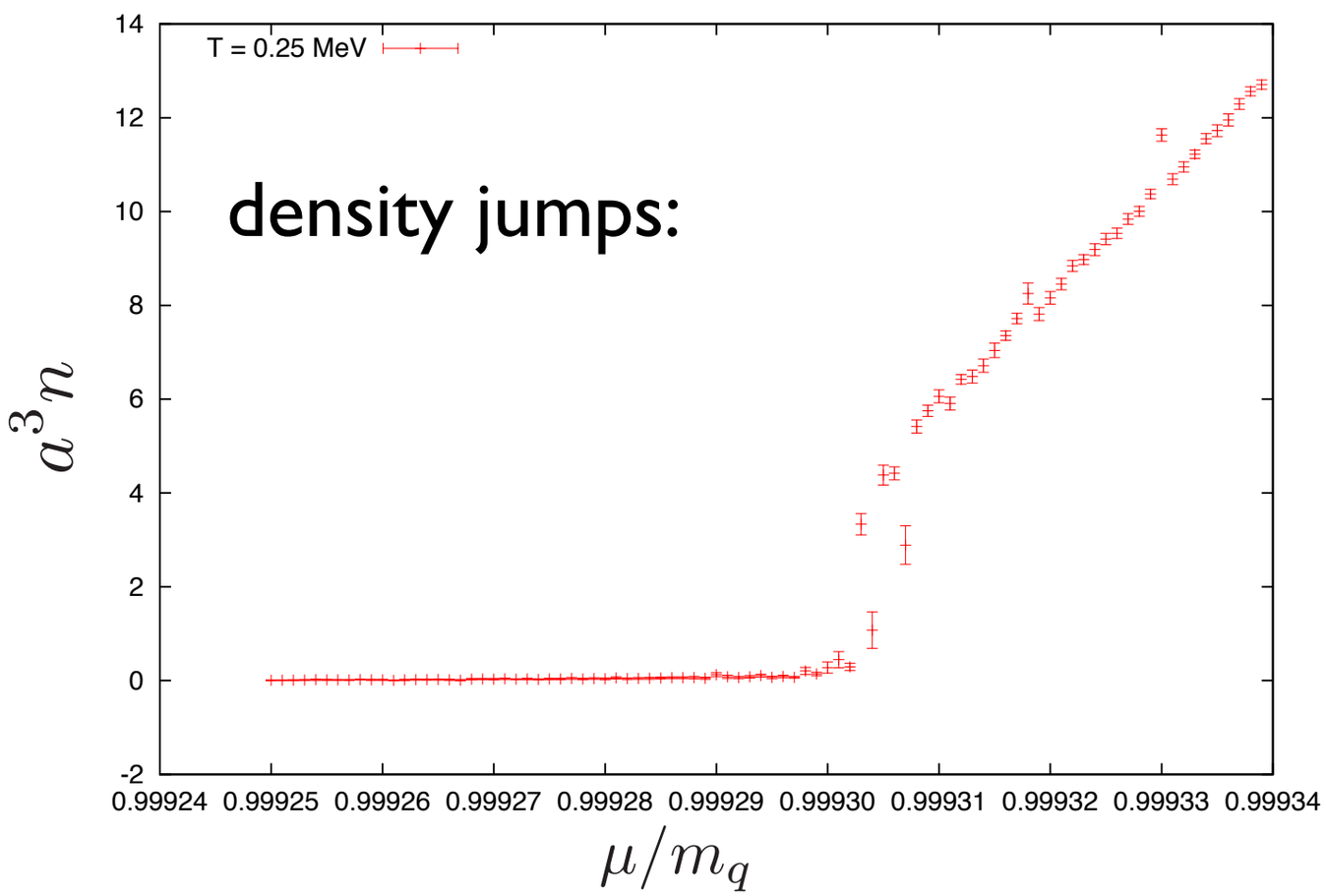

- phase coexistence: first order
- for higher $T = \frac{1}{aN_\tau}$ crossover
- nuclear liquid gas transition!

Phase diagram with increasing Nc

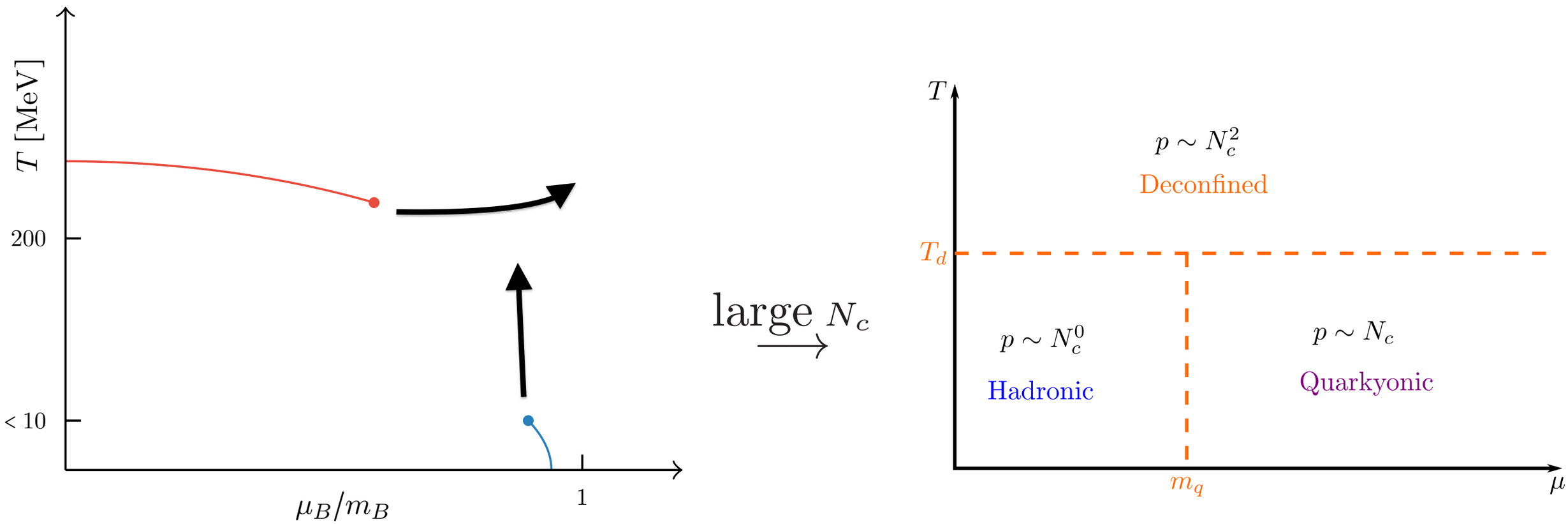

- Conjectured large N_c phase diagram emerges smoothly in heavy QCD
- Dense QCD is consistent with quarkyonic matter (=baryon matter for nucl. densities)
- No phase transition to quarkyonic matter besides nuclear liquid gas
- Should also hold for light quarks!

Including dynamical quarks

- Z(3) symmetry explicitly broken by $\frac{1}{m_q}$

  $\langle L \rangle \neq 0$ always!

- Deconfinement transition weakens, disappears at $\frac{1}{m_q^c} \Leftrightarrow m_\pi^c$

- Lattice determination in progress: $m_\pi^c \approx 4$ GeV
  [WHOT, Frankfurt]

- Dyson-Schwinger study $m_q^c \approx 460$ MeV
  [Fischer, Luecker, Pawlowski]

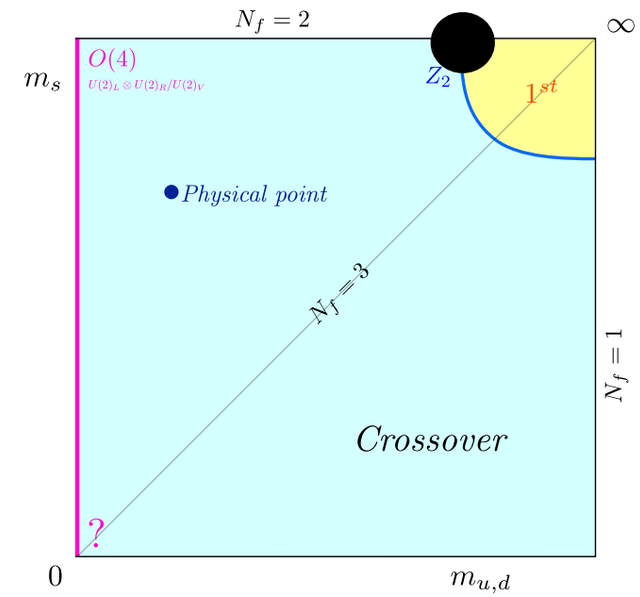

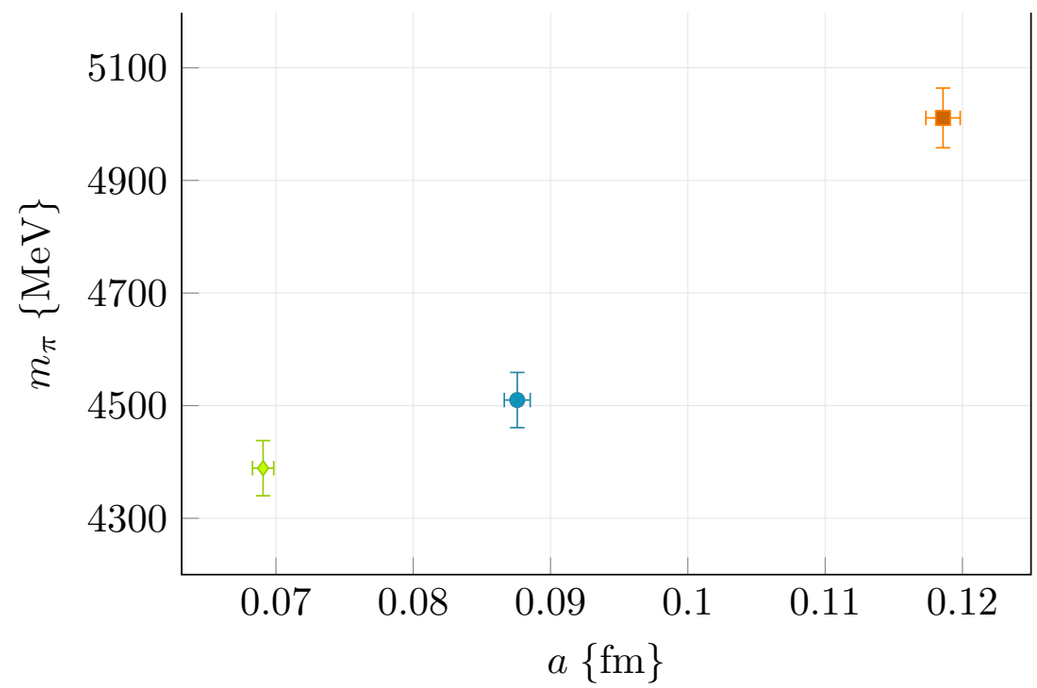

Cuteri, O.P., Schön, Sciarra, PRD 21

Binding energy per baryon, strong coupling limit

$$\epsilon \equiv \frac{e - n_B m_B}{n_B m_B} \overset{LO}{=} -\frac{4}{3}\frac{1}{a^3 n_B}\left(\frac{z_3}{z_0}\right)^2 \kappa^2$$

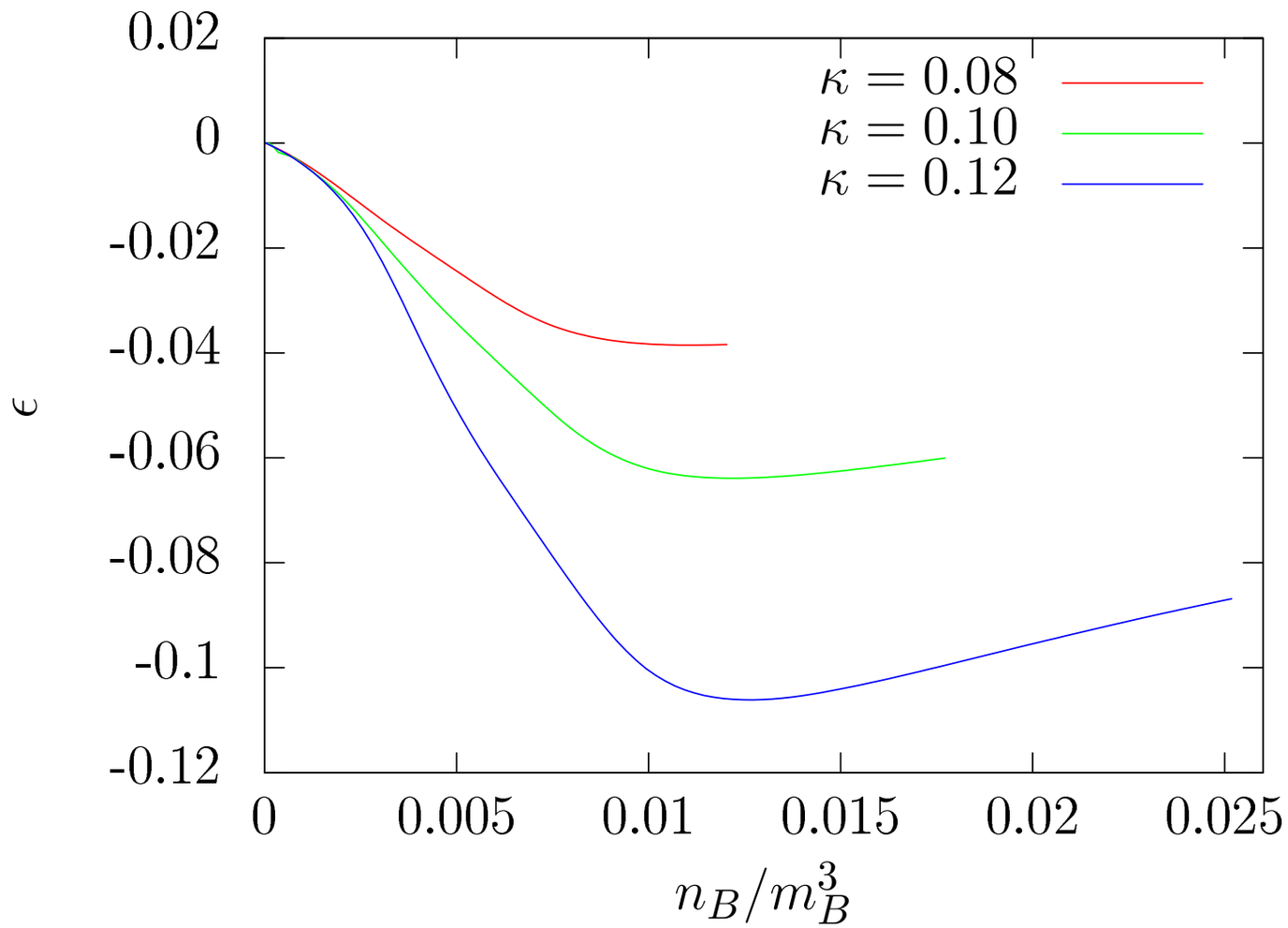

Charge Fluctuations and QCD phase boundary

Krzysztof Redlich (Wroclaw, Poland)

Direct comparison of Heavy ion data at LHC with LQCD

P. Braun- Munzinger et all.

χ_{NM} with $N,M=\{B,Q,S\}$ are expressed by particle yields: for Skellam distribution

- Is there a common temperature where all 2nd order cumulants constructed from ALICE data agree with LQCD result?

LQCD From ALICE DATA

$$\frac{\chi_B}{T^2}=\frac{1}{VT^3}(203.7\pm11.4)$$

$$\frac{\chi_S}{T^2}=\frac{1}{VT^3}(504.2\pm16.8)$$

$$\frac{\chi_{QS}}{T^2}=\frac{1}{VT^3}(191.1\pm12)$$

- The Volume at $T\approx154\ MeV$

$$V_{T_f}=3800\pm500\ fm^3$$

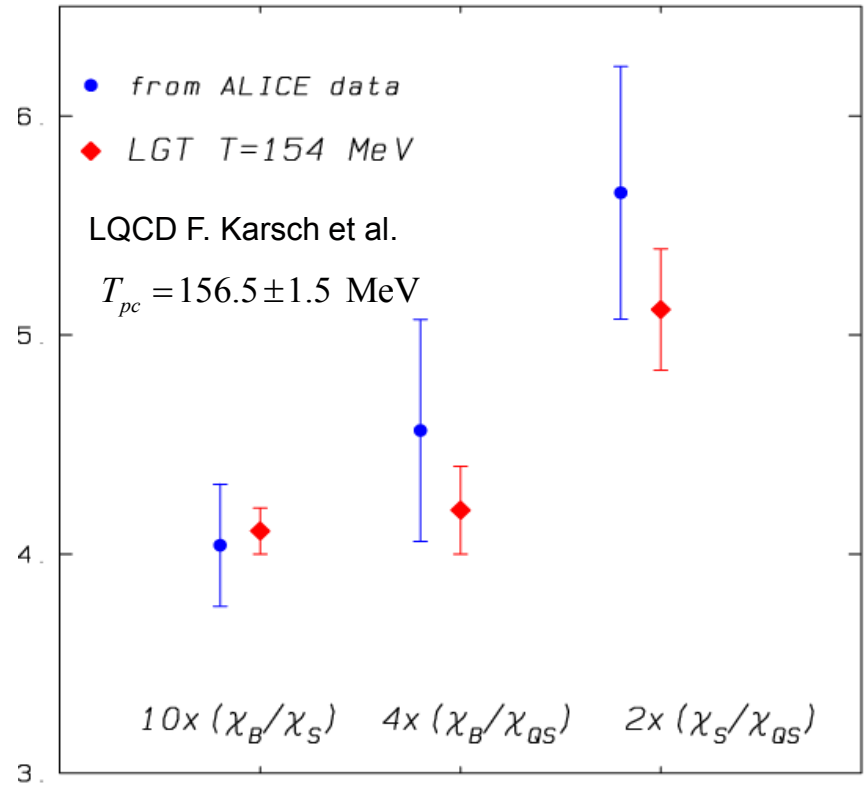

The 2nd cumulant ratios extracted from ALICE data are consistent with LQCD results at

$$T_f=154\pm6\ \text{MeV}$$

Evidence for thermalization and saturation of the 2nd order fluctuations near the QCD phase boundary

Probing non-strange baryon sector in πN - system importance of S-matrix also to explain proton yields

Pok Man Lo, B. Friman, C. Sasaki & K.R. , Phys.Lett. B778 (2018)

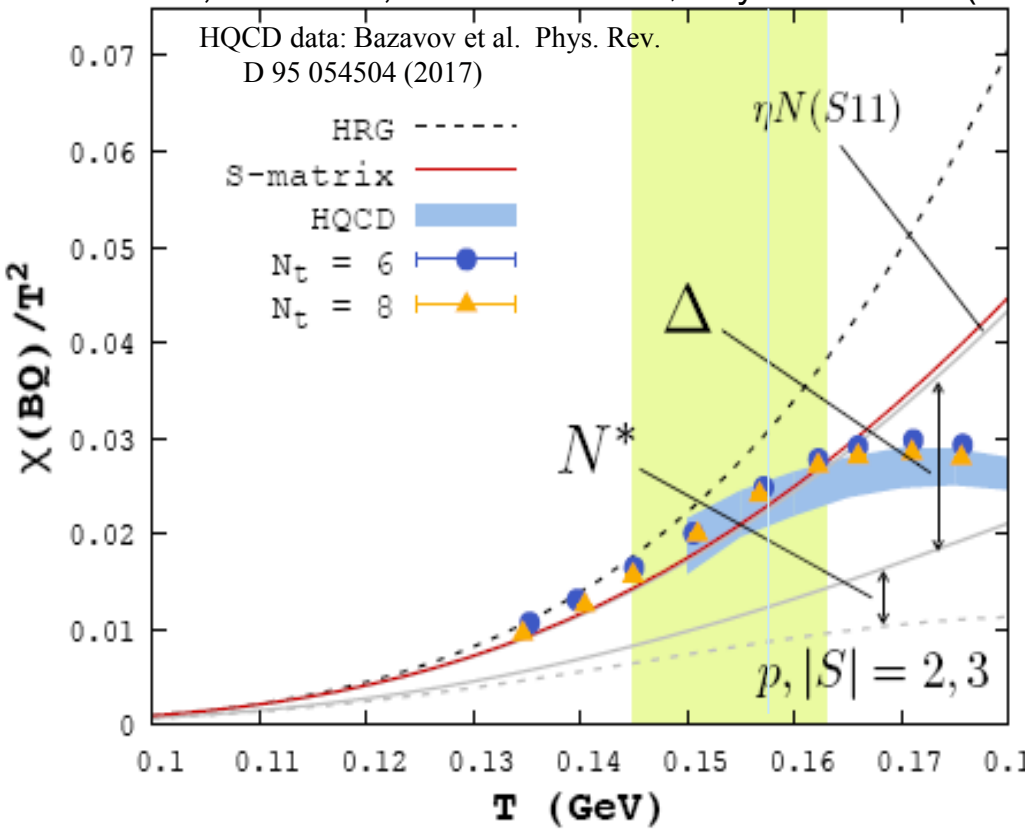

$$\chi_{BQ} = (\chi_{BB} - |\chi_{BS}|)/2$$

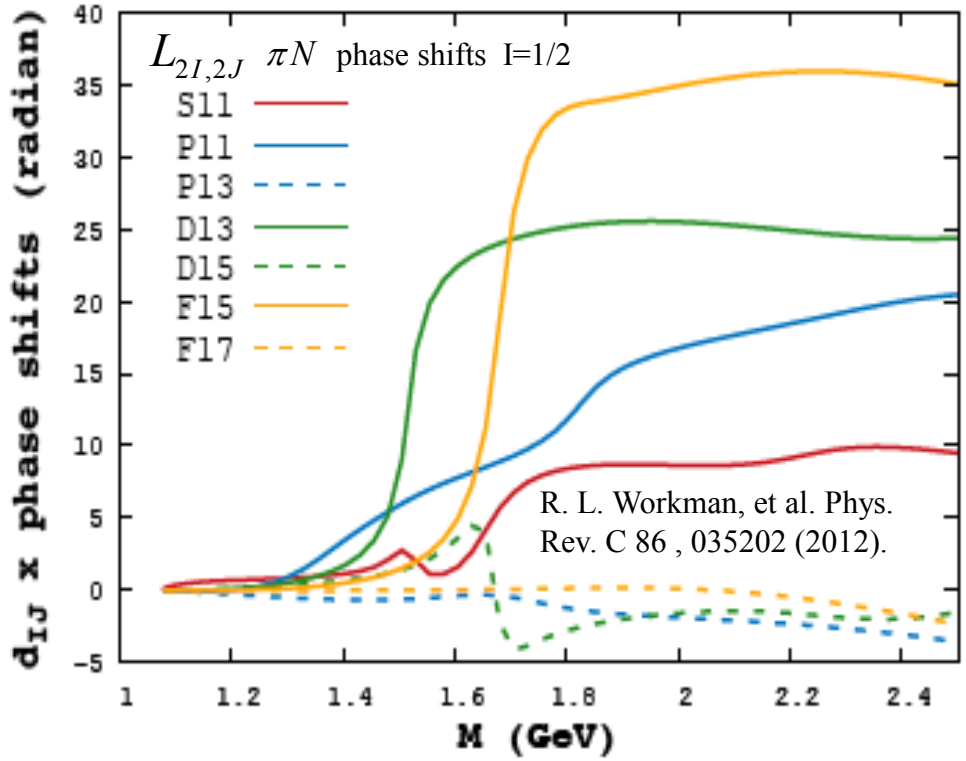

$$\Delta\chi_{BQ} \approx \sum_{I_z,j,B} d_j BQ \int dM \int d^3p \frac{1}{T} \frac{d\delta_j^I}{dM} \times e^{-\beta\sqrt{p^2+M^2}} (1+e^{-\beta\sqrt{p^2+M^2}})^{-2}$$

- Considering contributions of all πN $\delta_j^{I=(1/2),\ (3/2)}$ (N^*, Δ^* resonances) to χ_{BQ} within S-matrix approach, reduces the HRG predictions towards the LQCD in the chiral crossover $0.15 < T < 0.16\ GeV$

Strangeness canonical suppression with yields of charged particles explained with an exact strangeness conservation

- Strangeness conservation must be exact

J. Cleymans, Pok Man Lo, N. Sharma & K.R.
Phys. Rev. C103 014904 (2021)

$$Z^{GC}(\mu) = Tr[e^{-\beta(H-\mu S)}] \Rightarrow Z_S^C = Tr[e^{-\beta H}\delta_S]$$

$$Z^{GC}(\lambda) = \sum_{S=-\infty}^{\infty} \lambda^S Z_S^C \quad \Rightarrow Z_S^C \simeq \int_{-\pi}^{\pi} d\varphi e^{i\phi S} e^{\ln(Z^{GC}(\mu \to i\varphi))}$$

$$\ln Z^{GC}(\mu, T, V) = \sum_{s=-3}^{3} z_s e^{s\mu/T}$$

Interactions in z_s included: S-matrix

- This implies strangeness suppression effect

$$< N_s >_A^C \approx V_A n^{GC} \bullet \frac{I_s(2V_C n_{s=1}^{th}(T))}{I_0(2V_C n_{s=1}^{th}(T))}$$

where volume parameters $V_{A(C)} \sim dN_{ch}/d\eta$

V_C - full phase-space volume where S is exactly conserved

V_A - effective fireball volume in the acceptance

The suppression factor $I_S(x)/I_0(x) \le 1$, decreases with decreasing x, and increasing strange s-quantum number of hadron.

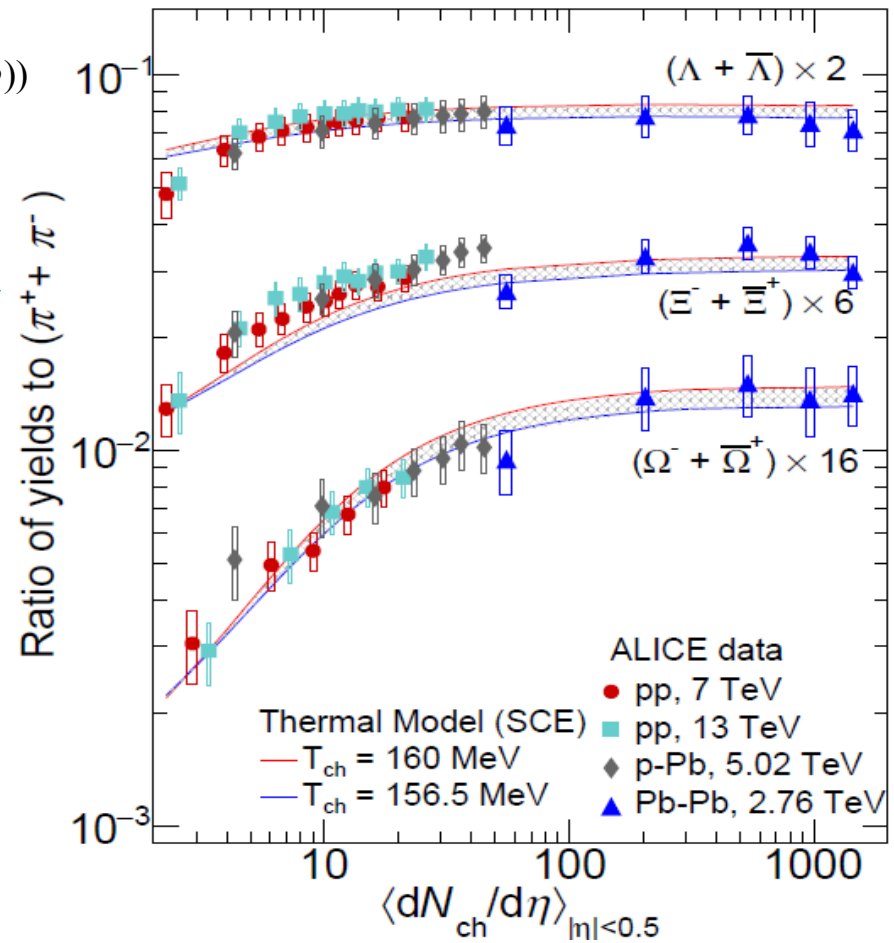

Ratios of cumulants: STAR data versus model: importance of exact baryon conservation law

P. Braun-Munzinger, B. Friman, A. Rustamov, J. Stachel & K.R. Nucl. Phys. A 1008 (2021)

Stars: STAR data

Adam *et al.* arXiv 2001.02852v2

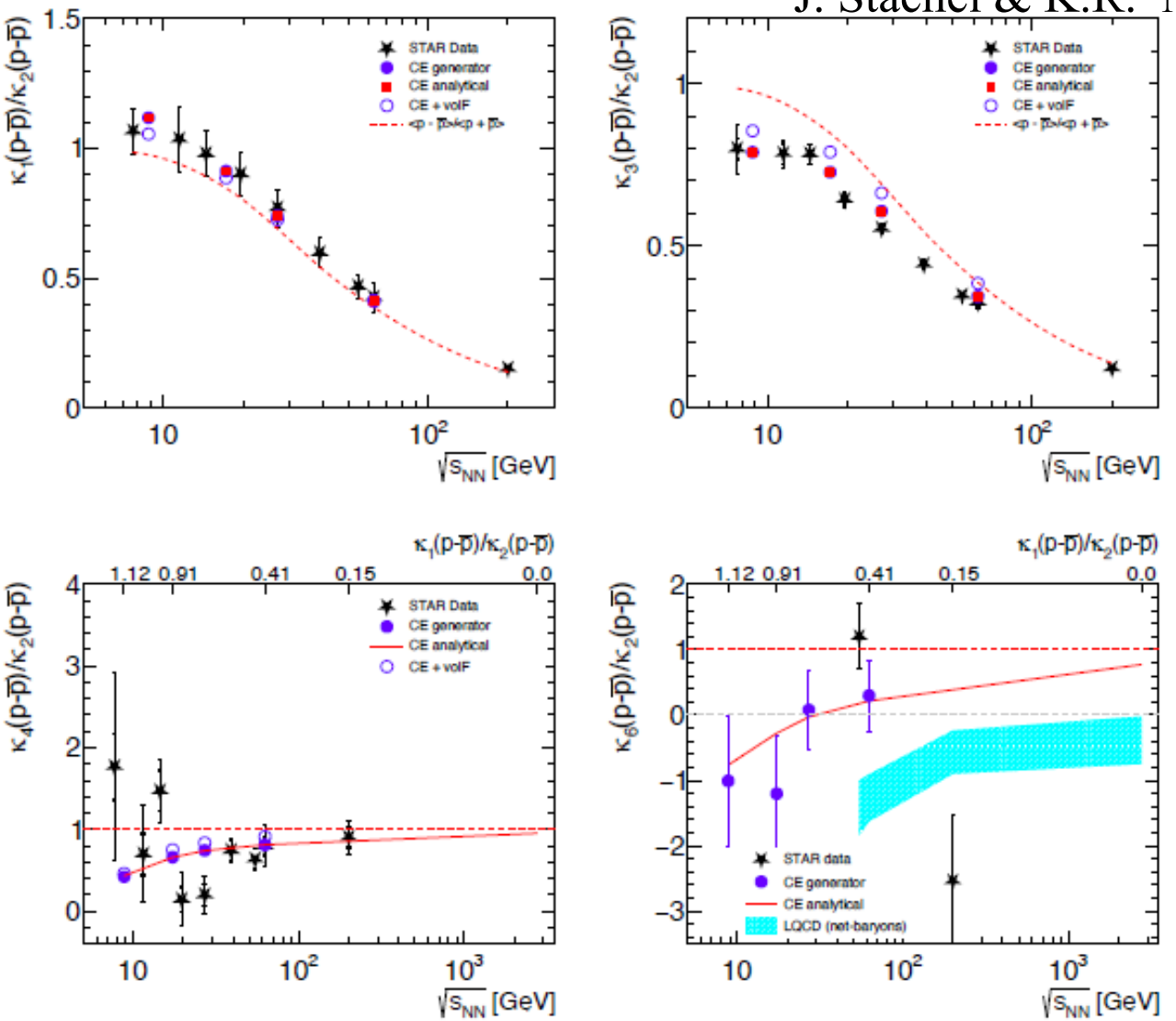

- Cumulants up to n<4 order follow the SATR data if exact baryon number conservation is accounted for
- Kurtosis data exhibit interesting deviations, however *not necessarily* of statistical significant

Symmetries and physics in QCD above T_c

Leonid Glozman (Graz, Austria)

Chiral spin symmetry

The electric interaction is defined via color charge (Lorentz-invariant)

$$Q^a = \int d^3x \Psi^\dagger(x) \frac{t^a}{2} \Psi(x).$$

It has both $U(1)_A$ and $SU(N_F)_L \times SU(N_F)_R$ symmetries.
On top of it it has a $SU(2)_{CS}$ chiral spin symmetry:

$$\Psi \to \Psi' = \exp\left(i \frac{\varepsilon^n \Sigma^n}{2}\right) \Psi$$

$$\Sigma = \{\gamma_k, -i\gamma_5\gamma_k, \gamma_5\}.$$

$SU(2)_{CS} \times SU(N_F) \subset SU(2N_F)$

$SU(2N_F)$ is also a symmetry of the color charge.

$U(1)_A \times SU(N_F)_L \times SU(N_F)_r \subset SU(2N_F)$

The color charge (and electric interaction) have a larger symmetry than symmetry of the QCD Lagrangian as the whole.

L.Ya.G., EPJA 51 (2015) 27; L.Ya.G., M. Pak,PRD, 92 (2015) 016001

Symmetries of spatial correlators above T_{pc}

C. Rohrhofer, Y. Aoki, G. Cossu, H. Fukaya, C. Gattringer, L.Ya.G., S. Hashimoto, C.B. Lang, S. Prelovsek, PRD 96 (2017) 09450; PRD 100 (2019) 014502.
$N_f = 2$ QCD with the chirally symmetric Domain Wall Dirac operator (JLQCD ensembles).

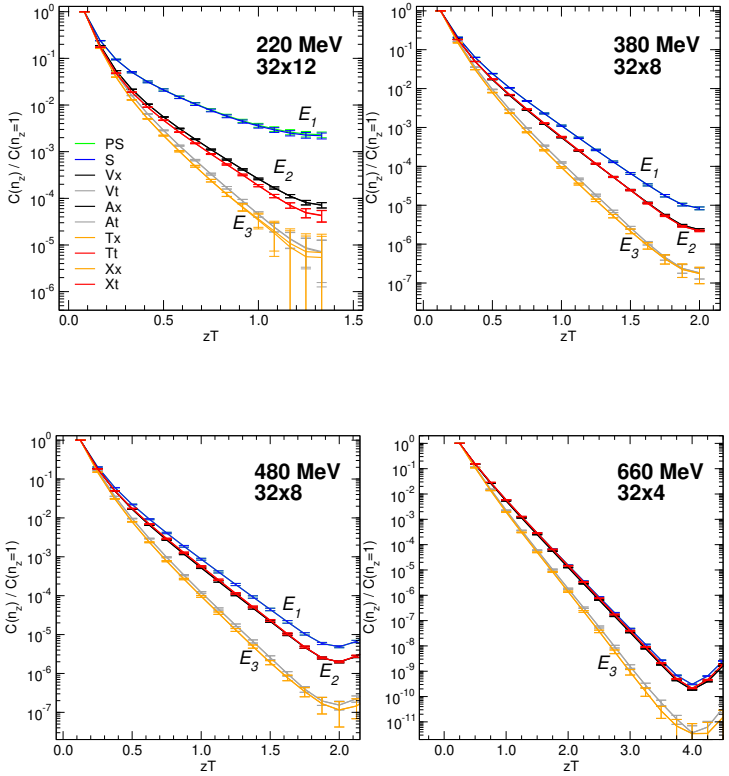

$E1$ - $U(1)_A$ symmetry; $E2$ & $E3$ - $SU(2)_{CS}$ and $SU(4)$ symmetries.
$SU(2)_{CS}$ and $SU(4)$ symmetries persist up to $T \sim 500$ MeV.

Temporal correlators above T_{pc}

C. Rohrhofer, Y. Aoki, L.Ya.G., S. Hashimoto, PLB 802(2020) 135245

$N_F = 2$ Domain wall Dirac operator at physical quark masses, 12×48^3 lattice at $T = 220$ MeV (JLQCD ensembles)

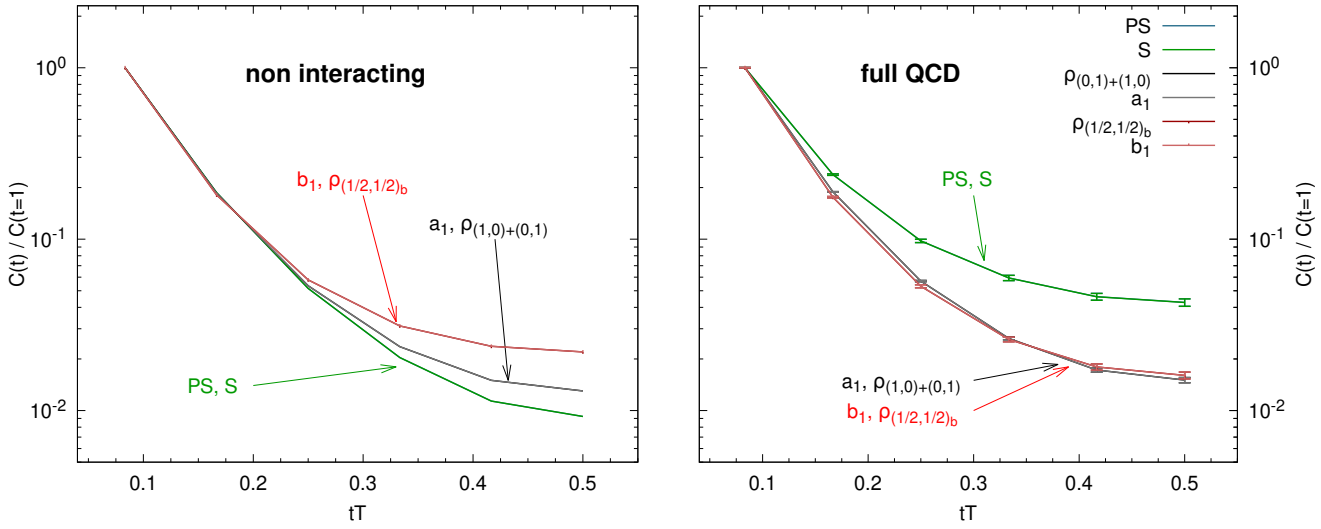

Free quarks: $SU(2)_L \times SU(2)_R$ and $U(1)_A$ multiplets.

Full QCD at $T = 220$ MeV: $U(1)_A$, $SU(2)_L \times SU(2)_R$, $SU(2)_{CS}$ and $SU(2N_F)$ multiplets.

Above T_{pc} QCD is approximately $SU(2)_{CS}$ and $SU(2N_F)$ symmetric.

Three regimes of QCD

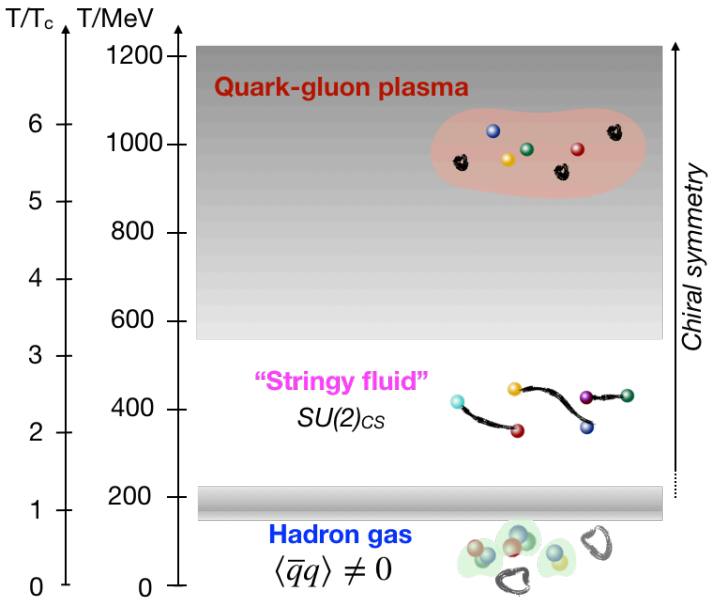

We can distinguish three different regimes according to symmetries and properties (degrees of freedom).

$0 - T_{pc}$ - Hadron Gas;

$T_{pc} - 3T_{pc}$ - Stringy Fluid (chiral, $SU(2)_{CS}$ and $SU(4)$ symmetries; electric confinement)

$T > 3T_{pc}$ - a smooth approach to QGP (chiral symmetry; magnetic confinement)

Conserved charge fluctuations at non-zero temperature and density

Jishnu Goswami (Bielefeld, Germany)

Comparison of LQCD with HRG models

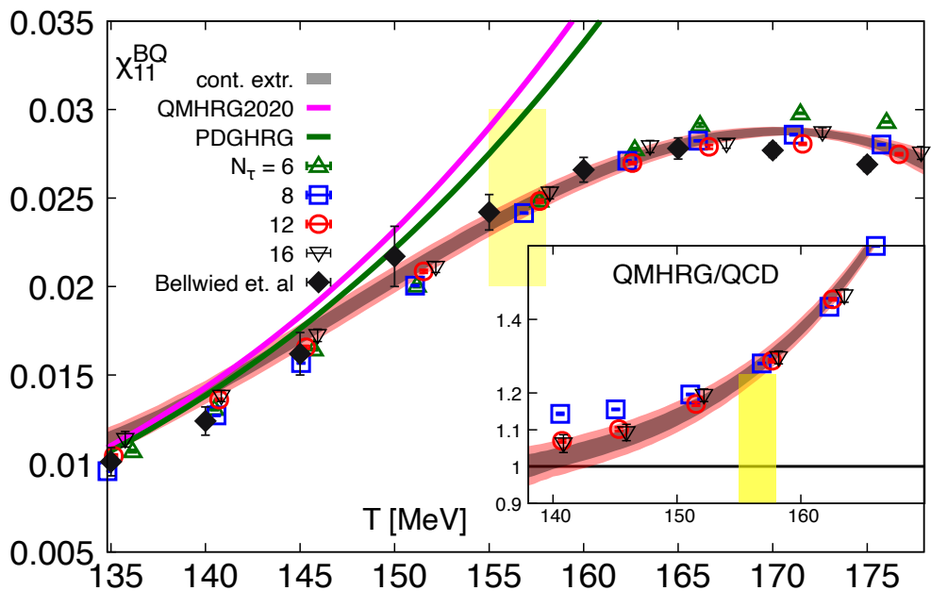

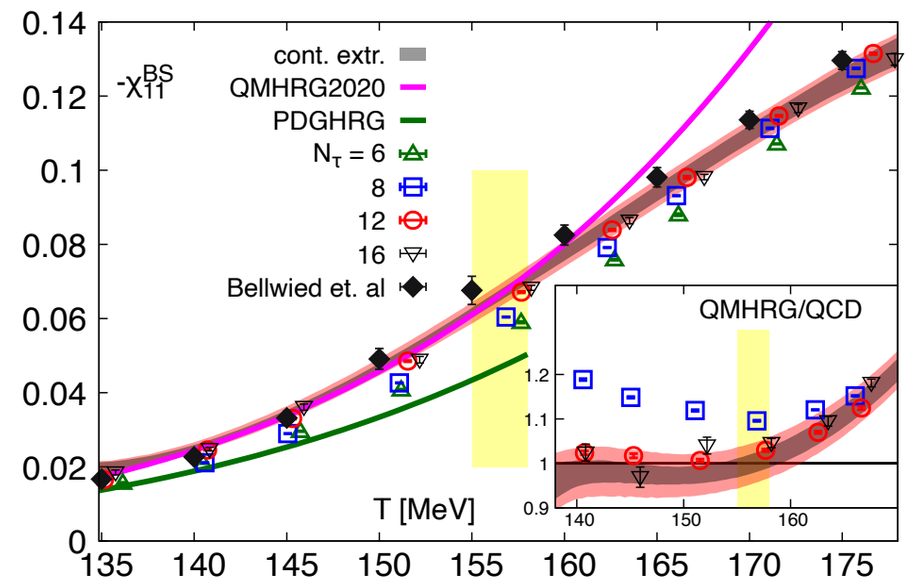

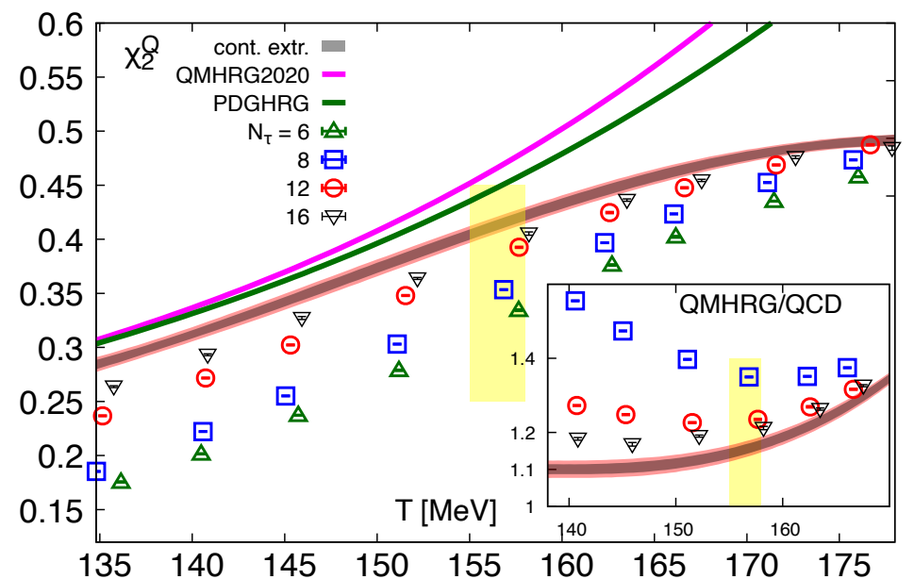

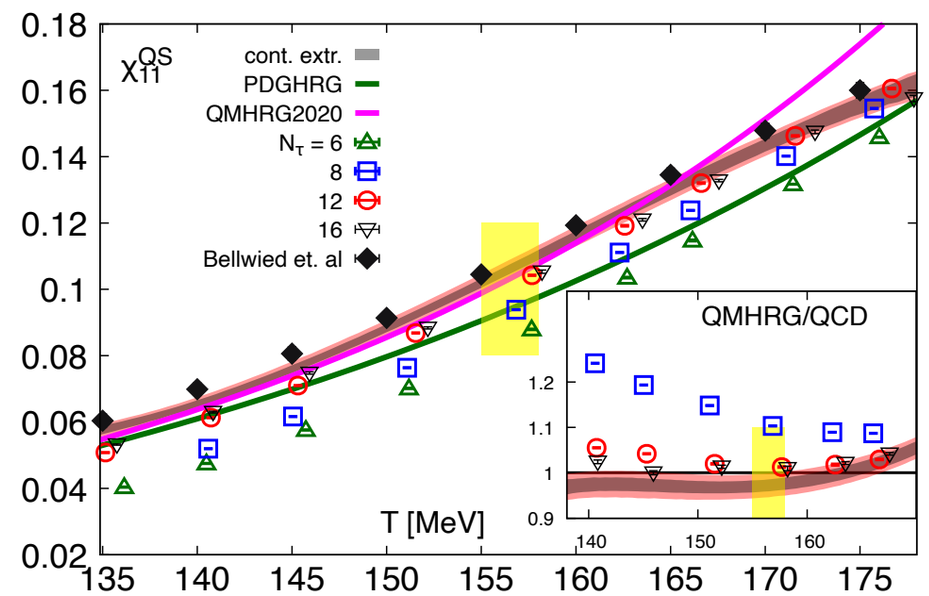

- **PDGHRG : Established resonances (3 and 4-star) from PDG**
- **QMHRG2020 : Additional resonances from PDG (1 and 2 star) and from Quark Model calculations.**
- **Uniqueness: Identification of 1 and 2-star resonances with QM prediction states.**
- **Different Quark model list have similar number of baryons/ mesons. The curves still differ from the use of different masses from different QM.**

The 2^{nd}order cumulants satisfy ($m_u = m_d$),

$$\chi_2^S = 2\chi_{11}^{QS} - \chi_{11}^{BS}$$

$$\chi_2^B = 2\chi_{11}^{BQ} - \chi_{11}^{BS}$$

D. Bollweg et al ,arXiv:2107.10011 ; J. Goswami et al, arXiv:2109.00268, SQM2021

S-matrix based calculations of Kaons $[K_0^*]$

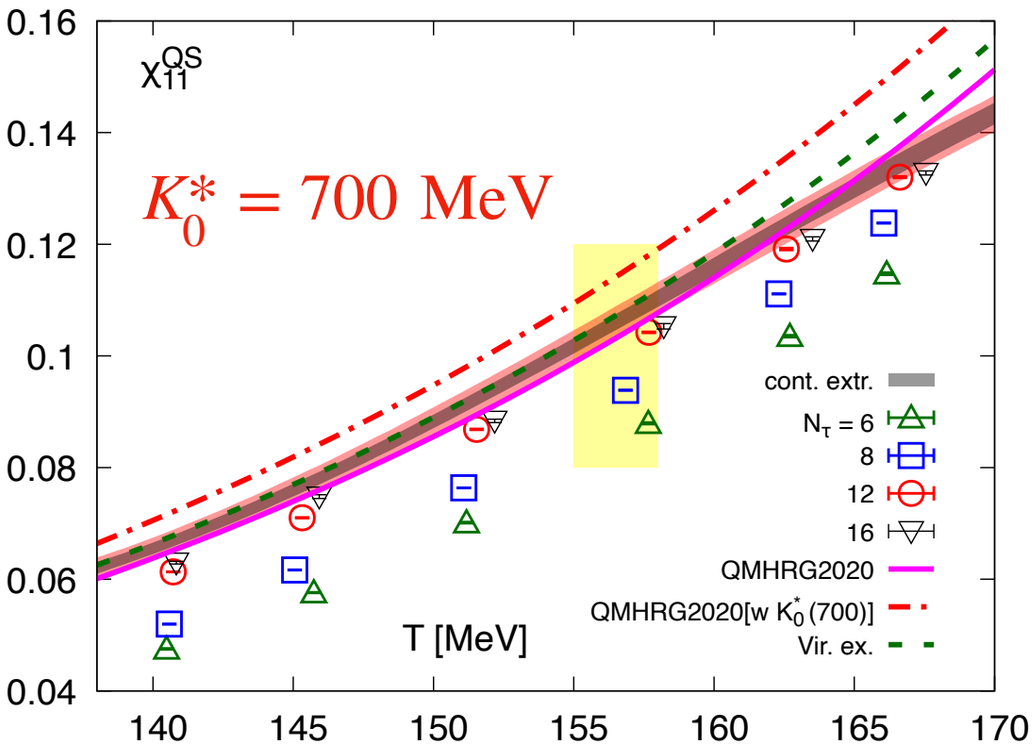

$$\chi_{1n}^{QS} \sim \sum_n Q_H S_H^n P_H$$

$$P_H \sim \exp(-m_H/T)$$

K_0^* does not contribute to the QCD thermodynamics as a point like non-interacting particle.

- K_0^* is not included in our QMHRG2020 list.
- At $T \sim 130$ MeV, the contribution of ground state kaon and its P-wave excitation $K^*(892)$ to χ_{11}^{QS} is more than $80\,\%$.
- Contribution of $K_0^*(700)$ as a point like non-interacting resonances would change the HRG model result by almost $10\,\%$.
- But the contribution is largely reduced in a virial expansion that makes use of information on scattering amplitudes in the S-wave $K - \pi$ channel.

B. Friman et al, Phys. Rev. D 92, 074003 (2015)

Nuclei, hypernuclei and exotica in relativistic nuclear collisions: access to the QCD phase diagram

Peter Braun-Munzinger (Darmstadt, Germany)

the QGP phase diagram, LatticeQCD, and hadron production data

note: all coll. at SIS, AGS, SPS, RHIC and LHC involved in data taking
each entry is result of several years of experiments, variation of μ_B via variation of cm energy

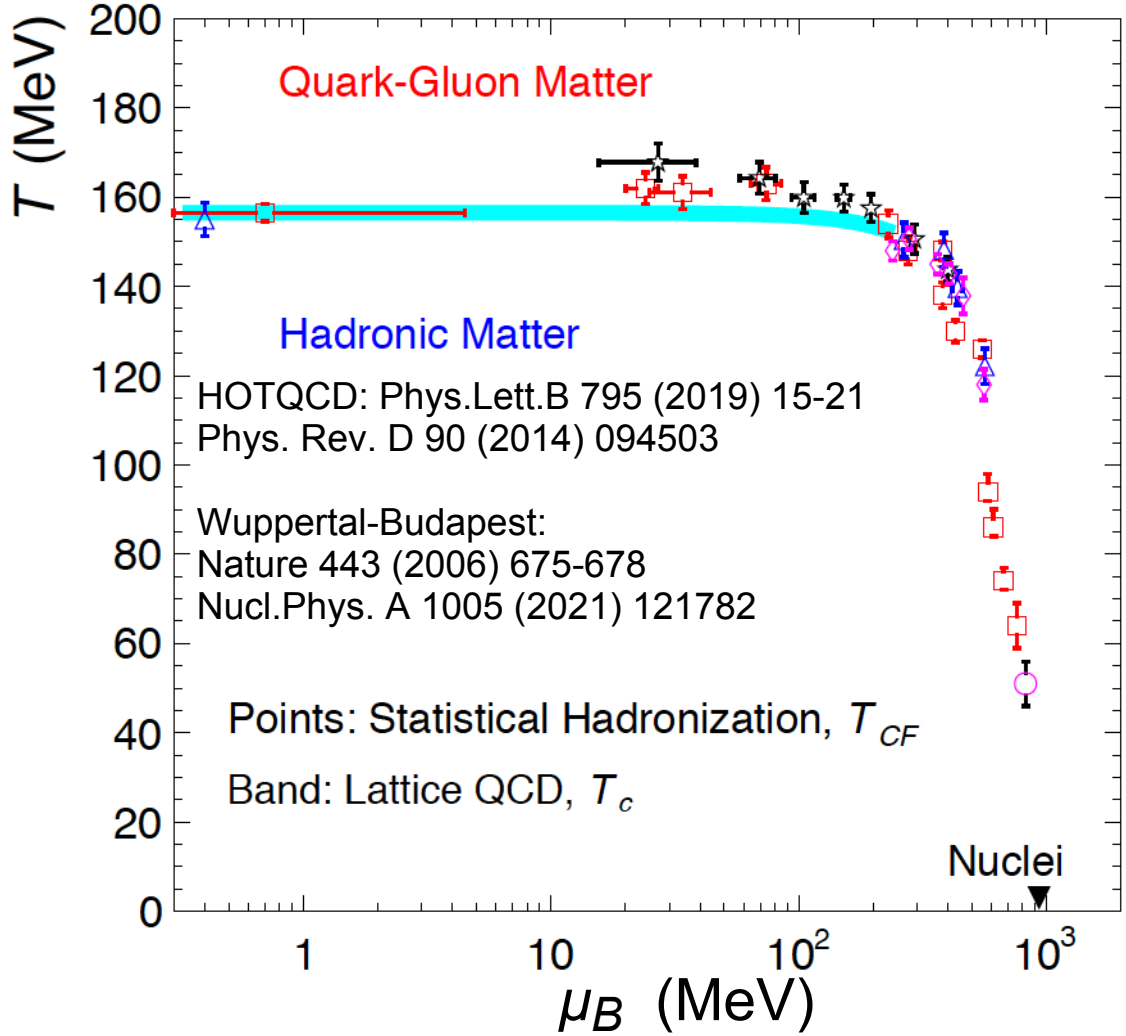

quantitative agreement of chemical freeze-out parameters with most recent LQCD predictions for baryo-chemical potential < 300 MeV

cross over transition at μ_B = 0 MeV, no experimental confirmation

should the transition be 1st order for large μ_B (large net baryon density)?

then there must be a critical endpoint in the phase diagram

experimental determination of phase boundary at
T_c = 156.6 ± 1.7 (stat.) ± 3 (syst.) MeV and μ_B = 0 MeV
Nature 561 (2018) 321

newest hyper-triton results

Lifetime
measurement

- Signal extracted in a wide *ct* range thanks to the BDT
- Most precise hypertriton lifetime determination so far
  - 5% stat. 6% syst.
  - Statistical uncertainty lower than the world average uncertainty
- Consistent with free Λ lifetime and previous ALICE measurement

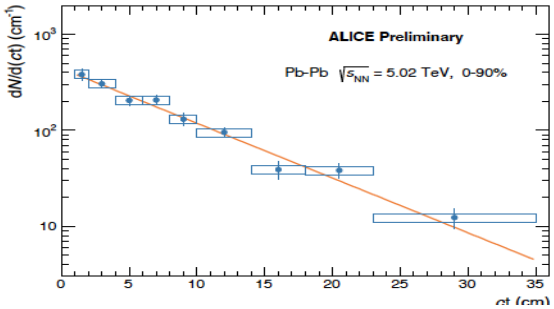

Lifetime
measurement

- Signal extracted in a wide *ct* range thanks to the BDT
- Most precise hypertriton lifetime determination so far
  - 5% stat. 6% syst.
  - Statistical uncertainty lower than the world average uncertainty
- Consistent with free Λ lifetime and previous ALICE measurement

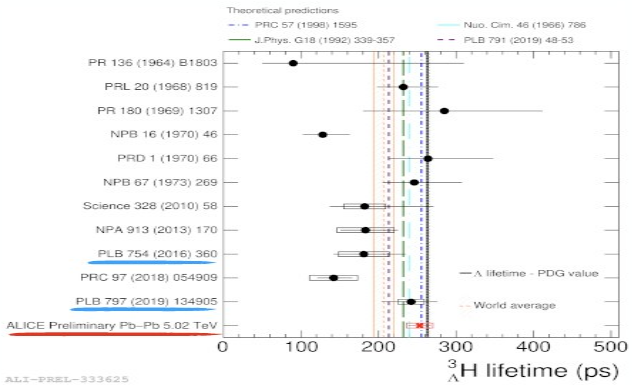

B_Λ

- Use Machine Learning (BDTs) to identify $^{3}_{\Lambda}$H candidates in Pb–Pb
- Most precise measurement of $^{3}_{\Lambda}$H lifetime
  - Favors $^{3}_{\Lambda}$H lifetime near free Λ lifetime
- Very precise measurements of $^{3}_{\Lambda}$H mass and binding energy
  - Binding energy compatible with 0.
  - Support loosely bound $^{3}_{\Lambda}$H

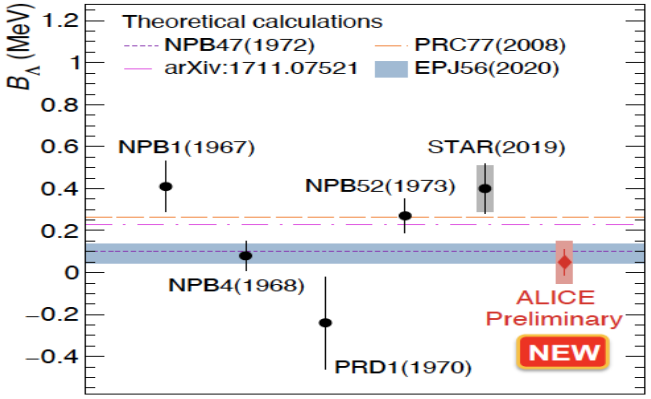

J/ψ and hyper-triton yields described with the same flow parameters in the statistical hadronization model

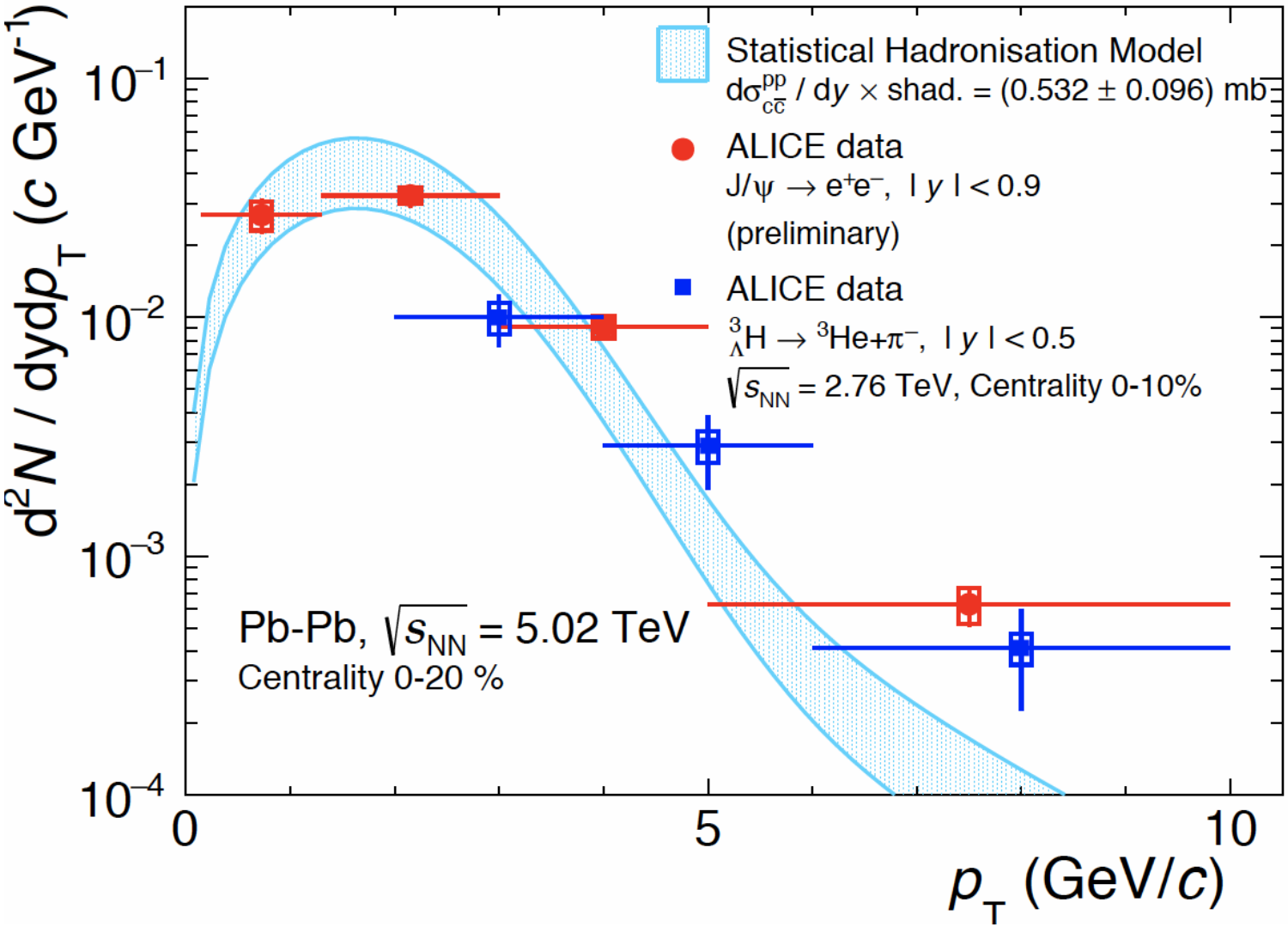

binding energies:
J/ψ 600 MeV
hypertriton 2.2 MeV
Lambda S.E. 0.13 MeV

from review: hypernuclei and other loosely bound objects produced in nuclear collisions at the LHC,
pbm and Benjamin Doenigus,
Nucl. Phys. A987 (2019) 144, arXiv:1809.04681

doorway state hypothesis:
all nuclei and hyper-nuclei, penta-quark and T,X,Y,Z states are formed as virtual, compact multi-quark states at the phase boundary. Then slow time evolution into hadronic representation. Excitation energy about 20 MeV, time evolution about 10 fm/c

Andronic, pbm, Redlich, Stachel
Nature 561 (2018) 321, arXiv :1710.09425

how can this be tested?

precision measurement of spectra and flow pattern for light nuclei and hyper-nuclei, multi-charm hadrons, penta-quark and X,Y,Z states from pp via pPb to Pb-Pb

a major new opportunity for ALICE Run3/4
and beyond 2030 for X,Y,Z, T_{cc} and penta-quark states

also new opportunities for
GSI/FAIR and JINR/NICA
experiments

Open heavy flavor in heavy-ion collisions

Ralf Averbeck (Darmstadt, Germany)

Charm baryons in pp collisions

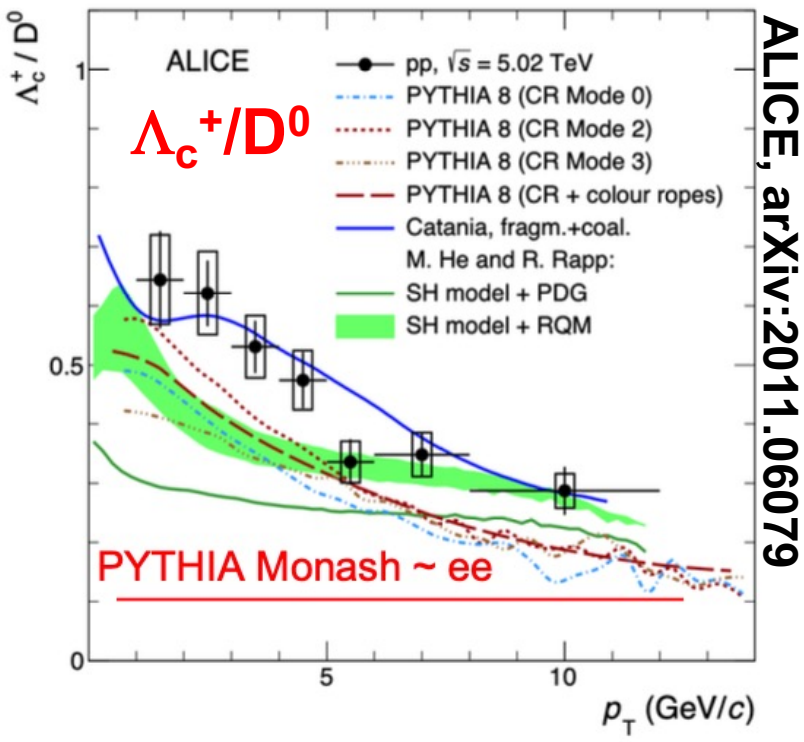

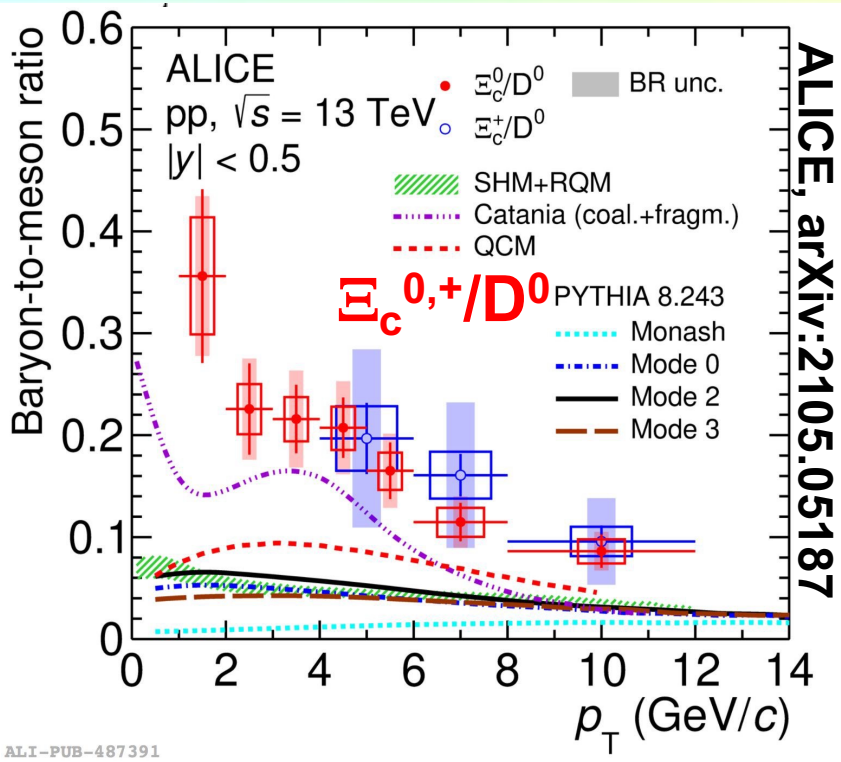

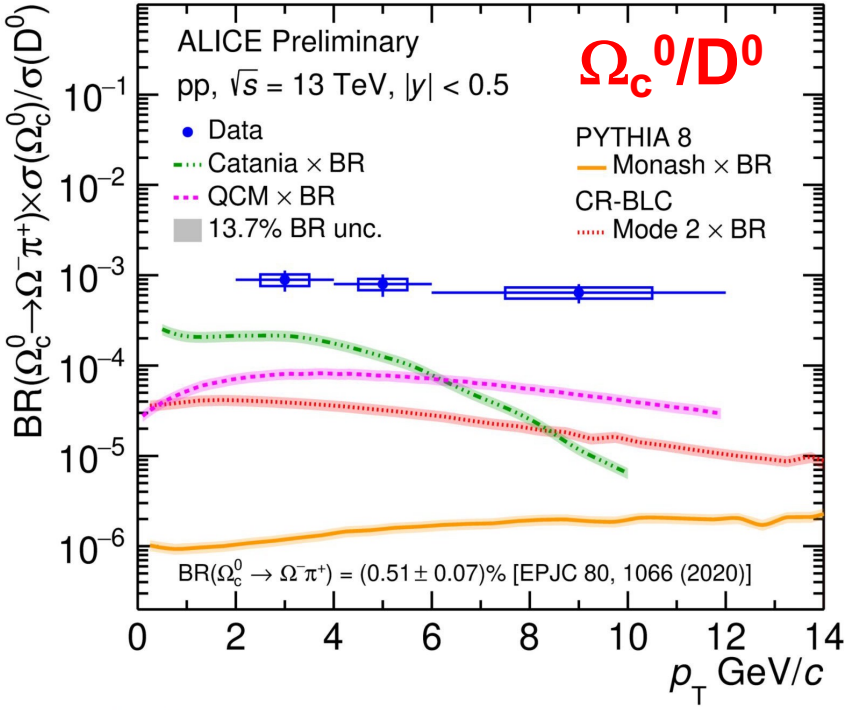

- baryon fraction (Λ_c, Ξ_c, Ω_c) at low p_T much larger than predicted by string fragmentation models tuned on e^+e^- data
- baryon measurements crucial for understanding of hadronization (see later)

total charm cross section needs baryon measurement!

Dead cone observed in D-jets in pp collisions

- **dead cone effect**
  (Dokshitzer, Khoze, Troian: J.Phys. G17(1991)1602)
  - radiation (medium induced and in vacuum) is suppressed at small angle ($\theta < m/E$)

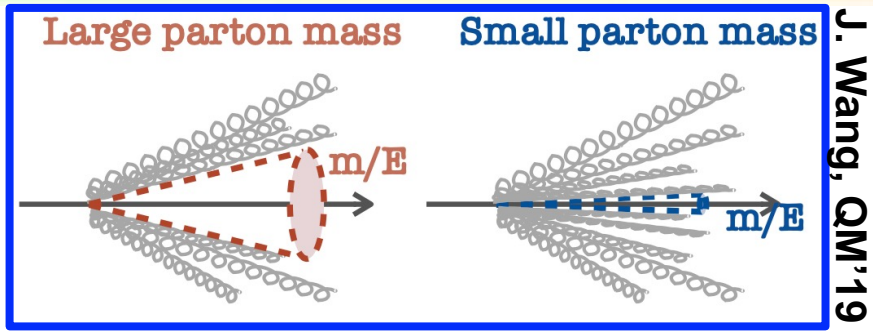

J. Wang, QM'19

- **first direct observation**
  - D^0-tagged vs. inclusive jets
  - analyze jet substructure via iterative declustering
  - radiator: leading quark proxy
  - radiation suppressed in expected angular region (shaded)
  - suppression vanishes for $m_q \ll E_{radiator}$

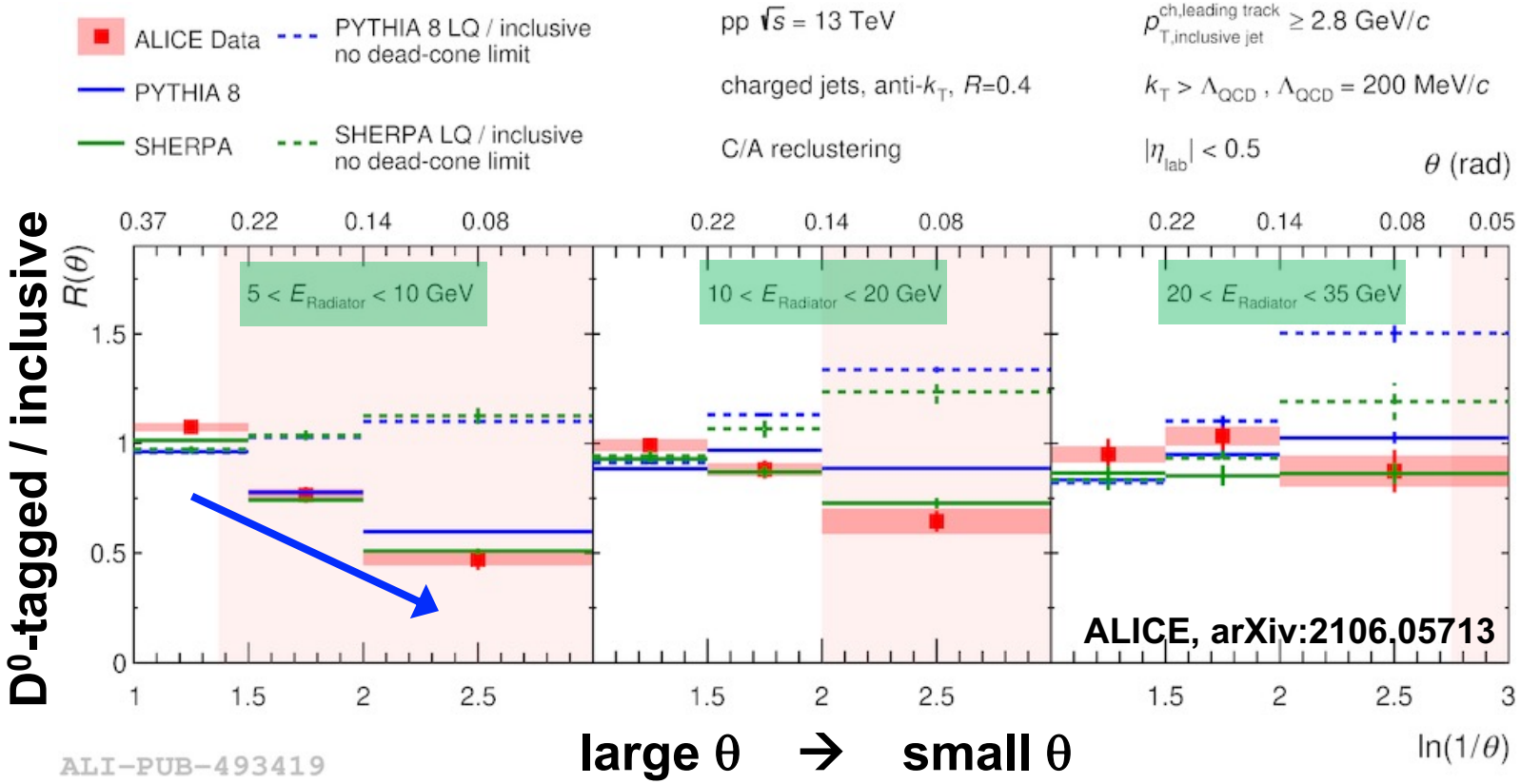

D^0-tagged / inclusive

ALICE, arXiv:2106.05713

large θ → small θ

Open and hidden heavy-flavor v_2

- p_T dependence of v_2 similar for π, D, J/ψ (with π > D > J/ψ)
  → indication for charm-quark flow & (re)combination
  → thermalization?
- no indication for Υ(1S) flow but $v_2 > 0$ for e from b hadrons
  - possible scenario:
    - b quarks do not flow
    - b-hadron flow via coalescence with light quarks
    - (re)combination small for Υ(1S)
- models describing data include
    - hydrodynamic expansion of the bulk
    - HQ interaction with the medium
    - hadronization via fragmentation and coalescence

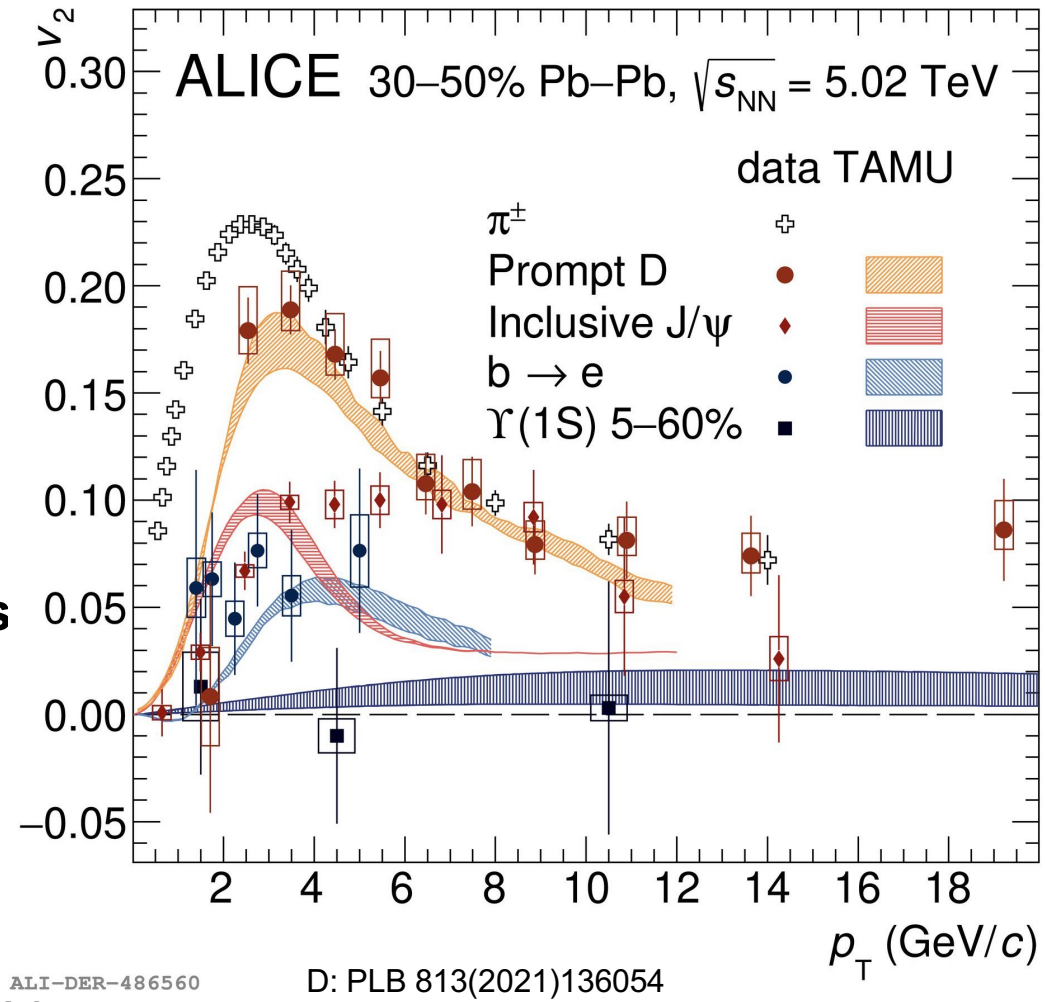

D: PLB 813(2021)136054
J/ψ: JHEP 10(2020)141
e←b: PRL 126(2021)162001
Υ(1S): PRL 123(2019)192301
TAMU: PRL 124(2020)042301

Quarkonia at the LHC as a probe of deconfinement

Johanna Stachel (Heidelberg, Germany)

Systematics of hadron production in SHMc

A.Andronic et al., PLB 797 (2019) 134836

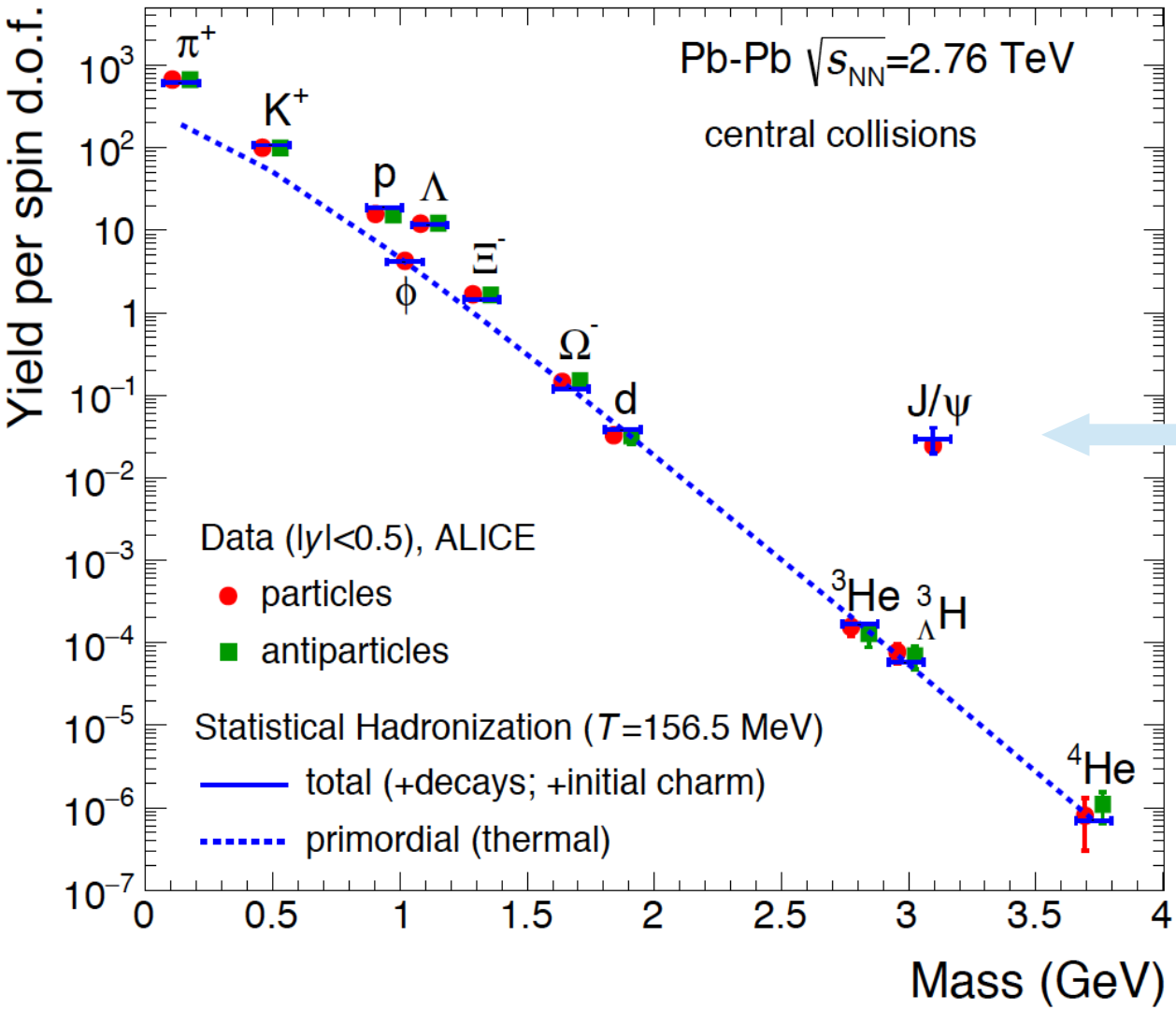

J/ψ enhanced compared to other M = 3 GeV hadrons since number of c-quarks is about 30 times larger than expected for pure thermal production at T = 156 MeV due to production in initial hard collisions and subsequent thermalization in the fireball.

enhancement factor 900 relative to purely thermal yield

Ratios of charm hadron to D^0 spectra

A. Andronic et al., JHEP07 (2021) 035

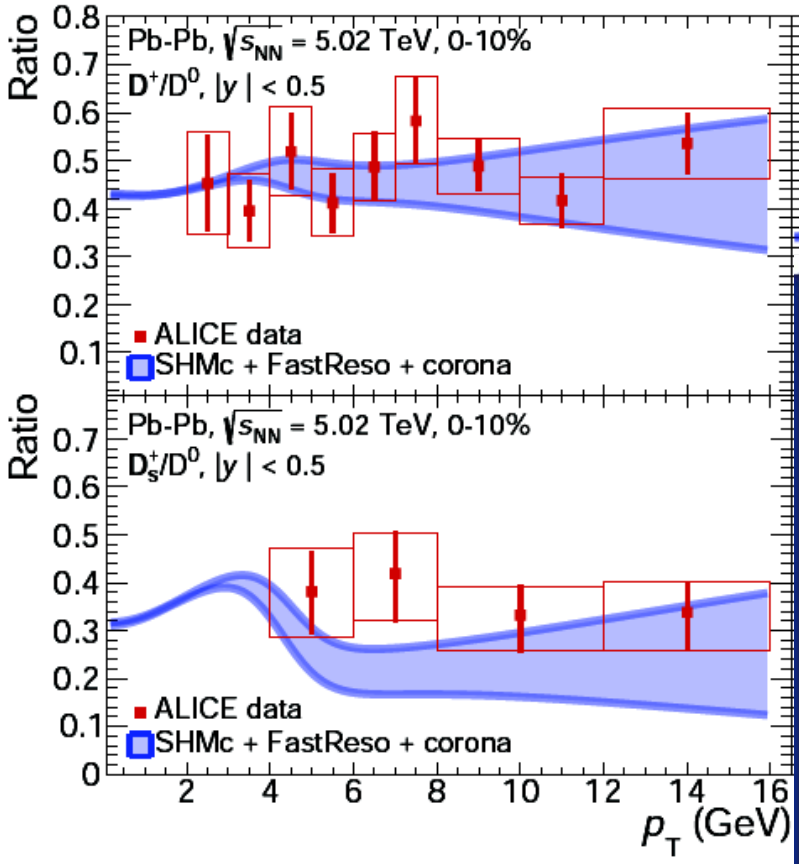

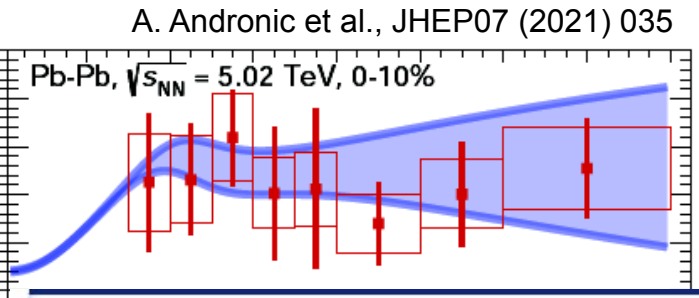

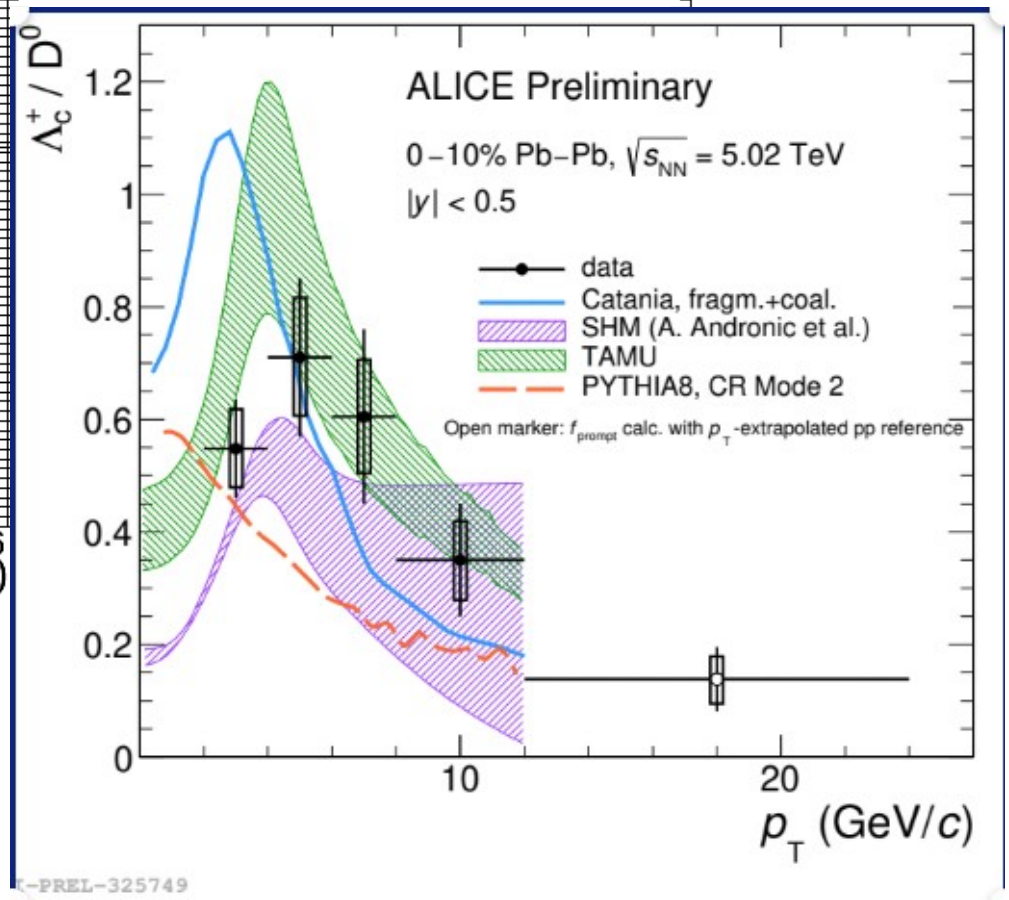

preliminary Lambda_c fits well into picture

The multi-charm hierarchy

open and hidden charm hadrons, including exotic objects, such as X-states, c-deuteron, c-triton, pentaquark, Ω_{ccc}

A. Andronic et al., JHEP07 (2021) 035

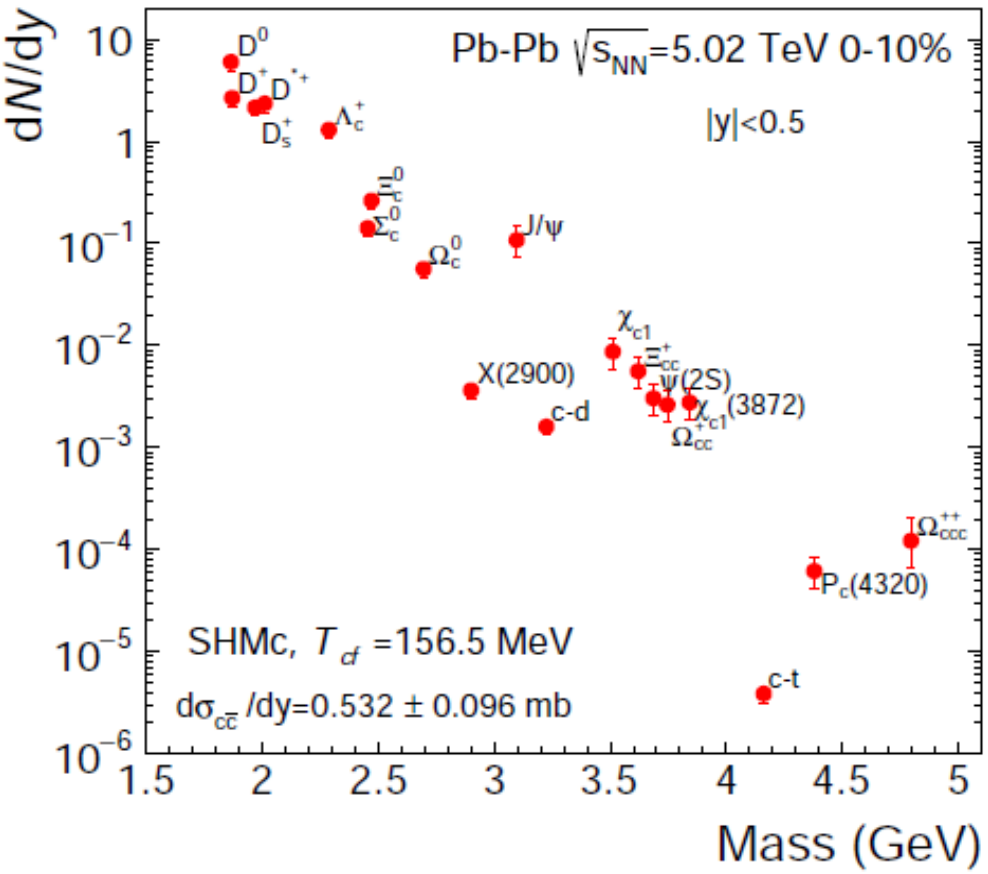

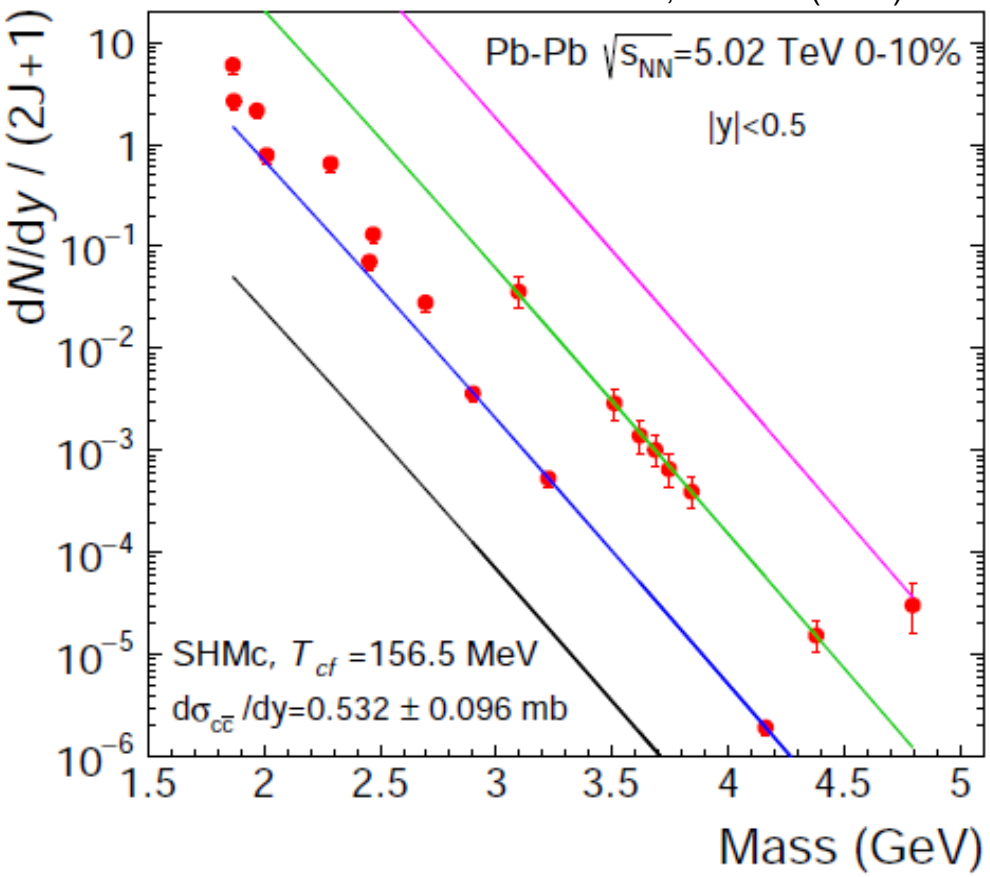

emergence of a unique pattern, due to g_c^n and mass hierarchy
perfect testing ground for deconfinement for LHC Runs3 and beyond

A new laboratory to study hadron hadron interactions

Laura Fabbietti (Munich,Germany)

What is inside neutron stars?

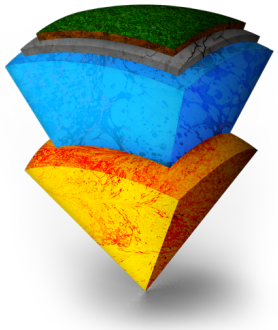

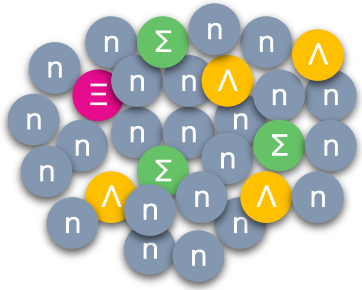

?

All two- and three-particle strong interactions can be measured at the LHC!

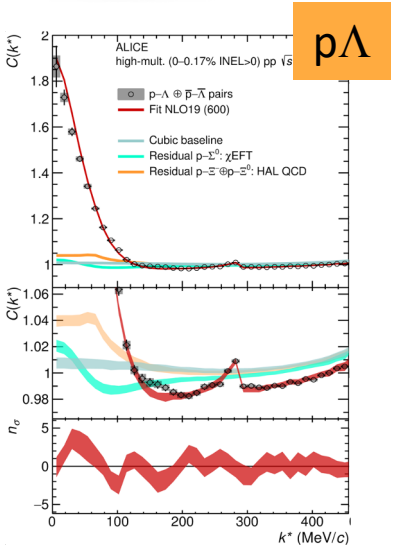

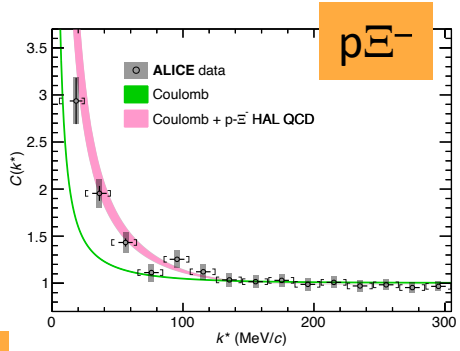

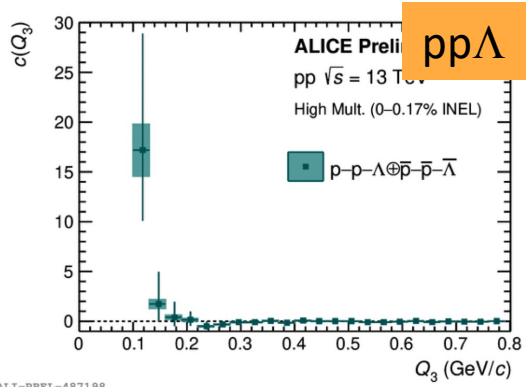

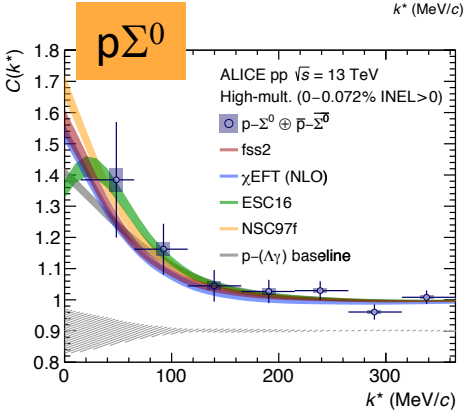

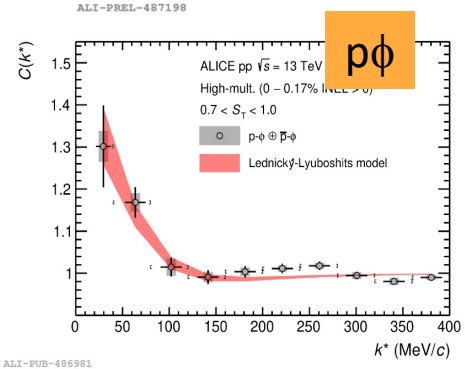

Test first principle calculations

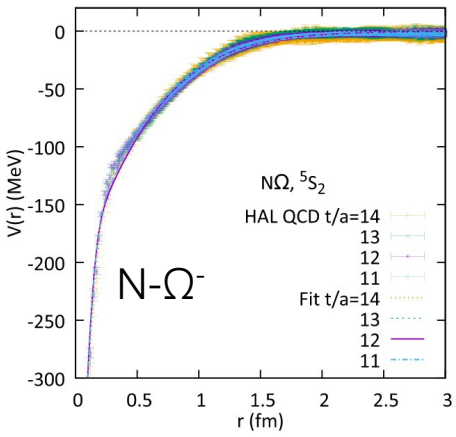

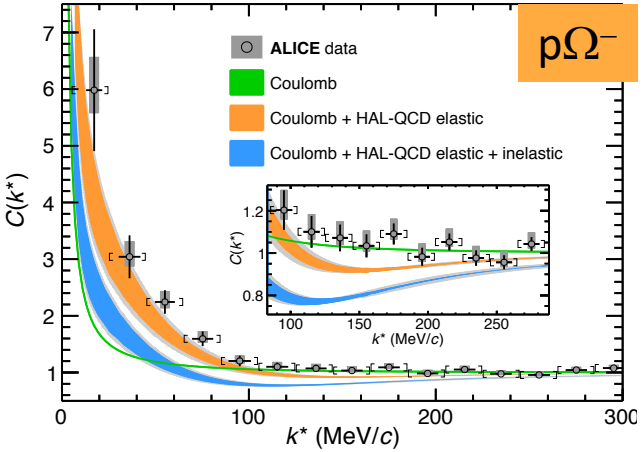

Data more precise than lattice calculation
No evidence of a bound state
Inelastic channels probably negligible since ΛΞ coupling very weak

HAL QCD potential: Predicted pΩ⁻ bound state with 1.54 MeV binding

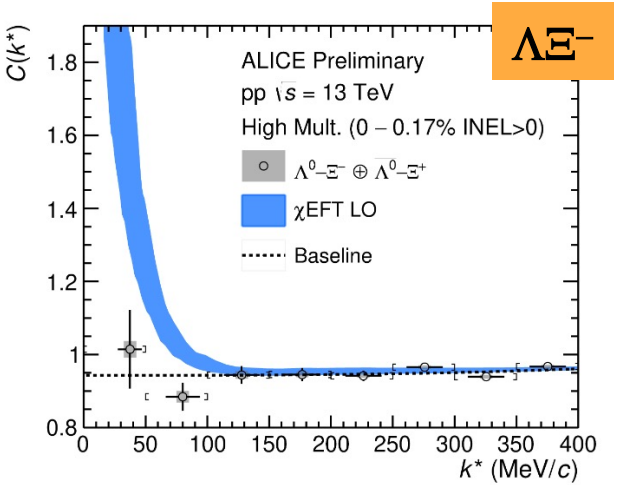

ALI-PREL-487007

Femtoscopy with Nuclei measures their emission time

Case II : delayed formation of d

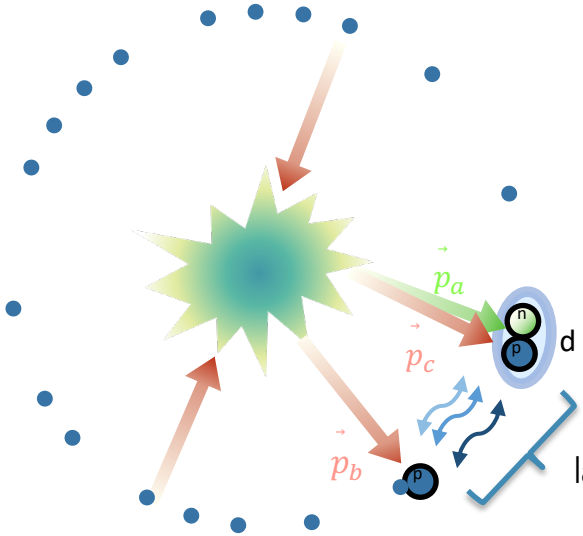

larger 'source' size ~10 fm

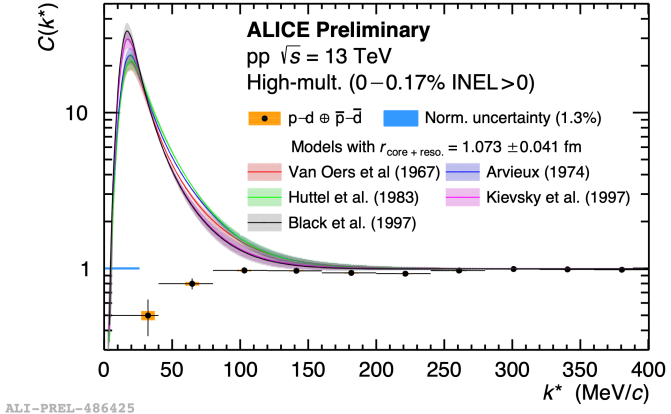

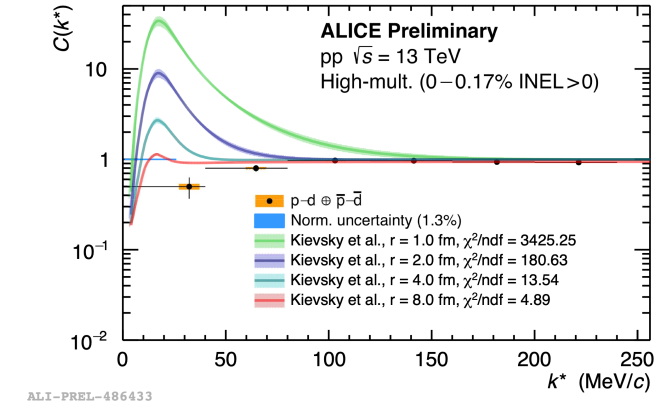

Charm sector opened

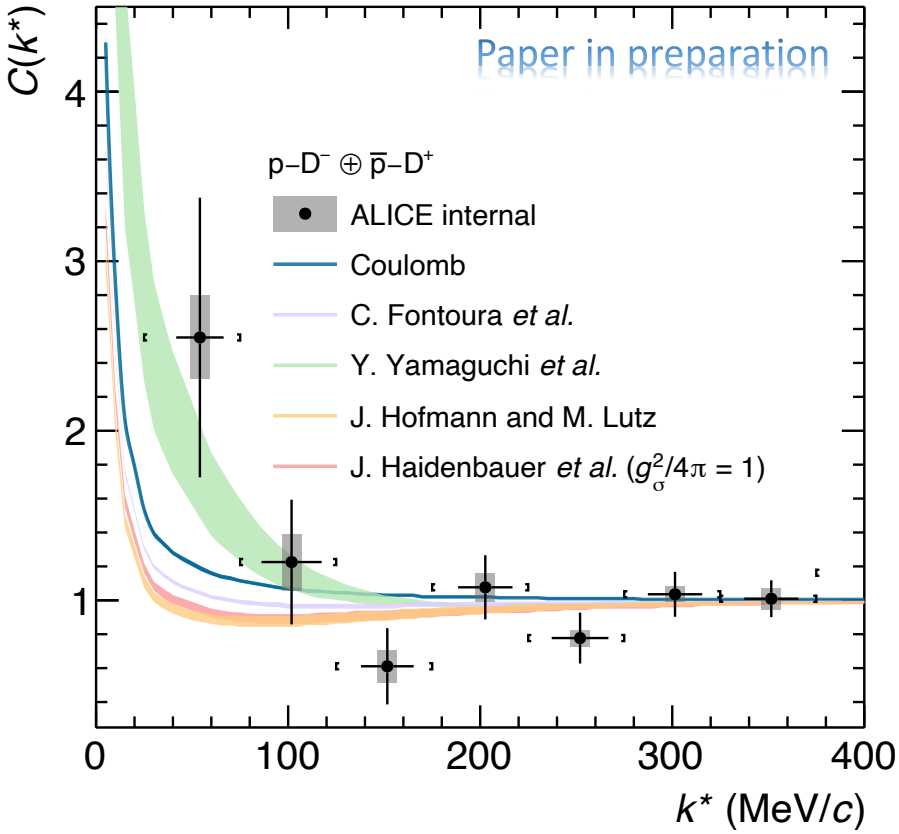

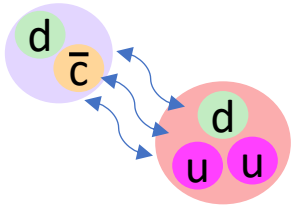

J. Haidenbauer et al, Eur. Phys. J. A33 (2007) 107-117
J. Hofmann and M. Lutz, Nucl. Phys. A 763 (2005) 90-139
Fontura et al, Phys. Rev. C 87 (2013) 025206
Yamaguchi et al, Phys. Rev. D84 (2011) 014032

Upcoming measurements of D-π, D-Kaon
Measurement of scattering lengths might be important for the interpretation of molecular states

Short distances is the new high densities

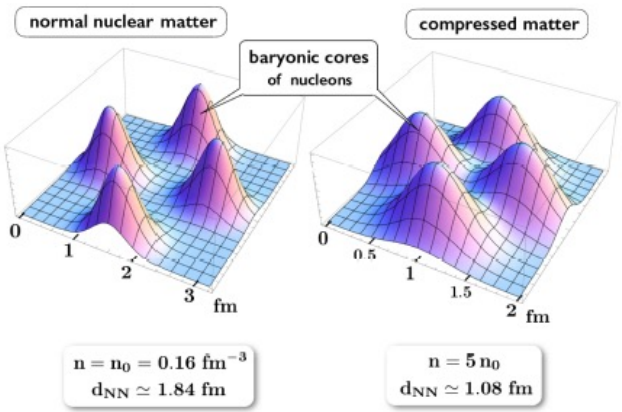

Future perspective:

Three- and four-body interactions measured and intra-particle distances of ~1-1.5 fm will provide access to interaction at high densities and very low (?) temperature

We can access the region of large μ_B at low temperatures

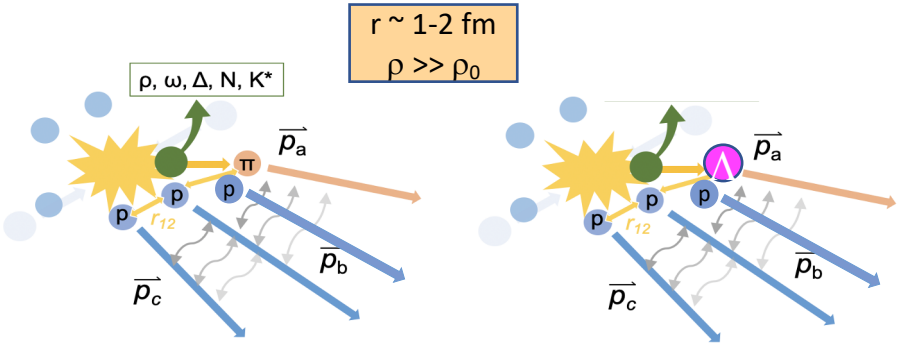

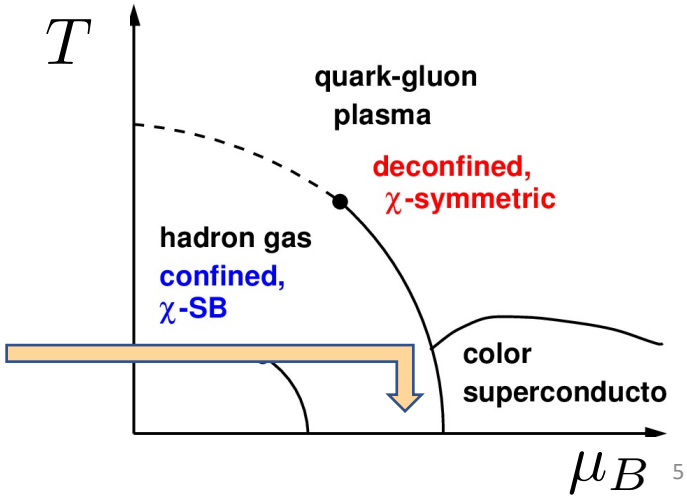

Investigating three-baryon interactions using femtoscopy in pp collisions with ALICE

Raffaele Del Grande (Garching, Germany)

Three-body femtoscopy in pp collisions with ALICE

- First measurement of three-baryon correlation functions
- Cumulants for p-p-p and p-p-Λ extracted with the Kubo's method

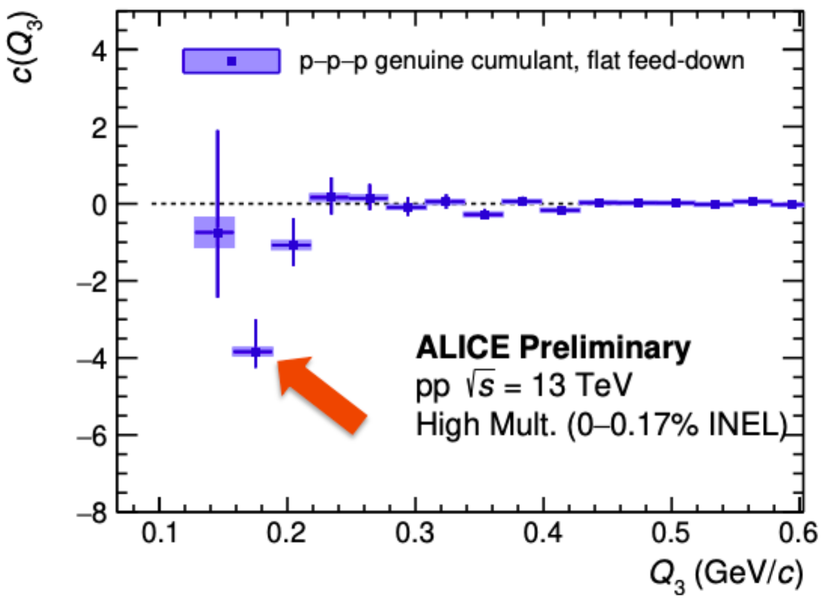

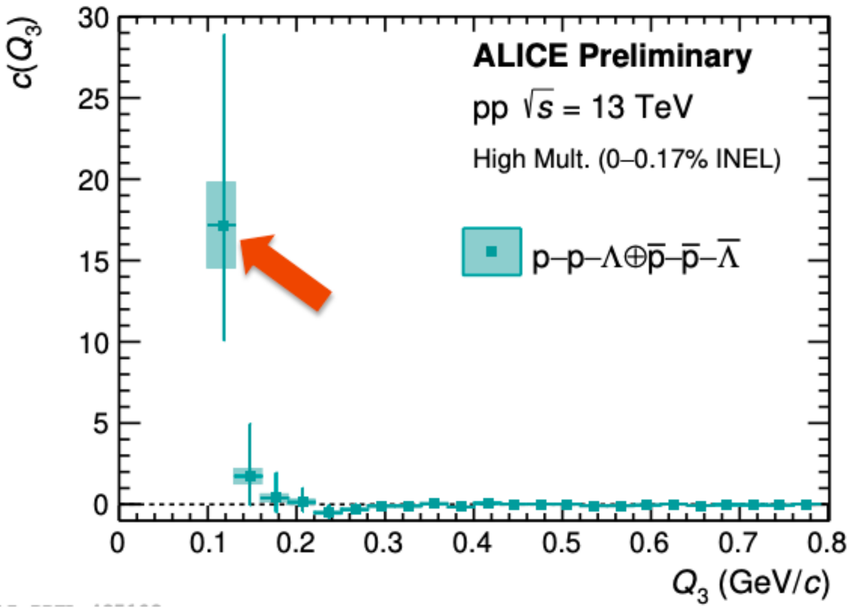

- **p-p-p:** significant deviation (**n_σ = 2.9** for $Q_3 < 0.4$ GeV/c)

  → FIRST HINT of genuine p-p-p correlation
- **p-p-Λ:** positive cumulant → ALICE Run 3 data should provide statistically significant result
- Calculations for the three-body scattering are needed

Antihelium-3 Inelastic Interactions at the LHC and in Our Galaxy

Laura Serksnyte (Garching, Germany)

Summary and outlook

- First measurements of the anti-^{3}He inelastic cross section in wide kinetic energy range from 0.04 GeV/A to 2.52 GeV/A.
- Impact of the ALICE measurements on anti-^{3}He fluxes near Earth:
  - High transparency of the Galaxy to anti-^{3}He fluxes
  - Uncertainties on cosmic ray fluxes from anti-^{3}He σ_{inel} measurements are small compared to other uncertainties in the field

Essential reference for any studies of anti-^{3}He in space!

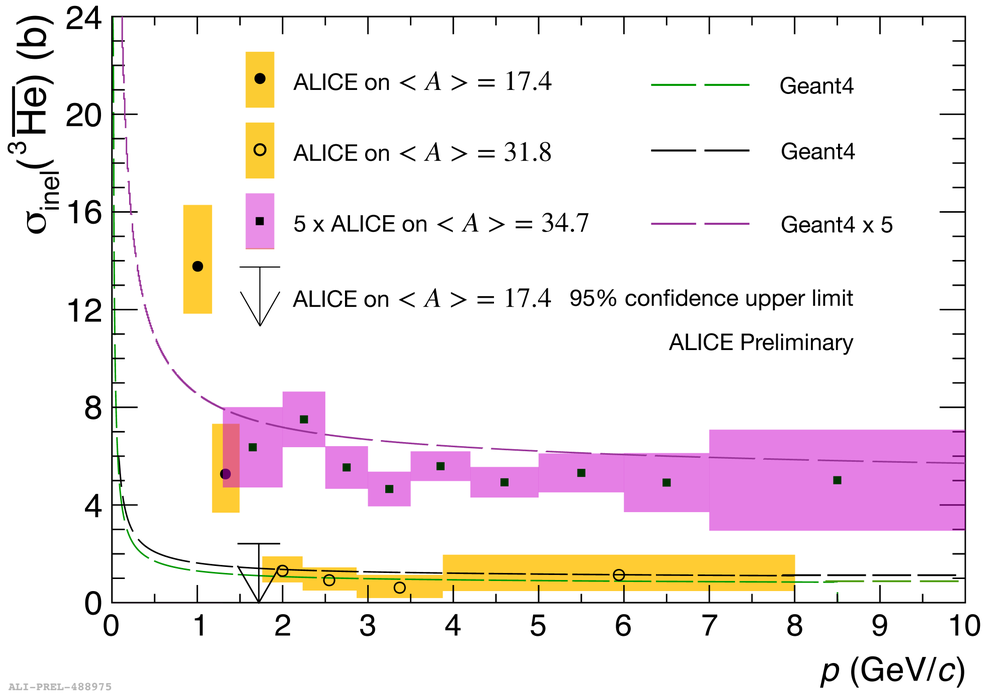

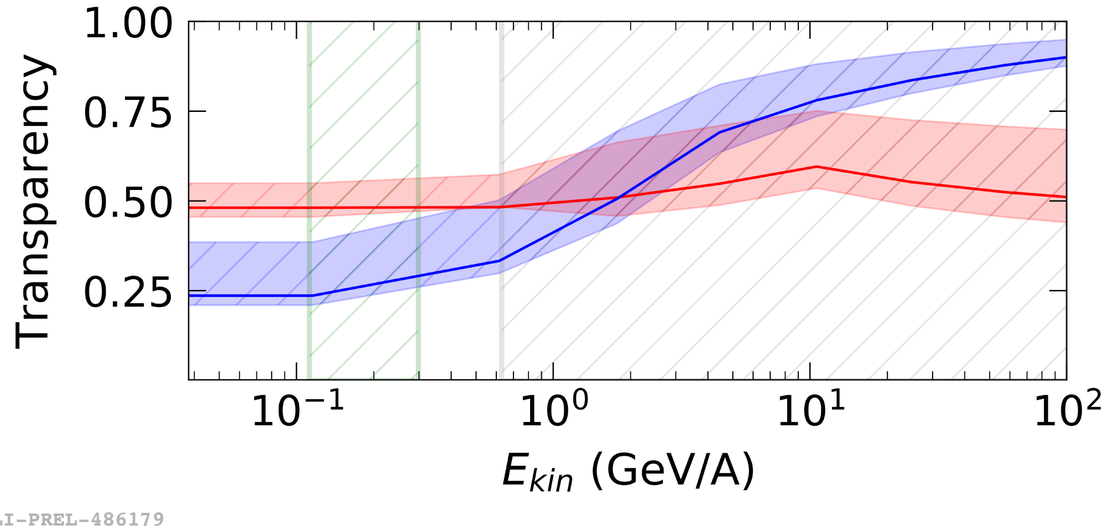

Initial state fluctuations effects on non-equilibrium phase transition on pp collisions at LHC energies

Irais Bautista (Puebla, Mexico)

Temperature Fluctuations

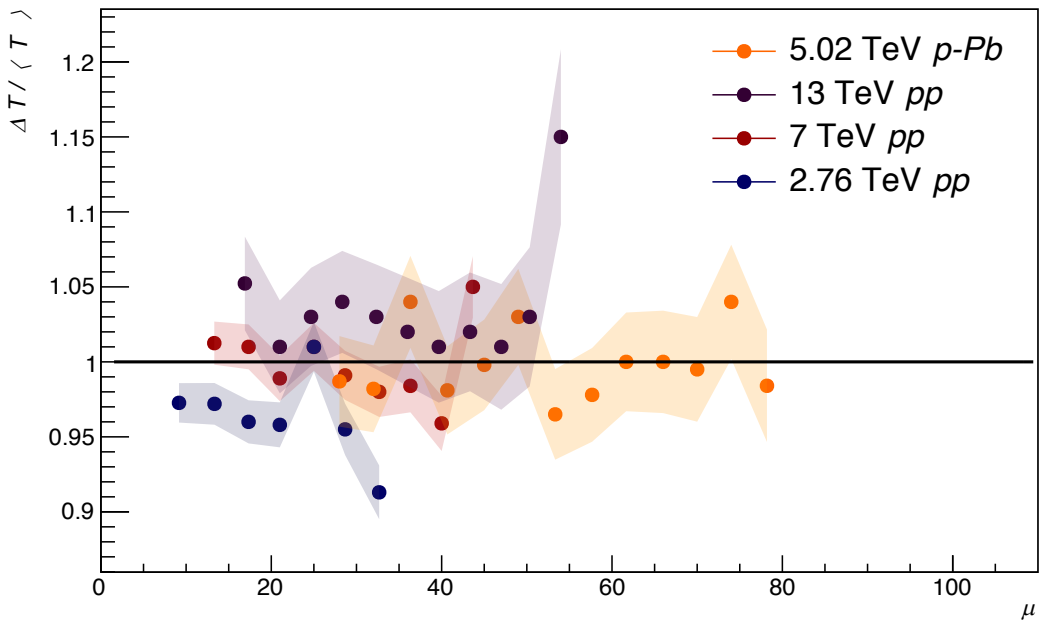

EbE <p_T> Fluctuations

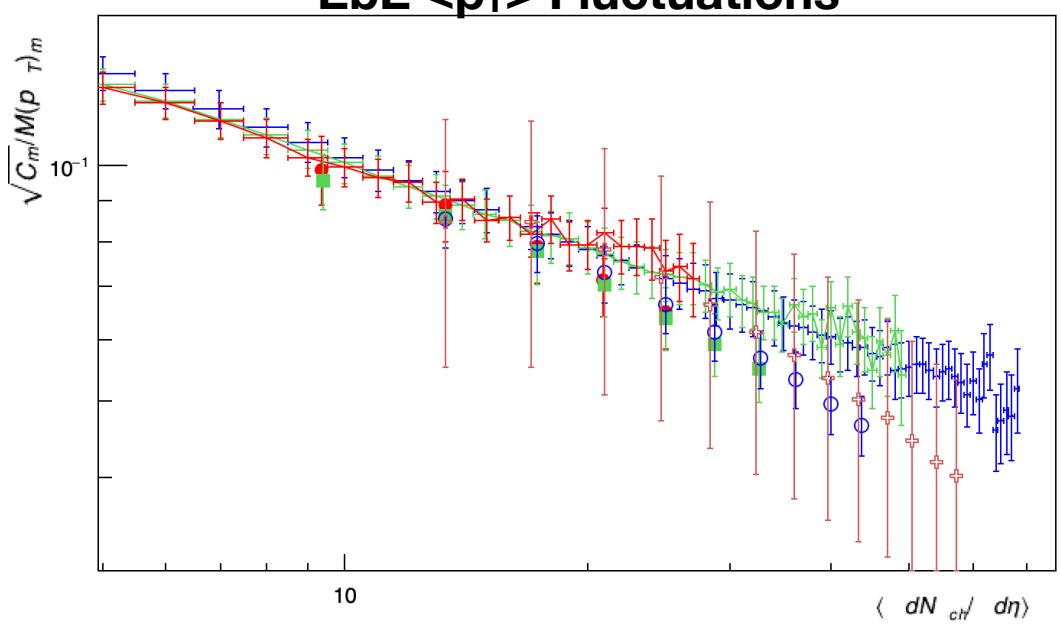

Mean transverse momentum fluctuations for pp collisions represented in blue lines for 7 TeV, green 2.76 TeV, red .9 TeV and brown 13 TeV dots come from SMP calculations and data from [ALICE Collaboration], Phys. Rept. 599 (2015)

Future opportunities with nuclear beams at the TeV scale

Urs Achim Wiedemann (Geneva, Switzerland)

Bottom-up is a more encompassing HI paradigm than the perfect fluid

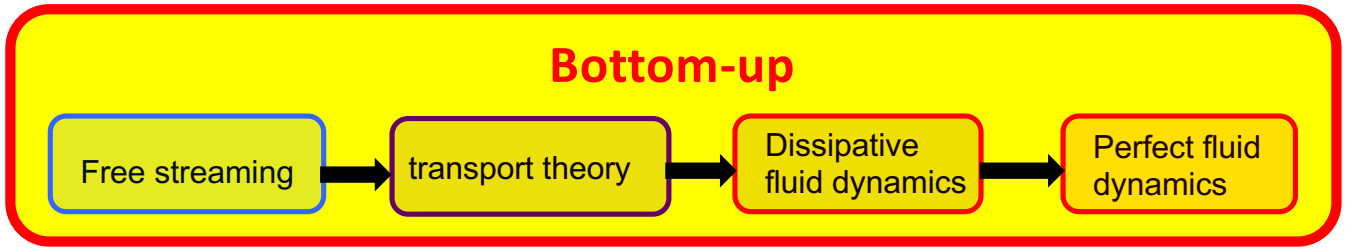

Bottom-up includes:

- pre-equilibrium dynamics*
  from $f \sim O(1/\alpha_s)$ to $f \sim 1$
- Close-to-perfect fluidity
  (with specific non-hydro modes)
- Jet quenching

Many open questions:

- Nature of non-hydro excitations?
- Onset of jet quenching
- Origin of hadrochemical equilibration
- Transport of heavy flavor
- …

*A. Kurkela, A. Mazeliauskas, J.F. Paquet, S. Schlichting, D. Teaney, "KOMPOST", Phys. Rev. Lett. 122 (2019) 12 and Phys. Rev. C99 (2019) 3

My escape from the GDR – from Leipzig via the Black Sea to Munich

Harald Fritzsch (Munich, Germany)